Molecular mechanisms of the age-related resistance in *Arabidopsis thaliana*.

By

Lanxi Hu

(Under the Direction of Li Yang)

Abstract

In animals and plants, immunity changes with the increase of age. The regulation of immune maturation remains largely underexplored. Heterochronic microRNAs are critical in regulating the developmental time. This work found that a conserved heterochronic microRNA (miRNA) in *Arabidopsis*, micro-RNA156, regulates the age-related resistance associated with the vegetative phase change, a transition from juvenile to adult during shoot development. With iR156-controlled SPL transcription factors obtaining distinct functions, the increase of disease resistance was integrated into the shoot development. Specifically, SPL10 bound and activated the key gene acting in defense, thereby enhancing the resistance in adult *Arabidopsis* leaves. In addition, I discovered that FLS2 (Flagellin-sensing 2), a plant immune receptor, mediated disease resistance in an age-dependent manner. The suppression of FLS2-controlled callose deposition by miR156 indicated the masked FLS2 function in juvenile phase. My work uncovered regulatory mechanisms that connect age-related resistance

with vegetative phase change. By determining the developmental regulation on immunity, we anticipate removing the aging barrier from plant immunity and provide a molecular guidance for disease managements in agriculture.

Index words: Aging, Immunity, crosstalk, vegetative phase change.

Molecular mechanisms of the age-related resistance in *Arabidopsis thaliana*.

By

Lanxi Hu

B.S, Nanjing Forestry University, China, 2015

MSc., The University of Manchester, UK, 2016

A Dissertation Submitted to the Graduate Faculty of The University of Georgia in

Partial Fulfillment of the Requirements for the Degree

DOCTOR OF PHILOSOPHY

ATHENS, GEORGIA

2023

Molecular mechanisms of the age-related resistance in *Arabidopsis thaliana*.

By

Lanxi Hu

Major Professor: Li Yang

Committee: Shavannor M. Smith

Brian Kvitko

Chang Hyun Khang

Electronic Version Approved:

Ron Walcott

Dean of the Graduate School

The University of Georgia

May 2023

DEDICATION

To Science—a lifestyle.

## ACKNOWLEDGEMENTS

I am grateful for the generous supports and profound scientific insights provided by my major supervisor, Dr. Li Yang. It is always very enjoyable to discuss scientific histories and new discoveries with Li. I have also developed deep appreciations to my committee members, Dr. Shavannor M. Smith, Dr. Brian Kvitko and Dr. Chang Hyun Khang, who not only gave numerous helpful suggestions and comments during each of my committee meeting as well as joint lab meetings, but also offered guidance for me to navigate the campus life and pursue a group leader position in academia as well as in the industry.

Then, I would like to thank my collaborators over several projects that I have been worked, including Alan Peper, Sorrel Tran, Peng Qi, Feng Kong and Stephanie Chen. Your dedication to our work is one of the best gifts that I can receive from our research.

A special thank you goes to Dr. Yao Yao at Animal & Dairy Science, UGA, who provided valuable insights about the career development for junior scientists and women in sciences.

Last but not the least, I am grateful for the time that I spent with my family and friends, online and in-person. I become more and more strong and happy because of you.

TABLE OF CONTENTS

Page

LIST OF TABLES

Page

LIST OF FIGURES

Page

APPENDIX

# CHAPTER 1

# INTRODUCTION AND LITERATURE REVIEW—

# TIME TO FIGHT: MOLECULAR MECHANISMS OF AGE-RELATED RESISTANCE.

Reproduced, by permission, from Hu, L., and Yang, L. 2019.

Time to Fight: Molecular Mechanisms of Age-Related Resistance.

Phytopathology Review, 109:9, 1500-1508.

**ABSTRACT**

Plant age is a crucial factor in determining the outcome of a host-pathogen interaction. In successive developmental stages throughout their life cycles, plants face dynamic changes in biotic and abiotic conditions that create distinct ecological niches for host-pathogen interactions. As an adaptive strategy, plants have evolved intrinsic regulatory networks that integrate developmental signals with those from pathogen perception and defense activation. As a result, amplitude and timing of defense responses are optimized, to balance the cost and benefit of immunity activation. A general term “age-related resistance” refers to a gain of disease resistance against a certain pathogen when plants reach a relatively mature stage. Age-related resistance is a common observation on fruits, vegetables, and crops for their resistance against viruses, bacteria, fungi, oomycetes and insect pathogens. This review focuses on the recent advances in understanding the molecular mechanisms of how plants coordinate developmental timing and immune response.

## INTRODUCTION

An innate immune system protects plants from most pathogens in the environment. Surface localized pattern recognition receptors (PRRs) in plant cells can detect conserved microbial-derived molecules, such as flagellin from bacteria, fungal chitin, and β-glucans from oomycetes, to activate Pattern-Triggered Immunity (PTI) (Saijo et al. 2018; Zipfel 2014). PTI leads to a spectrum of physiological and biochemical responses to counteract pathogen invasion, including the fortification of cell wall, accumulation of reactive oxygen species (ROS), synthesis of antimicrobial compounds and transcriptional reprogramming of the phytohormone crosstalk (Saijo et al. 2018). Successful pathogens can subvert PTI by proteinaceous virulence effectors. To execute their virulence function, effectors are delivered into plant cells or the apoplastic space where they interact with and further interfere with or redirect the function of host cellular components, resulting in compromised defense responses, and eventually, pathogen multiplication (Toruño et al. 2016). To counteract the effector-triggered susceptibility, plants have evolved a class of intracellular innate immune receptors known as nucleotide binding–leucine-rich repeat (NLR) receptors, which can recognize the presence of effectors either through direct binding or effector-triggered modifications of host proteins (Cui et al. 2015; Jones and Dangl 2006). The recognition of effectors by NLRs activates effector-triggered immunity (Cui et al. 2015; Jones et al. 2016), which often activates a rapid programmed cell death, known as hypersensitive

response (HR), as well as most outcomes that are shared with PTI (Cui et al. 2015; Jones and Dangl 2006).

Activation of immune responses is tightly regulated in a temporal and spatial pattern (Smakowska et al. 2016; Whalen 2005). Constitutive or ectopic immune response may lead to deleterious effects such as dwarfism, necrosis and/or yield loss (Bomblies and Weigel 2007; Brown 2002; Huot et al. 2014). Launching a robust and specific disease resistance at an optimal time minimizes the potential loss caused by pathogen attack and negative effects due to immunity activation. A positive correlation between host age and disease resistance has been observed in many flowering plants (Develey-Riviere and Galiana 2007; Panter and Jones 2002; Whalen 2005). The term “Age-Related Resistance (ARR)” describes the gain or reinforcement of disease resistance in the process of host maturation. Distinct modes of age-dependent host-microbe interactions are covered under this general term. Some ARR events occur during the transition between stages of shoot development; others may be activated during the maturation of an individual organ (Develey-Riviere and Galiana 2007; Panter and Jones 2002; Whalen 2005). ARR may trigger a broad-spectrum resistance against pathogens from multiple kingdoms, or it may only protect plants against a specific strain/race of a pathogen (Develey-Riviere and Galiana 2007; Panter and Jones 2002; Whalen 2005). Based on the heterogeneity of host species, host age, infected organ and causal pathogens, ARR may also be referred to as “ontogenic resistance”, “developmental resistance”, “mature seedling resistance” and “adult plant

resistance" (Develey-Riviere and Galiana 2007; Panter and Jones 2002; Whalen 2005). The complexity of nomenclature is indicative that there are multiple mechanisms acting behind developmentally acquired defense. While seasonal climate variations associated with plant age and microclimate with individual organs can contribute to acquired defense in mature plants, there is a growing body of evidence demonstrating that ARR is controlled by a sophisticated intrinsic regulatory network that directs plants to adjust their immunity for predictable changes of biotic stress occurring during their life cycles.

ARR is a common defense phenomenon among economically important fruits, vegetables and crops. Practices leveraging the correlation between plant age and defense capacity are routinely adopted in disease management. For example, planting date are often tested to minimize the cost of exposing plants at susceptible age to a certain disease in its peak season (Fry and Apple 1986; GARCIA-RUIZ and MURPHY 2001; Krupinsky et al. 2002). Morphological traits that are characteristic of a developmental stage are used as markers to predict disease incidence (Develey-Riviere and Galiana 2007; Panter and Jones 2002). ARR traits are targets of breeding programs to enhance disease resistance (Huang and Röder 2004; Panter and Jones 2002). Despite the potential value of ARR to agriculture, our knowledge of the molecular mechanisms of ARR are limited. Key questions in need of addressing include the following. What are the reliable molecular markers for predicting the timing of ARR? How do plants integrate developmental timing and defense activation at a molecular level? Do pathogens evolve virulence factors to counteract ARR? If so, how do they suppress ARR? Is

it possible to decouple the pace of developmental progression and the onset of ARR? What are potential tradeoffs caused by precocious activation of ARR? Studying the molecular mechanisms of ARR could be challenging due to complex interactions between environmental conditions, plant physiology and pathogen life cycle. The plasticity of morphological traits under varying environmental conditions (temperature, humidity and UV exposure etc.) complicates the quantification of "plant age". Distinct environmental conditions associated with each developmental stage may influence the outcome of disease resistance in addition to the action of an age-dependent immune response; for many plants, genetic tools are still limited to distinguish age-dependent innate immune response from secondary consequence caused by physiological and morphological changes, such as trichome density, cuticle thickness and leaf curling, associated with developmental transitions. Taking advantage of model pathosystems in which genetic resources are rich and control of growth conditions is feasible, researchers are beginning to understand the components and regulatory cascades of ARR.

An essential parameter of ARR is plant age. However, precisely quantifying plant age is not always straightforward. Plant age may refer to the developmental progression of individual organs (e.g., their size, color and/or shape) known as ontogenesis (Fig.1.1A). Plant organs undergo cell division, cell expansion, differentiation, ripening in the case of fruit, and finally, senescence. Leaves and fruits at early developmental stages are often protected by surrounding structures such as preexisting leaves, sepals or petals, which reduces the risk of pathogen attack. Elevated disease resistance in mature organs could be an adaptive

strategy that minimizes the risk of investment loss (Glander et al. 2018). For example, strawberry fruits and leaves show ontogenic resistance against powdery mildew *Podosphaera aphanis* (Asalf et al. 2014). When inoculated at bloom or green stages, the fruits are susceptible, but full resistance is apparent in white and pink stages of strawberries. When strawberry leaves are inoculated at a late development stage, the pathogen also produce less conidia than at early stage leaves (Asalf et al. 2014). Ontogenesis always occurs in the context of plant maturation. When a leaf or a fruit matures, the whole plant also changes its physiological and chronological age. Inevitably, ontogenic resistance could be influenced by maturation of the whole plant.

In many studies, plant age is defined as chronological age by the exact amount of time post planting or post organogenesis, such as “weeks after planting” or “days after pollination” (Develey-Riviere and Galiana 2007). The timing of ARR activation as well as progression of plant maturation are heavily influenced by environmental conditions. For example, under short day conditions (9 hours of light and 15 hours of darkness), *Arabidopsis thaliana* (hereafter Arabidopsis) gain enhanced resistance against the bacterial pathogen *Pseudomonas syringae* six weeks post germination, while under long day conditions (16 hours of light and 8 hours of darkness), ARR was activated three weeks after germination (Rusterucci et al. 2005). Hence, in complementation to chronological age, measurement of physiological age of a plant is useful in determining the timing of ARR onset.

Physiological age of a plant is defined by the appearance of characteristic morphological and physiological features, such as “flowering stage” or “adult vegetative stage” (Huijser and Schmid 2011; Poethig 2013) (Fig.1.1B). Most flowering plants go through successive developmental transitions in a predictable temporal pattern. The first transition is from the embryonic stage to the juvenile vegetative stage, which is characterized by seed germination. Next, plants grow from the juvenile vegetative stage to the adult vegetative stage, which is associated with heteroblasty, gain of flowering competence, reduction of rooting ability, and alteration of epidermal traits (Poethig 2013). A shoot further enters into reproductive stage that eventually results in inflorescence and floral organs. In many species, the meristem undergoes another change of identity from an inflorescence meristem that generates axillary buds to a floral meristem that generates floral organs (Wagner 2017). ARR is often associated with transitions between these developmental stages. ARR-associated with a transition from the embryonic stage to the juvenile vegetative stage is exemplified by distinct interactions between an oomycete and two *Brassicaceae* species. In the first interaction, cotyledons from Arabidopsis ecotype Col-0 are fully susceptible to downy mildew *Hyaloperonospora arabidopsidis* isolate Emco5, but true leaves exhibit resistance (McDowell et al. 2005). This postembryonic resistance is controlled by a single locus RPP31, although the causal gene is still unknown (McDowell et al. 2005). In the second interaction, *Hyaloperonospora parasitica* is virulent on cotyledons but not the true leaves of two broccoli cultivars (Coelho et al. 2009). Many studies have documented ARR against multiple pathogens after

a transition from the juvenile to the adult vegetative phase. For instance, adult leaves of Arabidopsis are more resistant to fungal (*Sclerotinia sclerotiorum*) and bacterial (*Xanthomonas oryzae* and *Pseudomonas syringae*) pathogens than are juvenile leaves (Xu et al. 2018). In maize, the adult stage is also associated with high resistance to common rust (*Puccinia sorghi*), European corn borer (*Ostrinia nubilalis*) and Southern leaf blight (*Cochliobolus carbonum*) (Abedon and Tracy 1996; Marla et al. 2018). Similarly, floral transition triggers age-dependent resistance. *Nicotiana tabacum* gains resistance to *Phytophthora parasitica* and *Hyaloperonospora tabacina* after switching to the flowering stage (Wyatt and Kuc 1992).

A summary of ARR observations is provided in Table 1.1. Only examples with known candidate causal genes are listed. For a more comprehensive summary of ARR events, please refer to these excellent reviews (Develey-Riviere and Galiana 2007; Panter and Jones 2002; Whalen 2005).

## MOLECULAR CONNECTIONS BETWEEN DEFENSE RESPONSE AND DEVELOPMENTAL TIMING

### ARR associated with organ maturation

Recently, genes and pathways associated with ontogenic resistance are identified by transcriptome analysis in Arabidopsis, apple, strawberry and cucumber (Ando et al. 2015; Gusberti et al. 2013; Mansfeld et al. 2017; Zou et al. 2018). These

studies shed lights on putative signaling cascades integrating developmental timing and the onset of ontogenic resistance. In Arabidopsis, resistance against *Pseudomonas syringae* is established between two- to six-day-old seedlings after germination (Zou et al. 2018). In two-day-old seedlings, high levels of TARGET OF EARLY ACTIVATION TAGGED 1 and 2 (TOE1 and TOE2) proteins suppressed the transcription of *FLAGELLIN-SENSITIVE 2 (FLS2)* by binding to an A/T rich motif in its promoter, named as TOE Binding Site in the FLS2 promoter (TBSF). *FLS2* encodes a leucine-rich repeat serine/threonine protein kinase that acts as a PRR to activate plant immunity after recognizing flagellin (Zipfel et al. 2004). In six-day-old seedlings, increased expression of microRNA172 (miR172) repressed TOE1/2 transcripts, thereby relieving the suppression of *FLS2* by TOE1/2. Hypersensitivity to bacterial elicitor flg22, a 22 amino acids peptide derived from flagellin, was observed in *toe1 toe2* double mutant and in plants overexpressing miR172, confirming their roles in regulating FLS2-mediated PTI. Another PRR, EF-TU RECEPTOR (EFR), which recognizes the bacterial elongation factor EF-Tu, was also suppressed by TOE1/2, suggesting that these two transcription factors regulate PTI triggered by multiple elicitors. Importantly, MIR172 precursors were activated by flg22 treatment. Therefore, the miR172-TOE1/2 module acts as an integrator of environmental and developmental cues to control the onset of PTI during cotyledon ontogenesis (Fig. 1.2A).

The miR172-TOE1/2 module is well documented as a regulator of vegetative phase change and flowering (Zhu and Helliwell 2010). In Zou et al.'s study, miR172 was shown to be induced by flg22 in both two-day-old and eight-week-old plants.

However, no changes of miR172 accumulation was found after flg22 treatment (Li et al. 2010) or *Pseudomonas syringae* infection (Zhang et al. 2011) in previous studies. These studies used four to five-week-old plants, suggesting that the upregulation of miR172 by PAMP is probably age-dependent. Pathogen-induced alteration of miR172 accumulation has been observed in mulberry infected with yellow dwarf disease, grapevine infected with grapevine leafroll disease and rice infected with blast fungus *Magnaporthe oryzae* (Alabi et al. 2012; Gai et al. 2014; Li et al. 2014). Plants used in these studies were beyond the cotyledon stage, so the temporal regulation of miR172 is likely to control ARR associated with different developmental processes. This is further corroborated by a study in *Solanum lycopersicum*, where overexpression of miR172 precursors enhanced resistance to *Phytophthora infestans* at the five-six leaf stage (Luan et al. 2018).

Strengthening physical barriers and chemical defense contribute to ontogenic resistance as well as activation of innate immunity in cucumbers and strawberries (Ando et al. 2015; Gusberti et al. 2013; Mansfeld et al. 2017). Cucumber fruits show ontogenic resistance against the oomycete pathogen, *Phytophthora capsica* (Ando et al. 2015). Young fruits at a rapidly elongating stage were most susceptible, resistance was developed when cucumber reaches maturity. Comparing the transcriptome of peel or exocarp isolated from susceptible (eight days postpollination) and resistance (sixteen days postpollination) fruits revealed candidate genes associated with ARR against *P. capsici* in cucumber (Ando et al. 2015). These genes represent pathways regulating cuticle synthesis, flavonoid biosynthesis, oxidative stress as well as PTI and ETI, suggesting that ARR is

composed of coordinated reinforcement in physical barriers, chemical defense and innate immunity (Ando et al. 2015). In another study, researchers compared the transcriptomic and metabolomic profile of peels from an ARR-capable (Vlaspik) and an ARR-defective (Gy14) cucumber cultivar at susceptible and resistant stages. The most abundant compounds uniquely presented in peel extracts from the ARR-capable cultivar at the resistant age were the terpenoid glycosides (Mansfeld et al. 2017). The role of these compounds in ARR against *P. capsica* is an intriguing question for future research. When comparing the transcriptomes between the young and old apple leaves inoculated with *Venturia inaequalis*, a gene encoding the homologue to Arabidopsis ENHANCED DISEASE SUSEPTIBILITY 1 (EDS1), a positive regulator of basal defense and ETI, was found to be down-regulated in old leaves (Gusberti et al. 2013). In contrast, an EDS1-like gene was preferentially expressed during ontogenic resistance in mature cucumber (Ando et al. 2015). These observations suggest that modulating the EDS1-regulated immune response may serve as a common strategy in ontogenic resistance. Given the distinct developmental and physiological status between exocarps, peels and leaves used in the cucumber and apple studies, it will be intriguing to dissect the shared and tissue-specific components of ontogenic resistance.

**ARR associated with vegetative phase change**

microRNA156/157 (miR156/157) is a conserved master regulator of vegetative phase change (Fouracre and Poethig 2016; He et al. 2018; Poethig 2013). From herbaceous to woody plants, the onset of vegetative phase change is tightly

associated with a reduction of miR156/157 level (Poethig 2013). The mature forms of miR156 and miR157 differ in three nucleotides and have comparable functions in suppressing the expression of SQUAMOSA PROMOTER BINDING PROTEIN-LIKE (SPL) transcription factors (He et al. 2018; Rhoades et al. 2002) . SPL proteins share a highly conserved 76 amino acids SBP box that is involved in both nuclear import and DNA binding (Birkenbihl et al. 2005; Liang et al. 2008). In the juvenile phase, *MIR156/157* genes are expressed at a high level, which suppress the accumulation of *SPL* transcripts and proteins (He et al. 2018; Poethig 2013). The expression of *MIR156/157* is gradually turned off during shoot maturation, allowing accumulated *SPL* proteins to specify adult traits. In both dicots and monocots, overexpression of *MIR156/157* precursors extends the time window to produce juvenile traits, while plants with reduced level or function of miR156/157 and plants expressing the resistant version of *SPL*s (*rSPL*s) to miR156/157 show early phase change (Poethig 2013). In most genomes, miR156/157 targets multiple members in the *SPL* gene family. They have overlapping and distinct functions in controlling a spectrum of morphological and physiological traits (Wang and Wang 2015). The Arabidopsis genome contains 17 *SPL* genes, 11 of them (*SPL2,3,4,5,6,9,10,11,13A/B,15*) are repressed by miR156/157 via mRNA cleavage and/or translational repression (Cardon et al. 1999; Rhoades et al. 2002).

The first genetic evidence linking miR156 levels to ARR comes from resistance of maize to common rust and European corn borer (Abedon and Tracy 1996). MiR156 over-accumulates in the *Corngrass1* (*Cg1*) mutant due to a transposon insertion in the promoter region of zma-miR156b/c locus (Chuck et al. 2007). The

*cg1* mutant extends the period of the susceptibility window as well as other juvenile traits in maize (Abedon and Tracy 1996; Chandler and Tracy 2007). In contrast, knocking down miR156 activity by target mimicry in rice reduced the number of tillers, rate of leaf initiation (Xie et al. 2012) and also enhanced resistance to rice brown planthopper (BPH, *Nilaparvata lugens* Stål) (Ge et al. 2018). However, BPH did not show a clear pattern of preference of plant age within tested cultivars (Baqui and Kershaw 1993), so it is still an open question whether endogenous miR156 contributes to ARR against BPH.

How temporal reduction of miR156/157 during vegetative phase change crosstalks with the plant immune response is revealed via characterizing individual miR156/157-targeted *SPL* genes (Fig. 1.3). In tobacco, NbSPL6 promoted resistance to Tobacco mosaic virus (TMV) by physically interacting with the Toll-interleukin-1 (TIR) type NLR immune receptor, N (Padmanabhan et al. 2013). Such interaction only occurred in the presence of the defense-eliciting TMV-p50-U1 effector. The gene homologue of NbSPL6 in Arabidopsis, AtSPL6, positively regulated race-specific resistance against *Pseudomonas syringae* effector avrRps4. Arabidopsis plants with reduced AtSPL6 by either overexpressing miR156 or RNAi were more susceptible to *Pseudomonas syringae* carrying avrRps4, but not to either avrRpt2 or avrRpm1 effectors (Padmanabhan et al. 2013). Therefore, SPL6 positively regulates a branch of ETI. It is unknown yet whether NtSPL6 contributes to the observed age-related pattern against TMV in tobacco (Ross 1961). Although *AtSPL6* expression is repressed by miR156 (Xu et al. 2016), there is no evidence to suggest that ETI against avrRps4 is age-

dependent. Future work is needed to validate that the temporal expression of SPL6 indeed contributes to age-dependent ETI.

Members of the SPL transcription factor family intersects phytohormone-mediated defense response and temporal expression of miR156. High levels of SPL9 in adult stage of Arabidopsis attenuated Jasmonic acids (JA) response by stabilizing JASMONATE-ZIM-DOMAIN PROTEIN 3 (JAZ3), a suppressor of JA signaling (Mao et al. 2017). Consistently, bioactive jasmonoyl-isoleucine levels and the expression of JA biosynthesis genes were significantly decreased in rice with reduced miR156 activity (Ge et al. 2018). However, Arabidopsis at the adult stage is more resistant to both the lepidopteran generalist *Helicoverpa armigera* and the specialist *Plutella xylostella*, which is contradictory to the observed low JA response in adult tissue (Howe and Jander 2008; Mao et al. 2017). Instead, it was found that importing of glucosinolates from preexisting leaves contributes to the increased insect herbivore resistance in adult plants (Mao et al. 2017). Such elevated resistance was still observed in plants overexpressing miR156 or expressing *rSPL9* (Mao et al. 2017). The authors proposed that constitutive accumulation of defense compounds compensates for the age-related attenuation of JA response (Mao et al. 2017). This proposition partially explains the enhanced resistance to insect herbivory, but the question would be that what is the biological significance of attenuated JA response in the adult plant stage. JA antagonizes salicylic acids (SA)-mediated defense against biotrophic or hemibiotrophic pathogens (Robert-Seilaniantz et al. 2011). It is conceivable that the SPL9-mediated suppression of the JA response may contribute to ARR against

biotrophic or hemibiotrophic pathogens by allowing high amplitude of SA response in the adult stage. Plants that express rSPL9 accumulate high level of ROS and transcribe high level of transcripts of basal SA responsive genes (Yin et al. 2019), but whether these phenotypes are due to a suppression of JA response by SPL9 remains to be tested. In rice, overexpressing *Ideal Plant Architecture 1 (IPA1)/OsSPL14* and *OsSPL7* enhanced resistance to bacterial blight (*Xanthomonas oryzae pv. oryzae*) by reducing the Gibberellin-mediated disease susceptibility (Liu et al. 2019). IPA1 and OsSPL7 both physically interact with and further stabilize SLR1, a DELLA transcriptional repressor of GA signaling (Liu et al. 2019) . Cumulatively, evidence indicates that diversified immune function of individual SPLs translate temporal decrease of miR156 into the coordinated onset of age-related defense during vegetative phase change.

Potential downstream events of miR156/157-controlled ARR is uncovered by comparing the transcriptome of juvenile and adult tissues. Beydler et al. compared the transcriptomes of juvenile and adult leaf primordia from maize and found that SA and JA pathways were up-regulated in juvenile primordia together with genes involved in oxidative stress and retrograde redox signaling (Beydler et al. 2016). This study provided candidate genes important for ARR associated with vegetative phase change in maize. Nevertheless, it should be noted that the comparison was done in leaf primordia in the absence of pathogen attack. It is unclear yet how these differences in gene expression may contribute to ARR against common rust and the European corn borer in mature leaves as documented in (Abedon and Tracy 1996). In Arabidopsis, genes involved in glucosinolate biosynthesis and

metabolism, oxalic acid catabolism, ROS accumulation and systemic acquired resistance (SAR) were differentially expressed in fully expanded juvenile and adult leaves from eight-week-old plants (Xu et al. 2018). Although no pathogen inoculation was used, this study offers a picture of differentiated gene expression in the leaf stage where actual infection occurs. It is noteworthy that a systematic search of miR156 binding sites in grape (*Vitis vinifera*) berries identified a NLR gene as a candidate target of miR156f/g/l (Cui et al. 2018). Thus, the miR156 regulated defense pathway may extend beyond the action of SPLs. It is reasonable to speculate that multiple defense pathways differentially activated in the juvenile and adult stages of plants collectively contribute to the observed broad-spectrum resistance associated with vegetative phase change.

**ARR associated with floral transition**

It has been a long-standing question whether ARR associated with floral induction is merely a physiological consequence of flowering or an independent program. Recent studies using mutants in flowering genes clearly demonstrate that the floral transition is not linked to the onset of ARR (Lyons et al. 2015; Wilson et al. 2013). Photoperiod-induced transient expression of FLOWERING LOCUS T (FT) triggered early flowering in short-day grown Arabidopsis, but the timing of ARR competence against *Pseudomonas syringae* was not affected (Wilson et al. 2013). On the other hand, in late flowering mutant, *constans-9* (*co-9*), ARR response was activated at the same time as in wild type (Wilson et al. 2013). In another case, deleting FLOWERING LOCUS C (FLC) in late flowering mutants accelerated

flowering without altering resistance against *Fusarium oxysporum* (Lyons et al. 2015). Although a positive covariation between immunity-related gene expression and flowering time was observed in a natural population of 138 Arabidopsis accessions from Sweden (Glander et al. 2018), this positive covariation can be genetically separated using a segregating recombinant inbred population (Glander et al. 2018). Taken together, these genetic evidence supports that the molecular programs regulating the timing of ARR onset, and the floral transition are two parallel pathways.

The study of SHORT VEGETATIVE PHASE (SVP)'s function in ARR and floral transition provides an elegant example of how this protein coordinates these two functions (Wilson et al. 2017). SVP represses flowering by integrating vernalization and themo-responsive pathways (Liu et al. 2009). In addition to early flowering, *svp* mutants are defective in ARR activation due to attenuated intercellular SA accumulation in mature plants (Wilson et al. 2013; Wilson et al. 2017). Expressing the *SVP* gene under a meristem specific promoter rescued the flowering time phenotype in *svp* loss-of-function mutant, but not the ARR defects, demonstrating that the leaf pool of SVP protein is responsible for activating defense and ARR is not a secondary physiological consequence of floral induction (Wilson et al. 2017). In leaves, SVP may promote SA accumulation by repressing SUPPRESSOR OF OVEREXPRESSION OF CO 1 (SOC1), a positive regulator of floral induction. SOC1 repressed the promoter activity of *ISOCHORISMATE SYNTHASE 1* (*ICS1*), a key enzyme in SA biosynthesis, and SA accumulation was reduced in a SOC1 gain-of-function mutant (Wilson et al. 2017; Zheng et al. 2015). In addition, SOC1

may also negatively regulate immunity by promoting stomatal opening (Kimura et al. 2015). Stomatal closure is a key defense mechanism in blocking pathogen entrance (Melotto et al. 2006). Constitutively open-stomata were observed in transgenic plants overexpressing SOC1-GFP in guard cells, and light-induced stomatal opening was significantly suppressed in the *soc1* mutant (Kimura et al. 2015). Thus, tissue specific function of SVP and SOC1 may explain how flowering genes regulate the timing of ARR.

*LEAFY* (*LFY*) is another dual regulator of flowering time and defense response (Winter et al. 2011) (Fig. 1.2B). LFY acts as an integrator of signals to promote flowering and also the transition from inflorescence meristem to floral meristem (Moyroud et al. 2010). A genome-wide search revealed that LFY bound to the promoter of *FLS2*, and repressed its activity (Winter et al. 2011). Flg22-triggered callose deposition was suppressed by inducing *LFY* expression in nine-day-old Arabidopsis seedlings (Winter et al. 2011), indicating that LFY directly suppresses PTI output. In addition, cauline leaves from *lfy* mutant were more resistance to *Pseudomonas syringae* (Winter et al. 2011). The authors proposed that LFY redirects plant resources from defense responses to flower and fruit development in order to maximize reproductive fitness (Winter et al. 2011).

Despite the fact that FLS2-mediated PTI is suppressed in cauline leaves due to a high level of LFY (Winter et al. 2011), cauline leaves are still more resistant to *Pseudomonas syringae* than rosette leaves (Xu et al. 2018). A compensatory mechanism must exist to enhance resistance in cauline leaves. Although such a

mechanism has not been discovered, a recent report showed that cauline leaves of Arabidopsis use shedding as a defense mechanism (Patharkar et al. 2017). Arabidopsis cauline leaves shed two days after being infected with *Pseudomonas syringae*, which is suggested to be a defense response to eliminate infected tissue and prevent pathogen spread. Unlike cauline leaves, rosette leaves infected with *Pseudomonas syringae* do not shed (Patharkar et al. 2017). Therefore, shedding is an age-dependent defense response associated with flowering. The shedding of cauline leaves requires genes involved in floral organ abscission and genes involved in SA accumulation and signaling (Patharkar et al. 2017), indicating an integration of a defense signaling pathway (SA response) into a local physiological response (floral organ abscission).

**ARR in successive developmental transitions**

Continuous increase of resistance against a pathogen occur in successive developmental stages throughout shoot maturation (Xu et al. 2018). The adult rosette leaves on Arabidopsis are more resistant to *Pseudomonas syringae* than juvenile leaves, while cauline leaves gain further resistance compared to adult leaves (Xu et al. 2018). Priming of defense by accumulative experience of biotic stresses could be an explanation for the reinforcement of defense in successive stages. However, the newly discovered genetic components of ARR detailed in this review strongly argue that intrinsic signaling cascades in successive developmental stages coordinates those ARR events (Fig. 1.3) As detailed above, the miR172-TOE1/2 module promotes ontogenic resistance in postembryonic

seedlings by regulating *FLS2* expression (Zou et al. 2018). In the transition from the juvenile to the adult vegetative phase, SPL9 (Wu et al. 2009) and SPL15 (Hyun et al. 2016) directly bind to miR172b promoter and activate its expression. It is reasonable to speculate that the *FLS2* promoter is de-repressed during vegetative phase change and flowering due to the reduction of TOE1/2. On the other hand, SPL3 is a direct activator of LFY in the meristem (Yamaguchi et al. 2009), which may lead to a suppression of *FLS2*. Therefore, a signaling relay from miR156 to FLS2 may regulate the age-related change of FLS2-mediated PTI associated with seedling ontogeny, vegetative phase and floral transition. SOC1 is another candidate to relay ARR from the vegetative phase change to the flowering stage. SOC1 suppressed the accumulation of intercellular SA by negatively regulating *ICS1*, which is important for the onset of ARR in Arabidopsis in a time window between five to eight weeks (Wilson et al. 2017). *SOC1* transcription is directly activated by SPL9, so it can potentially relay signals from temporal expression of miR156 to SA accumulation (Wang et al. 2009). SOC1 also forms a protein complex with AGAMOUS-LIKE 24 (AGL24) to activate *LFY* expression (Liu et al. 2008). Therefore, SOC1 may serve as a hub to suppress different aspects of age-dependent defense response by integrating developmental signals.

It should be noted that the speculated signaling relays mentioned above are based on epistasis studies learned from different developmental processes. For example, AGL24 is predominantly expressed in shoot apical meristem (Liu et al. 2008), so it is unclear whether the SOC1-AGL24 interaction can influence defense response

occurring in leaves. Similarly, the activation of *LFY* by SPL3 was only documented in the shoot apical meristem (Yamaguchi et al. 2009), further study is needed to validate the function of SPL3 in defense.

## SUPPRESSION OF ARR BY PATHOGENS

Pathogens have evolved a repertoire of virulence tools including toxins, hormone mimics and effector proteins to attenuate the host immune system or redirect nutrition distribution, which eventually promotes their multiplication. Conceivably, ARR could be a target of these pathogen-derived virulence factors. Pathogen infection can dramatically alter developmental timing of a host. Infection with the bacterial pathogens *Pseudomonas syringae* and *Xanthomonas campestris*, the oomycete pathogen *Peronospora parasitica*, and the root-infecting fungal pathogen *Fusarium oxysporum* accelerated flowering in Arabidopsis (Korves 2003). It is debatable whether this early flowering is a disease symptom caused by stress or a consequence associated with activation of ARR. Recent advances in computational prediction and functional studies on virulence effectors from bacteria, fungi and oomycetes start to reveal how ARR pathways might be manipulated by pathogens.

The effector SAP11 from the phytoplasma strain Aster Yellow Witches' Broom (AY-WB) delayed flowering when heterologously expressed in Arabidopsis, which was correlated with an altered expression of genes controlling flowering and ARR (Chang et al. 2018). For example, miR156 over-accumulated in SAP11 transgenic plants (Chang et al. 2018). It is hypothesized that delayed flowering is beneficial

for phytoplasmas and their insect vectors because it prolongs the susceptible time window for colonization. Alternatively, SAP11 may weaken immunity by manipulating key components required for ARR competence and flowering. Another phytoplasma effector PHYL1 from PnWB may directly or indirectly interfere with the miR396-mediated decay of SVP transcripts (Yang et al. 2015). Transgenic Arabidopsis expressing PHYL1 showed up-regulation of SVP as well as low miR396 level compared to wild type (Yang et al. 2015).

Large scale yeast-two-hybrid experiments have been carried out to identify host proteins that can interact with effectors or candidate effectors from *Pseudomonas syringae*, *H. arabidopsidis* and *Golovinomyces orontii* (Mukhtar et al. 2011; Weßling et al. 2014). In these screens, SOC1 was identified as a target of HaRxL45, a candidate effector from *H. arabidopsidis*. Transgenic Arabidopsis expressing HaRxL45 enhanced the susceptibility to *Pseudomonas syringae* (Fabro et al. 2011). One could speculate that HaRxL45 may have evolved as a virulence factor to suppress the onset or amplitude of ARR by stabilizing SOC1 or promoting its function. TOE2 was also found to interact with multiple effectors from *Pseudonas syringae*, namely avrPto, HopBB1 and HopR1 (Mukhtar et al. 2011). These discoveries open a door to study pathogen manipulation of host ARR.

*Rhodococcus fascians* infection exemplifies how a pathogen interferes with host hormone response to weaken ontogenic resistance. *Rhodococcus fascians* infection causes foliar distortion, witches broom and leaf gall in various plants

(Vereecke et al. 2000). The infected leaves and cotyledons are maintained at a young developmental stage (Depuydt et al. 2009), likely from the effect of cytokinin synthesized by the pathogen (Pertry et al. 2009). Infected cotyledons were shown to be maintained as a sink tissue for pathogen colonization (Dhandapani et al. 2016). It is conceivable that ontogenic resistance is delayed or impaired when the progression of organ maturation is blocked by *Rhodococcus fascians*.

## CONCLUSIONS AND FUTURE DIRECTIONS

Studies in the last decade provide great insights into the molecular mechanisms behind various types of age-dependent defense response. With the identification of key genes and regulatory cascades, we now have tools to decipher this complex phenomenon that integrates environmental cues, host physiology and pathogen life cycle. The newly discovered ARR components can serve as candidate molecular markers of plant age to guide the timing of pesticide application. These ARR genes could also be genetically engineered and used in molecular breeding for broad spectrum disease resistance. Introducing ARR genes into normally incompetent developmental stages can be a strategy to enhance disease resistance with low negative consequence. Some efforts are being made in this direction (Rinaldo et al. 2017).

The molecular links that integrate developmental timing and ARR activation is leading to some important emerging themes in ARR-related research. First, morphological alterations and ARR onset associated with plant maturation is genetically decouplable. This can be achieved by assigning tissue specific development or defense function to a master regulator. Second, ARR involves a collection of developmentally acquired consolidation in disease resistance including physical barriers, chemical defense and innate immunity. Third, ARR components are targeted by pathogen-derived virulence factors to dampen host immunity. Therefore, effectors can be useful probes to dissect the mechanism of ARR.

Exciting discoveries also lead to new challenges. Many ARR genes are conserved regulators of developmental transitions. Defense genes usually undergo fast evolution to escape and combat pathogen targeting. How do plants solve this paradox? Is the defense or development function the more ancient role of these genes? How do plants measure time to activate ARR? Neither the environmental nor the intrinsic cues triggering ARR have been elucidated. Do plants use the same set of signals for developmental transition and ARR, or are there unknown biotic signals to set the timing of ARR? Last but not least, phytohormones are versatile regulators of plant development and defense. How does hormonal crosstalk occur in an age-dependent manner for disease resistance? Dissecting the fundamental mechanisms for crosstalk between development and immunity provides an exciting direction for future research.

## LITERATURE CITED

Abedon, B., and Tracy, W. 1996. Corngrass 1 of Maize (Zea mays L.) delays development of adult plant resistance to common rust (Puccinia sorghi Schw.) and European corn borer (Ostrinia nubilalis Hubner). Journal of heredity 87:219-223.

Alabi, O. J., Zheng, Y., Jagadeeswaran, G., Sunkar, R., and Naidu, R. A. 2012. High-throughput sequence analysis of small RNA s in grapevine (V itis vinifera L.) affected by grapevine leafroll disease. Molecular plant pathology 13:1060-1076.

Ando, K., Carr, K. M., Colle, M., Mansfeld, B. N., and Grumet, R. 2015. Exocarp Properties and Transcriptomic Analysis of Cucumber (Cucumis sativus) Fruit Expressing Age-Related Resistance to Phytophthora capsici. PLoS One 10:e0142133.

Asalf, B., Gadoury, D. M., Tronsmo, A. M., Seem, R. C., Dobson, A., Peres, N. A., and Stensvand, A. 2014. Ontogenic resistance of leaves and fruit, and how leaf folding influences the distribution of powdery mildew on strawberry plants colonized by Podosphaera aphanis. Phytopathology 104:954-963.

Baqui, M., and Kershaw, W. 1993. Effect of plant age on host preference, honeydew production and fecundity of Nilaparvata lugens (Stål)(Hom., Delphacidae) on rice cultivars. Journal of Applied Entomology 116:133-138.

Beydler, B. D., Osadchuk, K., Cheng, C.-L., Manak, J. R., and Irish, E. E. 2016. The juvenile phase of maize sees upregulation of stress-response genes and is extended by exogenous JA. Plant physiology:pp. 01707.02015.

Birkenbihl, R. P., Jach, G., Saedler, H., and Huijser, P. 2005. Functional dissection of the plant-specific SBP-domain: overlap of the DNA-binding and nuclear localization domains. Journal of molecular biology 352:585-596.

Bomblies, K., and Weigel, D. 2007. Hybrid necrosis: autoimmunity as a potential gene-flow barrier in plant species. Nature Reviews Genetics 8:382.

Brown, J. K. 2002. Yield penalties of disease resistance in crops. Current opinion in plant biology 5:339-344.

Cardon, G., Höhmann, S., Klein, J., Nettesheim, K., Saedler, H., and Huijser, P. 1999. Molecular characterisation of the Arabidopsis SBP-box genes. Gene 237:91-104.

Century, K. S., Lagman, R. A., Adkisson, M., Morlan, J., Tobias, R., Schwartz, K., Smith, A., Love, J., Ronald, P. C., and Whalen, M. C. 1999. Developmental control of Xa21-mediated disease resistance in rice. The Plant Journal 20:231-236.

Chandler, M., and Tracy, W. 2007. Vegetative phase change among sweet corn (Zea mays L.) hybrids varying for reaction to common rust (Puccinia sorghi Schw.). Plant breeding 126:569-573.

Chang, S. H., Tan, C. M., Wu, C. T., Lin, T. H., Jiang, S. Y., Liu, R. C., Tsai, M. C., Su, L. W., and Yang, J. Y. 2018. Alterations of plant architecture and phase transition by the phytoplasma virulence factor SAP11. J Exp Bot.

Chuck, G., Cigan, A. M., Saeteurn, K., and Hake, S. 2007. The heterochronic maize mutant Corngrass1 results from overexpression of a tandem microRNA. Nature genetics 39:544.

Coelho, P. S., Valério, L., and Monteiro, A. A. 2009. Leaf position, leaf age and plant age affect the expression of downy mildew resistance in Brassica oleracea. European Journal of Plant Pathology 125:179-188.

Cui, H., Tsuda, K., and Parker, J. E. 2015. Effector-triggered immunity: from pathogen perception to robust defense. Annual review of plant biology 66:487-511.

Cui, M., Wang, C., Zhang, W., Pervaiz, T., Haider, M. S., Tang, W., and Fang, J. 2018. Characterization of Vv-miR156: Vv-SPL pairs involved in the modulation of grape berry development and ripening. Molecular Genetics and Genomics:1-22.

Depuydt, S., De Veylder, L., Holsters, M., and Vereecke, D. 2009. Eternal youth, the fate of developing Arabidopsis leaves upon Rhodococcus fascians infection. Plant physiology 149:1387-1398.

Develey-Riviere, M. P., and Galiana, E. 2007. Resistance to pathogens and host developmental stage: a multifaceted relationship within the plant kingdom. New Phytol 175:405-416.

Dhandapani, P., Song, J., Novak, O., and Jameson, P. E. 2016. Infection by Rhodococcus fascians maintains cotyledons as a sink tissue for the pathogen. Annals of botany 119:841-852.

Fabro, G., Steinbrenner, J., Coates, M., Ishaque, N., Baxter, L., Studholme, D. J., Körner, E., Allen, R. L., Piquerez, S. J., and Rougon-Cardoso, A. 2011. Multiple candidate effectors from the oomycete pathogen Hyaloperonospora arabidopsidis suppress host plant immunity. PLoS pathogens 7:e1002348.

Fouracre, J. P., and Poethig, R. S. 2016. The role of small RNAs in vegetative shoot development. Current opinion in plant biology 29:64-72.

Fry, W., and Apple, A. 1986. Disease management implications of age-related changes in susceptibility of potato foliage toPhytophthora infestans. American Potato Journal 63:47.

Gai, Y.-P., Li, Y.-Q., Guo, F.-Y., Yuan, C.-Z., Mo, Y.-Y., Zhang, H.-L., Wang, H., and Ji, X.-L. 2014. Analysis of phytoplasma-responsive sRNAs provide insight into the pathogenic mechanisms of mulberry yellow dwarf disease. Scientific reports 4:5378.

GARCIA-RUIZ, H., and MURPHY, J. F. 2001. Age-related Resistance in Bell Pepper to Cucumber mosaic virus. Annals of applied biology 139:307-317.

Ge, Y., Han, J., Zhou, G., Xu, Y., Ding, Y., Shi, M., Guo, C., and Wu, G. 2018. Silencing of miR156 confers enhanced resistance to brown planthopper in rice. Planta.

Glander, S., He, F., Schmitz, G., Witten, A., Telschow, A., and de Meaux, J. 2018. Assortment of flowering time and immunity alleles in natural Arabidopsis thaliana populations suggests immunity and vegetative lifespan strategies coevolve. Genome biology and evolution 10:2278-2291.

Gusberti, M., Gessler, C., and Broggini, G. A. 2013. RNA-Seq analysis reveals candidate genes for ontogenic resistance in Malus-Venturia pathosystem. PLoS One 8:e78457.

He, J., Xu, M., Willmann, M. R., McCormick, K., Hu, T., Yang, L., Starker, C. G., Voytas, D. F., Meyers, B. C., and Poethig, R. S. 2018. Threshold-dependent repression of SPL gene expression by miR156/miR157 controls vegetative phase change in Arabidopsis thaliana. PLoS genetics 14:e1007337.

Herrera-Foessel, S. A., Singh, R. P., Lillemo, M., Huerta-Espino, J., Bhavani, S., Singh, S., Lan, C., Calvo-Salazar, V., and Lagudah, E. S. 2014. Lr67/Yr46 confers adult plant resistance to stem rust and powdery mildew in wheat. Theoretical and applied genetics 127:781-789.

Howe, G. A., and Jander, G. 2008. Plant immunity to insect herbivores. Annu. Rev. Plant Biol. 59:41-66.

Huang, X.-Q., and Röder, M. S. 2004. Molecular mapping of powdery mildew resistance genes in wheat: a review. Euphytica 137:203-223.

Huijser, P., and Schmid, M. 2011. The control of developmental phase transitions in plants. Development 138:4117-4129.

Huot, B., Yao, J., Montgomery, B. L., and He, S. Y. 2014. Growth–defense tradeoffs in plants: a balancing act to optimize fitness. Molecular plant 7:1267-1287.

Hyun, Y., Richter, R., Vincent, C., Martinez-Gallegos, R., Porri, A., and Coupland, G. 2016. Multi-layered regulation of SPL15 and cooperation with SOC1 integrate endogenous flowering pathways at the Arabidopsis shoot meristem. Developmental cell 37:254-266.

Jones, J. D., and Dangl, J. L. 2006. The plant immune system. Nature 444:323.

Jones, J. D., Vance, R. E., and Dangl, J. L. 2016. Intracellular innate immune surveillance devices in plants and animals. Science 354:aaf6395.

Kimura, Y., Aoki, S., Ando, E., Kitatsuji, A., Watanabe, A., Ohnishi, M., Takahashi, K., Inoue, S.-i., Nakamichi, N., and Tamada, Y. 2015. A flowering integrator, SOC1, affects stomatal opening in Arabidopsis thaliana. Plant and Cell Physiology 56:640-649.

Korves, T. M. 2003. A Developmental Response to Pathogen Infection in Arabidopsis. Plant Physiology 133:339-347.

Krupinsky, J. M., Bailey, K. L., McMullen, M. P., Gossen, B. D., and Turkington, T. K. 2002. Managing plant disease risk in diversified cropping systems. Agronomy Journal 94:198-209.

Li, Y., Zhang, Q., Zhang, J., Wu, L., Qi, Y., and Zhou, J.-M. 2010. Identification of microRNAs involved in pathogen-associated molecular pattern-triggered plant innate immunity. Plant physiology 152:2222-2231.

Li, Y., Lu, Y.-G., Shi, Y., Wu, L., Xu, Y.-J., Huang, F., Guo, X.-Y., Zhang, Y., Fan, J., and Zhao, J.-Q. 2014. Multiple rice microRNAs are involved in immunity against the blast fungus Magnaporthe oryzae. Plant physiology 164:1077-1092.

Liang, X., Nazarenus, T. J., and Stone, J. M. 2008. Identification of a consensus DNA-binding site for the Arabidopsis thaliana SBP domain transcription factor, AtSPL14, and binding kinetics by surface plasmon resonance. Biochemistry 47:3645-3653.

Liu, C., Thong, Z., and Yu, H. 2009. Coming into bloom: the specification of floral meristems. Development 136:3379-3391.

Liu, C., Chen, H., Er, H. L., Soo, H. M., Kumar, P. P., Han, J.-H., Liou, Y. C., and Yu, H. 2008. Direct interaction of AGL24 and SOC1 integrates flowering signals in Arabidopsis. Development 135:1481-1491.

Liu, M., Shi, Z., Zhang, X., Wang, M., Zhang, L., Zheng, K., Liu, J., Hu, X., Di, C., and Qian, Q. 2019. Inducible overexpression of Ideal Plant Architecture1 improves both yield and disease resistance in rice. Nature plants:1.

Luan, Y., Cui, J., Li, J., Jiang, N., Liu, P., and Meng, J. 2018. Effective enhancement of resistance to Phytophthora infestans by overexpression of miR172a and b in Solanum lycopersicum. Planta 247:127-138.

Lyons, R., Rusu, A., Stiller, J., Powell, J., Manners, J. M., and Kazan, K. 2015. Investigating the association between flowering time and defense in the Arabidopsis thaliana-Fusarium oxysporum interaction. PLoS One 10:e0127699.

Mansfeld, B. N., Colle, M., Kang, Y., Jones, A. D., and Grumet, R. 2017. Transcriptomic and metabolomic analyses of cucumber fruit peels reveal a developmental increase in terpenoid glycosides associated with age-related resistance to Phytophthora capsici. Hortic Res 4:17022.

Mao, Y. B., Liu, Y. Q., Chen, D. Y., Chen, F. Y., Fang, X., Hong, G. J., Wang, L. J., Wang, J. W., and Chen, X. Y. 2017. Jasmonate response decay and defense metabolite accumulation contributes to age-regulated dynamics of plant insect resistance. Nat Commun 8:13925.

Marla, S. R., Chu, K., Chintamanani, S., Multani, D. S., Klempien, A., DeLeon, A., Bong-Suk, K., Dunkle, L. D., Dilkes, B. P., and Johal, G. S. 2018. Adult plant resistance in maize to northern leaf spot is a feature of partial loss-of-function alleles of Hm1. PLoS Pathog 14:e1007356.

McDowell, J. M., Williams, S. G., Funderburg, N. T., Eulgem, T., and Dangl, J. L. 2005. Genetic analysis of developmentally regulated resistance to downy mildew (Hyaloperonospora parasitica) in Arabidopsis thaliana. Molecular Plant-Microbe Interactions 18:1226-1234.

Melotto, M., Underwood, W., Koczan, J., Nomura, K., and He, S. Y. 2006. Plant stomata function in innate immunity against bacterial invasion. Cell 126:969-980.

Moyroud, E., Kusters, E., Monniaux, M., Koes, R., and Parcy, F. 2010. LEAFY blossoms. Trends in plant science 15:346-352.

Mukhtar, M. S., Carvunis, A. R., Dreze, M., Epple, P., Steinbrenner, J., Moore, J., Tasan, M., Galli, M., Hao, T., Nishimura, M. T., Pevzner, S. J., Donovan, S.

E., Ghamsari, L., Santhanam, B., Romero, V., Poulin, M. M., Gebreab, F., Gutierrez, B. J., Tam, S., Monachello, D., Boxem, M., Harbort, C. J., McDonald, N., Gai, L., Chen, H., He, Y., European Union Effectoromics, C., Vandenhaute, J., Roth, F. P., Hill, D. E., Ecker, J. R., Vidal, M., Beynon, J., Braun, P., and Dangl, J. L. 2011. Independently evolved virulence effectors converge onto hubs in a plant immune system network. Science 333:596-601.

Padmanabhan, M. S., Ma, S., Burch-Smith, T. M., Czymmek, K., Huijser, P., and Dinesh-Kumar, S. P. 2013. Novel positive regulatory role for the SPL6 transcription factor in the N TIR-NB-LRR receptor-mediated plant innate immunity. PLoS pathogens 9:e1003235.

Panter, S., and Jones, D. A. 2002. Age-related resistance to plant pathogens.

Panter, S. N., Hammond-Kosack, K. E., Harrison, K., Jones, J. D., and Jones, D. A. 2002. Developmental control of promoter activity is not responsible for mature onset of Cf-9B-mediated resistance to leaf mold in tomato. Molecular plant-microbe interactions 15:1099-1107.

Patharkar, O. R., Gassmann, W., and Walker, J. C. 2017. Leaf shedding as an anti-bacterial defense in Arabidopsis cauline leaves. PLoS genetics 13:e1007132.

Pertry, I., Václavíková, K., Depuydt, S., Galuszka, P., Spíchal, L., Temmerman, W., Stes, E., Schmülling, T., Kakimoto, T., and Van Montagu, M. C. 2009. Identification of Rhodococcus fascians cytokinins and their modus operandi

to reshape the plant. Proceedings of the National Academy of Sciences:pnas. 0811683106.

Poethig, R. S. 2013. Vegetative phase change and shoot maturation in plants. Pages 125-152 in: Current topics in developmental biology, vol. 105. Elsevier.

Rhoades, M. W., Reinhart, B. J., Lim, L. P., Burge, C. B., Bartel, B., and Bartel, D. P. 2002. Prediction of plant microRNA targets. cell 110:513-520.

Rinaldo, A., Gilbert, B., Boni, R., Krattinger, S. G., Singh, D., Park, R. F., Lagudah, E., and Ayliffe, M. 2017. The Lr34 adult plant rust resistance gene provides seedling resistance in durum wheat without senescence. Plant Biotechnol J 15:894-905.

Risk, J. M., Selter, L. L., Krattinger, S. G., Viccars, L. A., Richardson, T. M., Buesing, G., Herren, G., Lagudah, E. S., and Keller, B. 2012. Functional variability of the Lr34 durable resistance gene in transgenic wheat. Plant biotechnology journal 10:477-487.

Robert-Seilaniantz, A., Grant, M., and Jones, J. D. 2011. Hormone crosstalk in plant disease and defense: more than just jasmonate-salicylate antagonism. Annual review of phytopathology 49:317-343.

Ross, A. F. 1961. Systemic acquired resistance induced by localized virus infections in plants. Virology 14:340-358.

Rusterucci, C., Zhao, Z., Haines, K., Mellersh, D., Neumann, M., and Cameron, R. K. 2005. Age-related resistance to Pseudomonas syringae pv. tomato is associated with the transition to flowering in Arabidopsis and is effective

against Peronospora parasitica. Physiological and Molecular Plant Pathology 66:222-231.

Saijo, Y., Loo, E. P. i., and Yasuda, S. 2018. Pattern recognition receptors and signaling in plant–microbe interactions. The Plant Journal 93:592-613.

Saur, I. M., Kadota, Y., Sklenar, J., Holton, N. J., Smakowska, E., Belkhadir, Y., Zipfel, C., and Rathjen, J. P. 2016. NbCSPR underlies age-dependent immune responses to bacterial cold shock protein in Nicotiana benthamiana. Proc Natl Acad Sci U S A 113:3389-3394.

Smakowska, E., Kong, J., Busch, W., and Belkhadir, Y. 2016. Organ-specific regulation of growth-defense tradeoffs by plants. Current opinion in plant biology 29:129-137.

Torres, D. P., Proels, R. K., Schempp, H., and Huckelhoven, R. 2017. Silencing of RBOHF2 Causes Leaf Age-Dependent Accelerated Senescence, Salicylic Acid Accumulation, and Powdery Mildew Resistance in Barley. Mol Plant Microbe Interact 30:906-918.

Toruño, T. Y., Stergiopoulos, I., and Coaker, G. 2016. Plant-pathogen effectors: cellular probes interfering with plant defenses in spatial and temporal manners. Annual review of phytopathology 54:419-441.

Uauy, C., Brevis, J. C., Chen, X., Khan, I., Jackson, L., Chicaiza, O., Distelfeld, A., Fahima, T., and Dubcovsky, J. 2005. High-temperature adult-plant (HTAP) stripe rust resistance gene Yr36 from Triticum turgidum ssp. dicoccoides is closely linked to the grain protein content locus Gpc-B1. Theoretical and Applied Genetics 112:97.

Vereecke, D., Burssens, S., Simón-Mateo, C., Inzé, D., Van Montagu, M., Goethals, K., and Jaziri, M. 2000. The Rhodococcus fascians-plant interaction: morphological traits and biotechnological applications. Planta 210:241-251.

Wagner, D. 2017. Key developmental transitions during flower morphogenesis and their regulation. Current opinion in genetics & development 45:44-50.

Wang, H., and Wang, H. 2015. The miR156/SPL module, a regulatory hub and versatile toolbox, gears up crops for enhanced agronomic traits. Molecular plant 8:677-688.

Wang, J.-W., Czech, B., and Weigel, D. 2009. miR156-regulated SPL transcription factors define an endogenous flowering pathway in Arabidopsis thaliana. Cell 138:738-749.

Weßling, R., Epple, P., Altmann, S., He, Y., Yang, L., Henz, S. R., McDonald, N., Wiley, K., Bader, K. C., and Gläßer, C. 2014. Convergent targeting of a common host protein-network by pathogen effectors from three kingdoms of life. Cell host & microbe 16:364-375.

Whalen, M. C. 2005. Host defence in a developmental context. Mol Plant Pathol 6:347-360.

Wilson, D. C., Carella, P., Isaacs, M., and Cameron, R. K. 2013. The floral transition is not the developmental switch that confers competence for the Arabidopsis age-related resistance response to Pseudomonas syringae pv. tomato. Plant Mol Biol 83:235-246.

Wilson, D. C., Kempthorne, C. J., Carella, P., Liscombe, D. K., and Cameron, R. K. 2017. Age-Related Resistance in Arabidopsis thaliana Involves the MADS-Domain Transcription Factor SHORT VEGETATIVE PHASE and Direct Action of Salicylic Acid on Pseudomonas syringae. Mol Plant Microbe Interact 30:919-929.

Winter, C. M., Austin, R. S., Blanvillain-Baufume, S., Reback, M. A., Monniaux, M., Wu, M. F., Sang, Y., Yamaguchi, A., Yamaguchi, N., Parker, J. E., Parcy, F., Jensen, S. T., Li, H., and Wagner, D. 2011. LEAFY target genes reveal floral regulatory logic, cis motifs, and a link to biotic stimulus response. Dev Cell 20:430-443.

Wu, G., Park, M. Y., Conway, S. R., Wang, J.-W., Weigel, D., and Poethig, R. S. 2009. The sequential action of miR156 and miR172 regulates developmental timing in Arabidopsis. Cell 138:750-759.

Wyatt, S., and Kuc, J. 1992. The effect of leaf age, flowering, and senescence on the resistance of tobacco to blue mold. Phytopathology 80:1000.

Xie, K., Shen, J., Hou, X., Yao, J., Li, X., Xiao, J., and Xiong, L. 2012. Gradual increase of miR156 regulates temporal expression changes of numerous genes during leaf development in rice. Plant physiology:pp. 111.190488.

Xu, M., Hu, T., Zhao, J., Park, M.-Y., Earley, K. W., Wu, G., Yang, L., and Poethig, R. S. 2016. Developmental functions of miR156-regulated SQUAMOSA PROMOTER BINDING PROTEIN-LIKE (SPL) genes in Arabidopsis thaliana. PLoS genetics 12:e1006263.

Xu, Y. P., Lv, L. H., Xu, Y. J., Yang, J., Cao, J. Y., and Cai, X. Z. 2018. Leaf stage-associated resistance is correlated with phytohormones in a pathosystem-dependent manner. J Integr Plant Biol 60:703-722.

Yamaguchi, A., Wu, M.-F., Yang, L., Wu, G., Poethig, R. S., and Wagner, D. 2009. The microRNA-regulated SBP-Box transcription factor SPL3 is a direct upstream activator of LEAFY, FRUITFULL, and APETALA1. Developmental cell 17:268-278.

Yang, C.-Y., Huang, Y.-H., Lin, C.-P., Lin, Y.-Y., Hsu, H.-C., Wang, C.-N., Li-Yu, D. L., Shen, B.-N., and Lin, S.-S. 2015. MiR396-targeted SHORT VEGETATIVE PHASE is required to repress flowering and is related to the development of abnormal flower symptoms by the PHYL1 effector. Plant physiology:pp. 00307.02015.

Yin, H., Hong, G., Li, L., Zhang, X., Kong, Y., Sun, Z., Li, J., Chen, J., and He, Y. 2019. miR156/SPL9 Regulates Reactive Oxygen Species Accumulation and Immune Response in Arabidopsis thaliana. Phytopathology:PHYTO-08-18-0306-R.

Zhang, C., Liu, L., Wang, X., Vossen, J., Li, G., Li, T., Zheng, Z., Gao, J., Guo, Y., and Visser, R. G. 2014. The Ph-3 gene from Solanum pimpinellifolium encodes CC-NBS-LRR protein conferring resistance to Phytophthora infestans. Theoretical and applied genetics 127:1353-1364.

Zhang, W., Gao, S., Zhou, X., Chellappan, P., Chen, Z., Zhou, X., Zhang, X., Fromuth, N., Coutino, G., and Coffey, M. 2011. Bacteria-responsive

microRNAs regulate plant innate immunity by modulating plant hormone networks. Plant molecular biology 75:93-105.

Zheng, X.-y., Zhou, M., Yoo, H., Pruneda-Paz, J. L., Spivey, N. W., Kay, S. A., and Dong, X. 2015. Spatial and temporal regulation of biosynthesis of the plant immune signal salicylic acid. Proceedings of the National Academy of Sciences 112:9166-9173.

Zhu, Q.-H., and Helliwell, C. A. 2010. Regulation of flowering time and floral patterning by miR172. Journal of experimental botany 62:487-495.

Zipfel, C. 2014. Plant pattern-recognition receptors. Trends in immunology 35:345-351.

Zipfel, C., Robatzek, S., Navarro, L., Oakeley, E. J., Jones, J. D., Felix, G., and Boller, T. 2004. Bacterial disease resistance in Arabidopsis through flagellin perception. Nature 428:764.

Zou, Y., Wang, S., Zhou, Y., Bai, J., Huang, G., Liu, X., Zhang, Y., Tang, D., and Lu, D. 2018. Transcriptional Regulation of the Immune Receptor FLS2 Controls the Ontogeny of Plant Innate Immunity. Plant Cell.

Table 1.1 A summary of age-dependent defense responses with candidate genes

| **Host** | **Pathogen** | **Developmental transition** | **Genes involved** | **Reference** |
|---|---|---|---|---|
| maize | common rust and European corn borer | juvenile to adult | corngrassg1 (miR156) | (Abedon and Tracy 1996) |
| | *Cochliobolus carbonum* | juvenile to adult | Hm1 weak allele | (Marla et al. 2018) |
| | | | | |
| rice | *Xanthomonas oryzae* | juvenile to adult | Xa21 | (Century et al. 1999) |
| | | | | |
| Arabidopsis | *Pseudomonas syringae* | adult plant maturation | SVP, SOC1 | (Wilson et al. 2017) |
| | *HyaloPeronospora parasitica* | postembryonic to juvenile | RPP13 | (McDowell et al. 2005) |
| | *Pseudomonas syringae* | ontogenic resistance | miR172, TOE1, TOE2 | (Zou et al. 2018) |
| | insect | juvenile to adult | SPL9 | (Mao et al. 2017) |
| | *Pseudomonas syringae* | vegetative to flowering | HAE, HSL2; IDA, NEV | (Patharkar et al. 2017) |
| | | | | |
| tomato | *Phytophthora infestans* | vegetative to flowering | ph-3 | (Zhang et al. 2014) |
| | *Cladosporium fulvum* | vegetative to flowering | Cf-9B | (Panter et al. 2002) |

| | | | | |
|---|---|---|---|---|
| wheat | rust | adult plant resistance | Lr34 | (Risk et al. 2012); |
| | rust and mildew | adult plant resistance | Lr67 | (Herrera-Foessel et al. 2014) |
| | *P. striiformis f. sp. Tritici* | adult plant resistance | Yr36 | (Uauy et al. 2005) |
| | | | | |
| *Nicotiana Benthamiana* | *Pseudomonas syringae* | vegetative to flowering | NbCSPR | (Saur et al. 2016) |
| | | | | |
| Barley | powdery mildew | adult plant resistance | HvRBOHF2 | (Torres et al. 2017) |

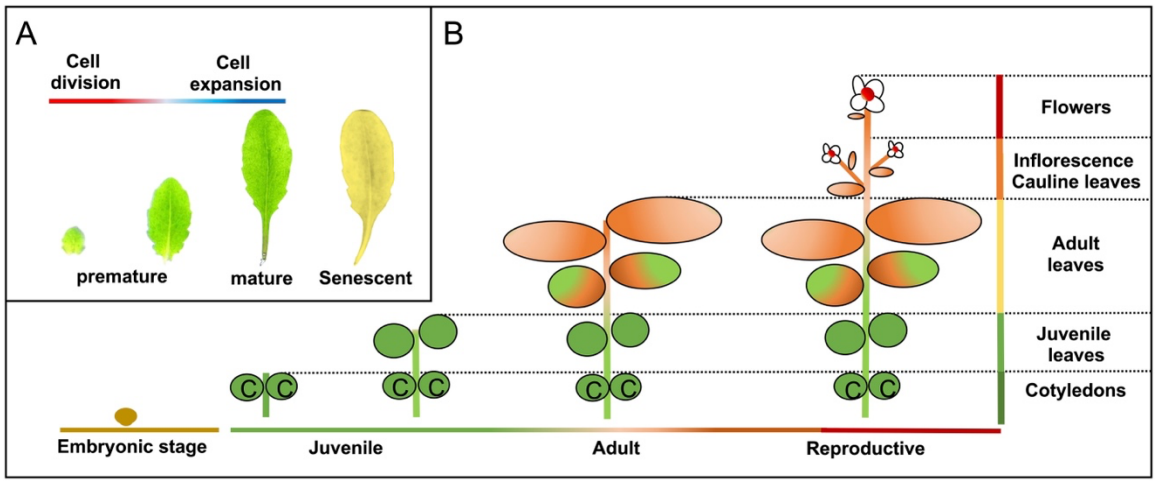


FIGURE 1.1 Diagram of organ maturation and successive developmental stages of a plant. A. Leaf maturation in Arabidopsis. B. The progression of shoot maturation. Capitalized “C” refers to cotyledon. Mature organs color-coded in orange. Dash lines point plant organs that is corresponding to labels below the dash lines.

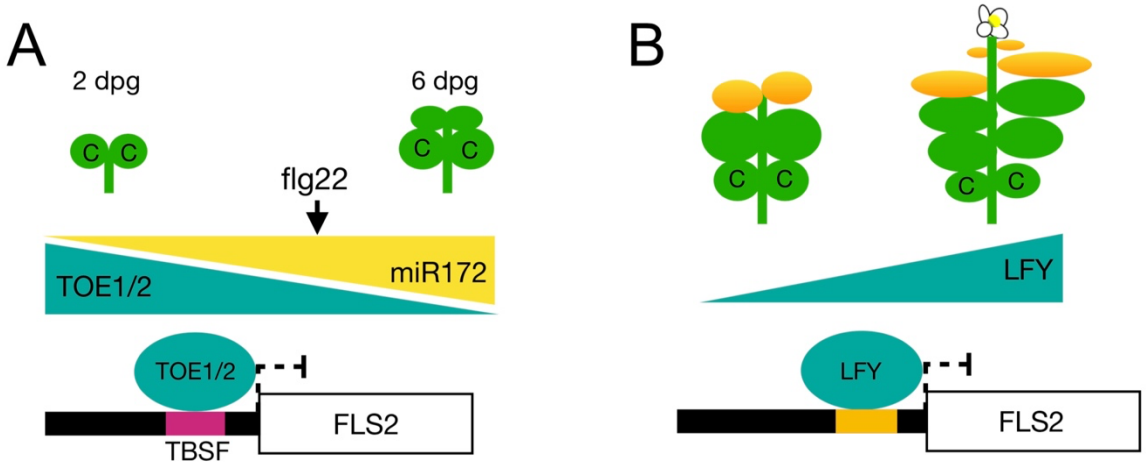


FIGURE 1.2 Age-dependent regulation of FLAGELLIN-SENSITIVE 2 (FLS2)-mediated PTI during plant maturation.

A. Onset of FLS2-mediated PTI during cotyledon maturation. Triangle bars indicate gene expression level. TOE1/2 binding motif upstream of *FLS2* promoter region is highlighted in magenta.

B. Suppression of *FLS2* expression by LFY in floral transition. LFY binding motif upstream of *FLS2* promoter is highlighted in orange.

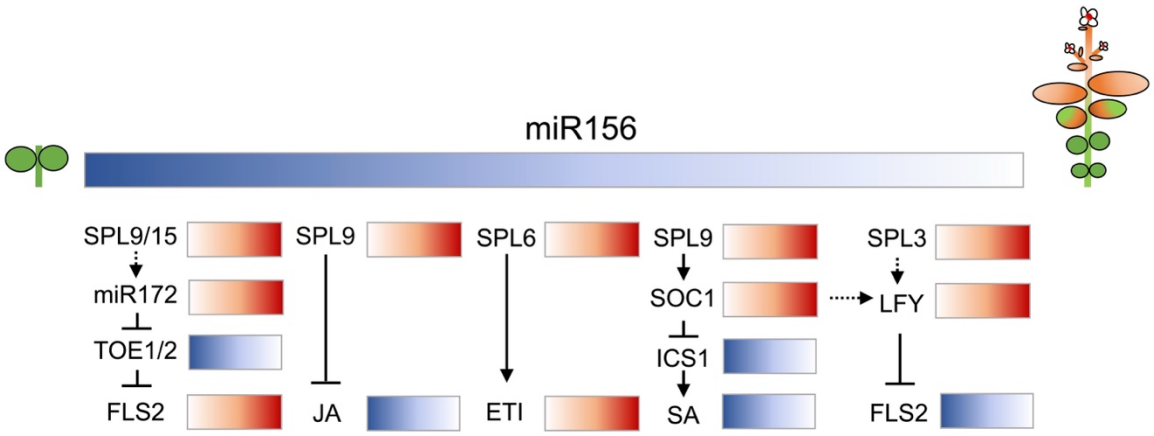


FIGURE 1.3 A hypothetical signaling relay in coordinating age-dependent defense responses associated with successive developmental stages. Color gradient indicates gene expression pattern from high (dark) to low (light). Temporally decreased genes are labeled in blue; temporally increased genes are labeled in red. Dashed arrows indicate that the genetic interactions have not been demonstrated in the ARR context.

# CHAPTER 2

# DISTINCT FUNCTION OF SPL GENES IN AGE-RELATED RESISTANCE IN ARABIDOPSIS.

Reproduced, by permission, from Hu, L., Peng Q., Peper A., Kong F., Yao Y., Yang Li. 2023. *Distinct function of SPL genes in age-related resistance in Arabidopsis*. *PLoS Pathogens*.

**ABSTRACT**

In plants, age-related resistance (ARR) refers to a gain of disease resistance during shoot or organ maturation. ARR associated with vegetative phase change, a transition from juvenile to adult stage, is a widespread agronomic trait affecting resistance against multiple pathogens. How innate immunity in a plant is differentially regulated during successive stages of shoot maturation is unclear. In this work, we found that *Arabidopsis thaliana* showed ARR against its bacterial pathogen *Pseudomonas syringae pv. tomato* DC3000 during vegetative phase change. The timing of the ARR activation was associated with a temporal drop of miR156 level. The microRNA miR156 maintains juvenile phase by inhibiting the accumulation and translation of *SPL* transcripts. A systematic inspection of the loss- and gain-of-function mutants of 11 *SPL* genes revealed that a subset of *SPL* genes, notably *SPL2*, *SPL10*, and *SPL11,* activated ARR in adult stage. The immune function of SPL10 was independent of its role in morphogenesis. Furthermore, the SPL10 mediated an age-dependent augmentation of the salicylic acid (SA) pathway partially by direct activation of *PAD4*. Disrupting SA biosynthesis or signaling abolished the ARR against *Pto* DC3000. Our work demonstrated that the miR156-SPL10 module in *Arabidopsis* is deployed to operate immune outputs over developmental timing.

## INTRODUCTION

Both animals and plants suffer from infectious diseases, particularly at a young age [1, 2]. The function of their immune systems can be enhanced with the progression of organismal maturation. In many plant species, a gain of disease resistance against certain pathogens during shoot maturation is termed age-related resistance (ARR). Plant ARR can launch robust and wide spectrum resistance against a variety of pathogens, and such trait is often selected in breeding [3].

Age-associated disease resistance is often coupled with successive developmental transitions, such as germination, [4] vegetative phase change [5] and flowering [6, 7]. The heterogeneity of host age, maturing stage of infected organs and virulence of causal pathogens suggest that multiple layers of signaling are intertwined between aging and immunity [3, 8]. ARR-associated juvenile-to-adult vegetative phase change (hereafter $ARR_{VPC}$) has been observed among economically important vegetables, crops and fruits, such as tomato, rice and grapevine [9]. The juvenile and adult phases refer to vegetative development prior to floral induction, and predicable changes of morphological and physiological traits are associated with this transition [10-12]. Several factors were speculated to impact $ARR_{VPC}$. Compared to juveniles, adult plants are exposed to environmental conditions that are not optimal for disease development (such as high UV) [2]; adult tissues may carry tough physical barriers (e.g., cell wall components, cuticle) [13]; and leaves of adult stage are

primed by previous exposure to pathogens [2]. Such factors complicate the investigation of intrinsic molecular mechanisms governing the onset of $ARR_{VPC}$. Nevertheless, accumulating evidence suggests that intrinsic signaling pathways govern ARR [3, 14].

MicroRNA156s (miR156), a conserved microRNA family [10], regulates the onset of vegetative phase change [10, 15]. MiR156 targets genes encoding SPLs (SQUAMOSA PROMOTER BINDING PROTEIN-LIKE) transcription factors, which contains a SQUAMOSA promoter binding protein (SBP) box for nuclear import and DNA binding [16-18]. In *Arabidopsis*, leaves generated in the juvenile shoot, e.g., juvenile leaves (usually leaves 1-4 under a short-day condition) accumulate high level of miR156 [19, 20]. Throughout the expansion of juvenile leaves, they maintain the morphological (e.g., no abaxial trichome) and molecular identities (e.g., high miR156 level) of the juvenile fate. A temporal decline of miR156 level, followed by the high expression of *SPL*s, initiates the vegetative phase change [18-21]. SPLs have overlapping yet distinct functions to promote adult traits such as adult leaf morphogenesis, floral induction, and reduced rooting [22-24]. A total of 11 *SPL* genes encoded in *Arabidopsis* Columbia-0 (Col-0) ecotype are suppressed by miR156 via mRNA cleavage and/or translational repression [18, 25]. Recent studies showed that the miR156-SPL pathway involved in plant immunity. Disrupting miR156 function in *Arabidopsis* by mutating SQUINT (SQN), an *Arabidopsis* orthologue of cyclophilin 40, compromised jasmonic acid signaling and disease resistance against

necrotrophic pathogen *Botrytis cinerea* [26]. Furthermore, overexpressing miR156-targeted *SPL9* in juvenile plants enhanced accumulation of reactive oxygen species and induced salicylic acid (SA) signaling, leading to enhanced resistance of *Arabidopsis* against bacterial pathogen *Pseudomonas syringae* [27]. Yet, a systematic dissection of the link between ARR and miR156-SPL signaling pathway is still lacking.

Here, we systemically analyzed the miR156-SPLs module in $ARR_{VPC}$. We demonstrated that the ARR to *Pseudomonas syringae pv. tomato* DC3000 (*Pto* DC3000) in *Arabidopsis* is associated with vegetative phase change. Altering the temporal expression of miR156-SPL pathway was sufficient to change the timing of $ARR_{VPC}$ onset. A sub-class of SPL transcription factors (SPL2/10/11) promoted disease resistance in adult stage, and such function was independent of their roles in leaf morphology. Transcriptomic analysis unveiled multiple mechanisms that collectively contribute to $ARR_{VPC}$, including priming, activating adult-specific defense programs, and strengthening juvenile defense after infection. Finally, we found SPL10 strengthened SA signaling in the adult stage by directly enhancing the transcription of PAD4. Our work provides molecular insights into the intrinsic clock that coordinates disease resistance outcomes with developmental timing.

## MATERIALS AND METHODS

### Plant material and growth conditions

*Arabidopsis* wild type, transgenic lines and mutants used in this study were in a Columbia-0 (Col-0) genetic background unless mentioned otherwise. The genetic cross of *MIM156/sid2-1* and *r10/eds1.2* were generated from this research and progenies from F3 or F4 generation were used for phenotypic test. Information for mutants and transgenic lines can be found in Table 2.1. Juvenile leaves were fully expanded leaves 1-2, or 3-4 from soil-grown 4- or 5-week-old plants. Adult leaves were fully expanded leaves that derived from 7-week-old plants. The adult phase of a leaf was confirmed by appearance of abaxial trichomes [40]. Plants were sown on Fafard #3 Mix propagation soil. The planted seeds were then placed under 4 °C for 2 days and transferred to a growth room under 23 °C/19 °C day/night and with 45% humidity. Nine hours light and 15 hours dark photoperiod with 180 μmol $m^{-2}s^{-1}$ was used as short-day condition. Lighting was made through a 5:3 combination of white (USHIO F32T8/741) and red-enriched (interlectric F32/T8/WS Gro-Lite) fluorescent lights. Plant age was counted from the first day when seeds transferred to the growth room. Only plants used for Figure 5E were grown on ½ MS plates in 24h with continuous light.

## Sampling strategy for studying $ARR_{VPC}$

In our short-day growth condition, plants produced 50-60 leaves before bolting. The ontogenic age of a leaf influenced defense gene expression (Figure 1- figure supplement 1A). To minimize the influence of ontogenic age of individual leaves (Figure 1- figure supplement 1B), we measured the expansion rate of juvenile and adult leaves and harvested fully expanded juvenile and adult leaves from plants of different ages (Figure 1- figure supplement 1C). Fully expanded leaves 1-4 derived from a 4- to 5-weeks old plants were sampled as juvenile leaves; fully expanded leaves (range from 8-13 depending on variations in plants) from 7-weeks old plants were sampled as adult leaves. Adult leaves showed characteristic abaxial trichome(s), blade serration and elongated petiole [20]. Plants for adult samples were planted 2-3 weeks earlier than those for juvenile leaves. Juvenile and adult samples were collected at the same time for disease assay and transcriptome analysis.

## Bacterial growth assay

*Pto* DC3000 strain was grown under 28°C on King's B solid medium (40 g/L proteose, 20 g/L glycerol and 15 g/L agar). The medium contained rifamycin for selection and cycloheximide to inhibit fungi growth. Glycerol stock of the bacterial strains stored under -80°C. Bacterial stock was streaked on plate for a 2-day growth and was re-streaked one day before inoculation. For infiltration, bacteria were collected from the plate and suspended in 10 mM $MgCl_2$ solution. Bacterial

suspension with concentration of 1 x $10^5$ CFU/mL was infiltrated in *Arabidopsis* leaves with a needless syringe. After inoculation, plants were covered by transparent lids for one hour. Day 0 samples were collected immediately after removing lids. Each sample contained four leaf discs that were derived from four individual leaves. Leaf samples were collected using the corer (the same size for all plants) and ground with homogenizer (OMNI International) and diluted serially. KB plates with 10 µL of bacteria suspension per sample were placed under room temperature for 2 days. Colony forming units were counted manually and normalized according to inside area of the corer. Day 2 samples were collected as described above two days post-infiltration (dpi). The method was modified from Holt *et al.* [60].

**RNA sequencing and analysis**

*Pto* DC3000 (1 x $10^8$ CFU/mL suspended in 10mM $MgCl_2$) was infiltrated into juvenile and adult of wild type (Col-0) leaves and leaves 1-2 from *rSPL10* plants, as described above in the bacterial growth assay. 10 mM $MgCl_2$ was used as the mock treatment. Three hours after inoculation, 20 leaf discs with comparable size from 5-10 individual plants were cored and collected as one biological repeat per genotype per treatment. Three biological repeats were prepared for each genotype/treatment. For RNA isolation, plant tissues were flash-frozen in liquid nitrogen and then ground to fine powders using homogenizer (OMNI International). Total RNAs were extracted using E.Z.N.A. Total RNA kit (Omega BIO-TEK). RNA quality was assessed with a 2100 Bioanalyzer instrument

(Agilent, RIN score ≥ 7, 28S/18S ≥ 1). RNA concentration was measured using a Nanodrop spectrophotometer (Thermo Scientific, RNA concentration ≥ 50 ng/μL, 260/280 ~2.0). RNA samples were sequenced at BGI San Jose lab. Oligo dT based mRNA enrichment was followed by random N6 primer based reverse transcription. The synthesized DNA nanoballs were then sent for strand-specific mRNA sequencing (PE100) on a DNA Nanoball Sequencing (DNBseq) platform. The data was filtered using SOAPnuke software in BGI. ~48 M clean reads with average Q30 ≥ 88.81% per sample were obtained.

Files of RNA-seq raw reads together with processed data were uploaded to NCBI with access No. GSE208657. The clean RNA-seq data were aligned against the TAIR10 reference genome using HiSAT2 (v.2.1.0, [61]) with following parameters, hisat2 -p 4 -x TAIR10indexed -1 sample_strand1.fq.gz -2 sample_strand2.fq.gz -S aligned_sample.sam. The aligned reads were assembled into transcripts according to the TAIR10 annotation [62, 63] using Stringtie [64]. ~ 99% overall alignment rate was reached for each sample. Differential expression analysis was done by comparing transcript levels between pairwise normalized samples using DEseq2 package in R (LFC ≥ ±0.58, padj ≤ 0.05) [65]. Gene ontology was analyzed first against the whole *Arabidopsis* genome at TAIR Gene Ontology terms website, http://geneontology.org/ [66], and which was then confirmed using total detected 22,622 (covers 88.7% of known genes in *Arabidopsis* genome) genes of the RNA-seq results on agriGO website http://systemsbiology.cau.edu.cn/agriGOv2/# [67]. Figures were

generated in R, with ComplexHeatmap package that was specifically used for Figure 3 B-D and 4 [68].

**Motif discovery and enrichment analysis**

The de novo motif discovery analysis was carried on the website (https://www.arabidopsis.org/tools/bulk/motiffinder/index.jsp). Frequencies of 6-mer motifs were compared between 1000 bp upstream sequences of each input gene and the current *Arabidopsis* genomic sequence set (33518 sequences). A total of 15 motifs containing the consensus SPL binding site, GTAC, were identified. A frequency-based sequence logo was generated through the weblogo, (https://weblogo.berkeley.edu/logo.cgi). To assess the enrichment of experimentally validated TF binding sites, we used the SEA (https://meme-suite.org/meme/tools/sea). 1000 bp upstream sequences of the 203 Adu/*r10* co-upregulated DEGs (Figure 6 A) were extracted from TAIR. Shuffled input sequences were chosen as control sequences. The DAP motif database [46] were selected to identify the enriched motifs.

**qRT-PCR**

Bacterial suspension with 1 x $10^8$ CFU/mL was infiltrated in *Arabidopsis* leaves. Leaf samples were harvested at 3 hours hpi. Each sample had 16-20 leaf discs derived from 6-10 individual plants. The leaf age of plants in soil was measured following the same standard as the above. For plants on ½ MS plates, 15-20

leaves were harvested per genotype per treatment as one biological rep. leaves 8-13 from 45-day-old of Col-0 with abaxial trichomes were used as adult leaves, leaves 1-2 from 18-day-old Col-0 were used as juvenile leaves. In comparison, leaves 1-2 from 21-day-old of *rSPL10* were used. For each bio-rep, three to six technical replicates were used in one qPCR run. RNA extraction was performed using Omega biotek EZNA plant RNA kit. The qPCR was performed in the Applied Biosystems QuantStudio 1 Real-Time PCR system with SYBR Green master mix (Applied Biosystems). PCR conditions were set as follows: 95°C for 5 mins, 40 cycles of 95°C for 15s, 56°C for 30s and 72°C for 20-30s. *SAND* (*AT2G28390*) or *TUB2* (*AT5G62690*) was used as reference genes. The relative expression was calculated using relative standard curve methods. Delta-delta CT was also used for calculation when knowing that the PCR efficiency for the primers was at least more than 95% in previous standard curve results. The oligonucleotides used here can be found in Table S1.

**Estradiol-induced gene expression**

The estradiol-inducible *MIM156* and *rSPL3* was constructed using a Gateway compatible version of the XVE system, as described by Brand et al., [69]. The *MIM156* and *rSPL3* sequence were cloned into pMDC160. Transgenic plants were crossed to plants containing pMDC150-35S [69] and generated homozygous. The estradiol-inducible *rSPL10* was generated by cloning *rSPL10* into a modified pMDC7 vector tagged with Citrine and HA.

**HPLC-MS**

Ten (experimental replicate 1) or sixty (experimental replicate 2) leaves 1-2 of Col-0 and *r10* each and three adult Col-0 leaves (plants sawn in soil) were collected as one biological repeat for each genotype or a developmental stage. 3 to 6 biological replicates from five and six (for juvenile and adult tissues in experimental replicate 1), or thirty and six (for juvenile and adult tissues in experimental replicate 2) individual plants were collected in total. The leaves were then lyophilized, powdered, and weighted for getting a comparable dry weight for all samples (weighting error $\leq$ 0.1 mg). Metabolites from 1.5 mg or 8.5 mg (in separate experimental repeats) of dry tissue of each biological replicate were extracted and were detected under Liquid chromatography-mass spectrometry (HPLC-MS). Samples were added into 200 µL of prechilled metabolite extraction buffer, which consist of 1:1 methanol:chloroform (v/v) supplemented with $^{13}C_6$-cinnamic acid, $D_5$-benzoic acid, and resorcinol as internal standards [70]. Sonication of the samples took 30 min within an ice-chilled water bath. Then, adding 100 µL of high-performance (HPLC)-grade water, vortexing for 30 sec and centrifuging for 5 min to extract the aqueous phase of each sample, which was transferred to a new tube and stored at -80ºC until analysis. Reverse-phase high-performance liquid chromatography-mass spectrometry (HPLC-MS) was used to detect Free SA and SA-conjugates [70]. Amount of salicylic acid beta-glucoside (SAG) and salicylic acid (SA) were measured and calculated in the unit of nmole metabolite per gram of dry weight (nmole/g DW).

**ChIP-qPCR assay**

The procedure and the preparation of reagents were modified from protocols [71-73] . In brief, 1 gram of non-treated fully expanded adult leaf tissues were collected from the pro*SPL10::rSPL10-YFP* line. Leaves from 2-3 plants were harvested as one biological sample. Three biological replicates in total from two independent experiments were used. The tissue was crosslinked, and the chromatin was extracted and sonicated using nuclei extraction buffers and a bioruptor UCD-200 with chilling pump. 15 µL of post-sonicating chromatin solution was saved as the input. The remaining chromatin solution was immunoprecipitated by using GFP-trap Magnetic Agarose (ChromoTek, cat no. gtma). Diluted input and DNA eluted after IP were used for qPCR using primers designed for probing the indicated positions (Figure 6B; Table S1). We used the following formula to calculate the estimated CT value for adjusting CT values of input and IP samples, DCt [normalized ChIP] = (Ct [Input] – Log2 (dilution factor for Input)) – ((Ct [ChIP] – Log2 (dilution factor for ChIP)), and the final output % input = 100 * 2 ^ (DCt [normalized ChIP] [73].

**GUS staining assay**

Plants carrying pro*PR2*::GUS were harvested at six week after planting. The GUS solution was prepared as following and was vacuum infiltrated into plants, 0.1 M $NaPO_4$, pH 7.0, 10 mM EDTA. 0.1% Triton X-100, 1 mM $K_3Fe(CN)_6$, 2 mM X-Gluc (X-Gluc was dissolved in N ,N-DMF and made fresh). After 24 h incubation at 37°C, the staining solution was replaced with 70% ethanol. Tissues were washed several times with 70% ethanol until the chlorophyll in leaves was cleared. The GUS-stained leaves were imaged using a dissecting microscope (VWR).

**RESULTS**

**The age-related resistance to *Pto* DC3000 is associated with a reduction of miR156 level.**

To assess the $ARR_{VPC}$, we measured the multiplication of *Pto* DC3000 in juvenile (without abaxial trichomes) and adult (with abaxial trichomes) leaves of *Arabidopsis thaliana* Col-0 ecotype. During the expansion of an individual leaf,

defense genes are differentially expressed (Figure 2.1; Figure 2.8 A-B), which is known as ontogenic resistance [4, 28-31]. Ontogenic resistance occurs during the maturation of both juvenile and adult leaves (Figure 2.1; Figure 2.8 C). Because juvenile leaves are produced in early shoot development, juvenile and adult leaves on a same plant are always at different ontogenic age (Figure 2.1, Figure 2.8 C and 2.8 E). To avoid the impact of ontogenic resistance, we sampled fully expanded juvenile leaves (leaves 1-4) from 4- to 5-week-old plants and adult leaves (leaves 8) from 7-week-old plants, respectively. To avoid the influence of flowering-associated ARR [32, 33], plants were grown in a short-day condition and bolting was not observed before 10 weeks after planting. Bacterial multiplication in leaves 8 was lower than that in leaves 1, 2, 3 and 4 (Figure 2.1A, 2.1B). No significant differences were observed between leaves 1-2 and 3-4 (Figure 2.1 B). We concluded that the increased resistance to *Pto* DC3000 was associated with vegetative phase change in Col-0.

Since miR156 level in fully expanded leaves drops from the juvenile to adult transition [34], we hypothesized that a high level of miR156 suppresses immunity in juvenile stage. We compared bacterial growth in adult leaves (leaves ≥ 8) from Col-0 and leaves at the same position from transgenic plants overexpressing *MIR156A* under a constitutive 35S promoter from TMV (*35S::MIR156A*). Expressing *MIR156A* in adult leaves led to accelerated production of juvenile leaves, marking the prolonged juvenile phase as previously reported [19, 20]

(Figure 2.1 C). Interestingly, it also led to an increase in bacterial growth when compared with leaves at the same position in Col-0 (Figure 2.1 D). Consistently, knocking down miR156 activity by a target mimicry, 35S::*MIMICRY156* [35] (*MIM156*) displayed enhanced disease resistance (Figure 2.1 E, 2.1 F). These evidences suggests that high accumulation of miR156 suppresses resistance to *Pto* DC3000 in the juvenile phase.

**miR156-regulated SPL10 promotes ARR in adult phase.**

To test which miR156-targeted *SPL* contributes to $ARR_{VPC}$, we first screened disease phenotype in the gain-of-function mutants carrying miR156-resistant *SPL* genes (*rSPLs*, Figure 2.2A). We examined the disease phenotype in juvenile leaves expressing individual *rSPL* gene from 9 out of 11 members under its own native promoter [23]. Low levels of endogenous *SPL* transcripts in juvenile leaves provided a sensitized background to test the function of *rSPLs*. We found that leaves 1-2 from *rSPL2*, *10*, *9* and *13* showed increasing resistance compared to wild type, but *rSPL3*, *4*, *6*, *11* and *15* did not change resistance to *Pto* DC3000 (Figure 2.2A; Figure 2.9). Thus, a subset of miR156-regulated SPLs was sufficient to enhance immunity in juveniles.

To check the necessity of SPLs in adult conferred immunity, we tested disease phenotypes in adult leaves with loss of function *spl* combinatorial mutants based on amino acid sequence similarity (Figure 2.2 A; Figure 2.9). There are 5

phylogenic clades for miR156-targeted *SPL* genes, *SPL3/4/5*, *SPL6*, *SPL2/10/11*, *SPL9/15*, and *SPL13A/13B* (Figure 2A) [25, 36]. In Col-0 background, *SPL10* and *SPL11* (78% amino acid identity) reside in a 1.6 kb tandem duplication [25]. S*pl2/10/11* showed enhanced susceptibility to *Pto* DC3000 (Figure 2.2 A). While the phenotypes of *spl2 and spl10* single mutants were wild type-like, *spl10/11* mildly reduced disease resistance, indicating that *SPL2, 10* and *11* redundantly contributed to immunity in adult leaves. Importantly, although *rSPL10* carried a higher resistance than wild type in juvenile leaves (Figure 2.2 A, 2.2 B), the difference between the two genotypes was much smaller in the adult stage (Figure 2.2 B), supporting that SPL10 enhanced resistance is age dependent. *Spl3*/*4*/*5* triple or *spl6* single mutations did not alter resistance to *Pto* DC3000 (Figure 2.2 A). The lack of disease phenotypes against *Pto* DC3000 in the gain- and loss-of-function mutants of *SPL6* is consistent with a previous report [37]. *rSPL9* enhanced resistance, but the *spl9/15* double mutant displayed unstable phenotypes, which may be resulted from redundancy among other SPL members (Figure 2.2 A). Altogether, the data confirmed the specialized function of SPLs in $ARR_{VPC}$.

To further determine whether the disease phenotypes of *SPL10* mutants were pleiotropic effects caused by SPL10-mediated leaf morphogenesis, we assayed bacteria multiplication in transgenic plants expressing either estradiol inducible *rSPL3*, *rSPL10* or *MIM156* (Figure 2.2 C). Transgenic plants growing on ½ MS medium supplemented with estradiol showed typically early phase change phenotypes, indicating that the transgenes were functional [23, 38]. In line with

the data above (Figure 2 A), applying estradiol 12 hrs before inoculation suppressed bacterial multiplication in juvenile leaves of inducible *rSPL10* and inducible *MIM156* lines, but not for that from inducible *rSPL3* plants (Figure 2.2 D). Notably, the leaf morphology was comparable between wild type and estradiol induced plants (Figure 2.2 C), indicating that miR156-SPL10 controlled disease resistance and leaf morphology can be decoupled.

**The basal expression of defense genes is high in the adult stage.**

To explore the transcriptional signature of $ARR_{VPC}$, we performed RNA sequencing to compare juvenile (leaves 1-2) and adult (leaves ≥ 8) transcriptomes at 3 hours after mock treatment or *Pto* DC3000 infection (Figure 2.3 A). An early time point was chosen because change of chromatin accessibility could be detected at 3 hrs post *Pto* infection [39]. Under mock treatment, we identified 2002 and 2320 genes that were respectively up- or down-regulated in adult leaves compared with juvenile leaves, hereafter $Adu_{no\ infection\ (nof)}$ (LFC = 0.58, padj < 0.05) (Figure 2.3 B; Figure 2.10 C, 2.10 D). As expected, *SPL3/4/5* were up-regulated in adult samples. In addition, the Gene Ontology (GO) enrichment analysis revealed that vegetative phase change related GOs, such as adaxial/abaxial axis specification [40] were enriched in the $Adu_{nof}$ DEGs (Figure 2.3 D), confirming that our juvenile and adult samples represented two distinct developmental phases (Figure 2.3; Figure 2.10 A and

2.10 B). Intriguingly, we observed that immunity related GOs were also enriched in the up-regulated $Adu_{nof}$ DEGs, including defense response to bacterium/fungus and response to SA (Figure 2.3 D). Here, jasmonic acid (JA) signaling-mediated defense was downregulated, coinciding with the antagonistic interaction between JA and SA in plant immunity [41]. The enrichment of pro-defense genes in up-regulated $Adu_{nof}$ indicated that adult plants had primed defense signaling.

For defense induction state, we investigated genes that were differentially induced/suppressed by infection in juvenile and adult stages. *Pto* treatment triggered 3027 and 4728 DEGs in juvenile and adult leaves, respectively (Figure 2.10 C and 2.10 D). Among the 2163 *Pto*-triggered DEGs shared between juvenile and adult leaves (2163 = 239+1924 in Figure 2.3 C; Figure 2.10 C and 2.10 D), the shared up-regulated DEGs were enriched with well-characterized defense responses such as respiratory burst, defense response to bacterium and response to salicylic acid (Figure 2.3 D). Meanwhile, photosynthesis and light harvesting signaling pathways were enriched in down-regulated DEGs, indicating that a pathogen-induced transcriptomic reprogramming switched from development to defense regardless of plant age (Figure 2.3 D). A total of 864 DEGs were only induced/repressed by *Pto* in the juvenile stage, and there are 2565 DEGs were adult-specific (Figure 2.3 C). Cutin biosynthetic and wax biosynthetic processes were enriched in adult-specific *Pto*-induced DEGs,

consistent with a previously suggested consolidation of constitutive defense in ARR [42].

Among genes that were specifically induced by *Pto* in the adult stage but not the juvenile stage, a portion of them did not eventually have higher transcription level when we compared infected adult and juvenile leaves (red bar only, Figure 2.3 C). It is arguable whether inducibility of a gene alone contributes to ARR. So, we further searched for genes whose absolute expression levels were different between juvenile and adult leaves after *Pto* DC3000 treatment (hereafter $Adu_{pto}$). Genes that were specifically induced/repressed by infection in the adult stage count for 20.6% (934 out of 4528) of the $Adu_{pto}$ (red bar/black bar, Figure 2.3 C). There, cellular response to hypoxia, defense response to bacterium and response to heat were over-represented, indicating an age-dependent *Pto* response that may cope with abiotic stresses (Figure 2.3 D). A 5.3% (239 out of 4528) of $Adu_{pto}$ were also triggered by *Pto* in the juvenile stage, but the amplitude of change was preferentially higher in the adult stage (Figure 2.3 C). Thus, $ARR_{VPC}$ strengthened a sector of juvenile-defense regulon as well as activated adult-specific defense genes. In addition, 38% (1722 out of 4528) of $Adu_{pto}$ were not *Pto*-triggered but already had differential expression between juvenile and adult leaves before infection (Figure 2.3 B). Of the 38%, GOs pertaining to defense, such as SA signaling, together with adult-related developmental pathways were enriched (Figure 2.3 D). Finally, 20.1% $Adu_{Pto}$ (910 out of 4528) was not induced either by infection or age alone. These DEGs could be resulted

from a synergistic interaction between age and infection (Figure 2.3; Figure 2.10 C). Taken together, we discovered that ARR transcriptome changes could contribute to the elevation of defense signaling at non-infected state, the adult-specific inducible defense as well as the strengthened juvenile defense.

**Overexpressing SPL10 recapitulates the ARR transcriptomic landscape in juvenile leaves.**

To delineate the contribution of SPL10 to ARR at the transcriptomic level, we investigated the *rSPL10 (r10)* induced DEGs at non-infected and *Pto*-infected states (Figure 2.3 A). A total of 3211 genes (1859 up-regulated and 1352 down-regulated) were differentially expressed in leaves 1-2 between Col-0 and *r10* at non-infected state ($r10_{nof}$). Out of 3211 genes, 1316 of them overlapped with $Adu_{nof}$ (Figure 2.4 A). A 936 of the 1316 $r10_{nof}$ were co-regulated in adult leaves in the same trend, attributing to 21.7% (936/4322) of the $Adu_{nof}$, being consistent with the function of SPL10 in specifying adult fate (Figure 2.4 A). GO terms associated with immune signaling including systemic acquired resistance were enriched in the 936 co-upregulated DEGs between $r10_{nof}$ and $Adu_{nof}$ (Adu/$r10_{nof}$) (Figure 2.4 C). After bacterial infection, we identified 2621 DEGs between leaves 1&2 from *r10* and Col-0. Out of 2621 DEGs, 1006 of them overlapped to $Adu_{pto}$ (Figure 2.4 B), with 604 out of the 1006 were co-regulated in the same trend, occupying 13.3% (604/4528) of total $Adu_{pto}$ (Figure 2.4 B). Defense-related GOs were enriched in those co-regulated DEGs (Figure 2.4 C). The observations support that SPL10 activated a sector of adult immune response to *Pto* DC3000.

**Disrupting SA signaling compromised the SPL10-mediated ARR.**

Since SA-related GO terms were enriched in the co-upregulated Adu/*r10*$_{nof}$ (Figure 2.4 C), we first measured the age- and SPL10- effects on SA signaling. We assembled a core SA regulon by overlapping DEGs induced by SA and its synthetic inducer benzothiadiazole (BTH) [43, 44] (Figure 2.5 A). 81.3% of the core SA regulon (527 activated and 239 repressed genes) were detected in the gene count matrix generated from a combination of all our RNA sequencing samples. SA-activated (199/527) and -repressed (50/239) markers were enriched in Adu$_{nof}$ (Figure 2.5 B). SA-activated genes were also enriched in *r10*$_{nof}$ (Figure 2.5 B), denoting that SPL10 contributed to enhancing SA signaling in the adult phase. Consistently, accumulation of Salicylic acid beta-glucoside (SAG) (an inactive SA form, stored in vacuole) was higher in adult than that in juvenile leaves (Figure 2.5 C). The accumulation of free SA showed a similar trend (Figure 2.5 C). Next, we sought to validate whether elevated SA response in adult phase depended on the temporal expression of *SPL10*. We selected four age-dependent SA-activated genes, *AT3G60470, BG3, ATLTP4.4* and *PR5* (Fig 5B). Their expressions were compromised in the adult leaves of *spl2/10/11* (Figure 2.5 D). Noticeably, the upregulation of the four SA responsive genes were also observed in adult or *r10* leaves when plants were grown on sterile plates (Figure 2.5 E). In conclusion, the age-related increase of SA response in leaves required *SPL10* and was not primed by pre-exposure to microbes. The

EDS1-PAD4 protein complex is essential for SA-mediated defense signaling [45]. We found that both genes were upregulated in adults and *r10* (Figure 2.4 A). Furthermore, a significant overlap was found between the EDS1-PAD4 core regulon (EP-core, [45] and genes co-upregulated by adults and *r10* (Figure 2.5 F), implying that the EDS1-PAD4 mediated SA signaling pathway could be differentially activated in juvenile and adult stage due to the temporal expression of SPL10.

Out of the 936 DEGs co-regulated by adult stage and *rSPL10* (Figure 2.4 A), 400 of them were associated with SPL10-binding sites identified in a ChIP-seq experiment of SPL10 by Ye *et al* (Figure 2.6 A) [24], indicating that these genes are likely direct targets of SPL10. A de novo motif discovery algorism identified potential SPL-binding sites in 203 of the co-up-regulated DEGs (Figure 2.6 A), but not in the 197 down-regulated genes. In addition, experimentally validated SPL TF binding sites [46] were enriched in the promoter of the 203 genes (Figure 2.6; Figure 2.11). Interestingly, the promoter region and gene body of *PAD4* contains two potential SPL10-binding GTAC-containing motifs (Figure 2.6 B) [24]. We generated a genomic reporter line of SPL10 (*proSPL10::rSPL10-YFP*). The transgenic line showed similar early phase change phenotypes observed in the *proSPL10::rSPL10-GUS* line, indicating that the fusion had a normal SPL10 function (Figure 2.6-Figure 2.11). Using ChIP-qPCR, we validated that the motif 1 (M1, 186-182 bp away from the TSS), but not motif 2 was associated with SPL10 at uninfected state (Figure 2.6 B). Furthermore, the transcript level of *PAD4* was

reduced only in the *spl2/10/11* adult leaves but not in the juvenile leaves (Figure 2.6 C), indicating that the temporal expression of *PAD4* depends on SPL10. Taken together, these observations suggest that SPL10 directly promotes *PAD4* expression in the adult stage.

To probe the genetic interactions of SA signaling and the miR156-SPL10 mediated ARR, we first tested the $ARR_{VPC}$ phenotype in the mutant of *SALICYLIC ACID INDUCTION DEFICIENT 2* (*sid2-1*, defective in pathogen-induced SA biosynthesis) and *NONEXPRESSER OF PR GENES 1* (*npr1-1*, defective in SA perception) mutants. Neither of those mutants altered the timing of vegetative phase change. As expected, both mutants in adult stage were more susceptible than Col-0 (Figure 2.7 A). The difference of bacterial growth between wild type and the mutants in juvenile stage was less pronounced (Figure 2.7 A), in agreement with the age-dependency of SA-mediated disease resistance. We then introduced *sid2-1* mutation into *MIM156* background (Figure 2.7 and ; Figure 2.12). Although precocious morphological traits were shared between *MIM156* and *MIM156/sid2-1*, the bacteria level in *MIM156/sid2-1* phenocopied that of *sid2-1* (Figure 2.7 B), suggesting that *SID2* acts downstream of miR156. Similarly, loss of function mutation of *EDS1* reversed the enhanced disease resistance phenotype in *r10* plants (Figure 2.7 C; Figure 2.12). The leaf morphology phenotype of *r10* plants was not changed by *eds1.2*, which further confirmed that age-associated leaf morphology and disease resistance can be decoupled (Figure 7C). Consistent with the molecular evidence that SPL10 binds to the promoter of *PAD4*, the $ARR_{VPC}$ phenotype was compromised in *pad4-1*

and *eds1.2* mutant (Figure 2.7 D). In essence, miR156-SPL10 promoted resistance through *SID2* and *EDS1-PAD4*-dependent SA signaling.

## DISCUSSION

In this research, we uncovered an ARR mechanism regulated by the miR156-SPL pathway, linking immune maturation to an intrinsic aging mechanism (Figure 2.13). In plants, ARR occurs during predicable developmental transitions that are often accompanied by morphological changes. Our research provides a potential mechanism for the temporally coordinated change of immunity and morphogenesis, where the same molecular clock, miR156, controls different *SPL* genes to specify immune and developmental traits. For instance, SPL2/10/11, but not SPL3/4/5/6, are required for resistance against *Pto* DC3000 (Figure 2.2 A). Interestingly, NbSPL6 is required in the N-mediated TMV resistance in tobacco [37]. The homologue of *NbSPL6* in *Arabidopsis*, *AtSPL6*, is necessary to the full ETI response triggered by *Pseudomonas syringae* effector AvrRps4, but not basal resistance to *Pto* DC3000 [37] (Figure 2.2 A). It is possible that the broad spectrum of resistance associated with ARR requires multiple SPL family members to activate different defense pathways. As rSPL10 only influenced 21.7% of $Adu_{nof}$ and 13.3% of $Adu_{pto,}$ other SPLs may contribute to the rest of adult defense to *Pto* and/or to other pathogens (Figure 2.4 A and 2.4 B). Alternatively, the coordinated maturation of development and immune system may be achieved by functional switch of the same SPL protein. In rice

plants, *Ideal plant architecture 1* (*IPA1*)/*OsSPL14* increases panicle size [47]. *IPA1* binds to an alternative cis-regulatory element to activate defense when challenged by the bacterial pathogen *Xanthomonas oryzae pv. Oryzae* (*Xoo*) [48]. In *Nicotiana benthamiana* and tomato plants, temporal reduction of miR6019/6020 allows its target, *N* gene, to mediate age-dependent resistance to tobacco mosaic virus (TMV) [49]. The temporal expression pattern of miR6019/6020 mimics that of miR156 in tobacco. It would be interesting to explore the genetic relationship between those two miRNAs in regulating ARR.

We showed that defense GO terms were enriched in up-regulated *rSPL10*$_{nof}$ and Adu$_{nof}$. Among those, components of SA pathway, such as *SID2* and *NPR1* were required for ARR$_{VPC}$ (Figure 2.6). We observed the up-regulation of SA response accompanied by a reduction of JA response in both Col-0 adults and the *rSPL10* line (Figure 2.3 and 2.4). JA and SA often act antagonistically to fine-tune immune response to multiple pathogens. Our ARR transcriptome results showed that the antagonism also occurred in an age-dependent manner (Fig 2.3 C). Upregulation of SA production and response have also been observed during vegetative-floral transition in both tomato and tobacco plants [50]. In *Arabidopsis*, *SVP* and *SOC1* genes regulating floral induction also transcriptionally promote age-dependent increase of SA, independent from flowering traits [32, 51]. We did not observe differential expression of *SVP* or *SOC1* in juvenile *vs* adult transcriptome, suggesting the *SVP-SOC1* module may not act in the ARR$_{VPC}$ of

*Arabidopsis*. On the other hand, we found that $ARR_{VPC}$ was *NPR1*-dependent (Figure 2.6 A), which is different from an age- and SA-associated but *NPR1*-independent gain of resistance observed before [52]. It is likely that there are parallel aging pathways strengthen SA signaling during plant maturation.

In co-upregulated Adu/$r10_{pto}$ DEGs, we noticed that cellular response to hypoxia was enriched (Figure 2.4 D). Response to hypoxia of plants has been reported for counteracting submergence and waterlogging stress [53]. Respiratory burst, as part of immune responses, is oxygen dependent. At the site of *Botrytis cinerea* infection, hypoxic response was induced, leading to the stabilization of subgroup VII of ETHYLENE RESPONSE FACTOR (ERF-VII) [54]. Members in the ERF-VII can activate defense gene as well as hypoxic response [54]. SPL10 may upregulate genes that react to low-oxygen environment when reactive oxygen species accumulates or respiration increases. How hypoxia response contributes to ARR against biotrophs and necrotrophs remains to be seen.

## LITERATURE CITED

1. Solana R, Pawelec G, Tarazona R.(2006). Aging and innate immunity. Immunity.24(5):491-4.

2. Develey-Rivière MP, Galiana E.(2007). Resistance to pathogens and host developmental stage: a multifaceted relationship within the plant kingdom. New Phytologist.175(3):405-16.

3. Hu L, Yang L.(2019). Time to fight: Molecular mechanisms of age-related resistance. Phytopathology.109(9):1500-8.

4. Zou Y, Wang S, Zhou Y, Bai J, Huang G, Liu X, et al.(2018). Transcriptional regulation of the immune receptor FLS2 controls the ontogeny of plant innate immunity. The Plant Cell. 30(11):2779-94.

5. Chandler M, Tracy W.(2007). Vegetative phase change among sweet corn (Zea mays L.) hybrids varying for reaction to common rust (Puccinia sorghi Schw.). Plant breeding.126(6):569-73.

6. Rusterucci C, Zhao Z, Haines K, Mellersh D, Neumann M, Cameron R.(2005). Age-related resistance to Pseudomonas syringae pv. tomato is associated with the transition to flowering in Arabidopsis and is effective against Peronospora parasitica. Physiological and molecular plant pathology.66(6):222-31.

7. Glander S, He F, Schmitz G, Witten A, Telschow A, de Meaux J.(2018). Assortment of flowering time and immunity alleles in natural Arabidopsis thaliana

populations suggests immunity and vegetative lifespan strategies coevolve. Genome biology and evolution.10(9):2278-91.

8. Paludan SR, Pradeu T, Masters SL, Mogensen TH.(2021). Constitutive immune mechanisms: mediators of host defence and immune regulation. Nat Rev Immunol.21(3):137-50. Epub 20200811. doi: 10.1038/s41577-020-0391-5. PubMed PMID: 32782357; PubMed Central PMCID: PMCPMC7418297.

9. Panter S, Jones DA.(2002). Age-related resistance to plant pathogens.

10. Poethig RS. Vegetative phase change and shoot maturation in plants. Current topics in developmental biology. 105: Elsevier; 2013. p. 125-52.

11. Brink RA.(1962). Phase change in higher plants and somatic cell heredity. The Quarterly Review of Biology.37(1):1-22.

12. Poethig RS.(1990). Phase change and the regulation of shoot morphogenesis in plants. Science.250(4983):923-30. Epub 1990/11/16. doi: 10.1126/science.250.4983.923. PubMed PMID: 17746915.

13. Alzohairy SA, Hammerschmidt R, Hausbeck MK.(2020). Changes in winter squash fruit exocarp structure associated with age-related resistance to Phytophthora capsici. Phytopathology.110(2):447-55.

14. Carella P, Wilson DC, Cameron RK.(2015). Some things get better with age: differences in salicylic acid accumulation and defense signaling in young and mature Arabidopsis. Frontiers in plant science.5:775.

15. Wang J-W, Park MY, Wang L-J, Koo Y, Chen X-Y, Weigel D, et al.(2011). miRNA control of vegetative phase change in trees. PLoS Genet.7(2):e1002012.

Epub 2011/03/09. doi: 10.1371/journal.pgen.1002012. PubMed PMID: 21383862; PubMed Central PMCID: PMCPMC3044678.

16. Birkenbihl RP, Jach G, Saedler H, Huijser P.(2005). Functional dissection of the plant-specific SBP-domain: overlap of the DNA-binding and nuclear localization domains. Journal of molecular biology.352(3):585-96.

17. Liang X, Nazarenus TJ, Stone JM.(2008). Identification of a consensus DNA-binding site for the Arabidopsis thaliana SBP domain transcription factor, AtSPL14, and binding kinetics by surface plasmon resonance. Biochemistry.47(12):3645-53.

18. Rhoades MW, Reinhart BJ, Lim LP, Burge CB, Bartel B, Bartel DP.(2002). Prediction of plant microRNA targets. Cell.110(4):513-20. Epub 2002/08/31. PubMed PMID: 12202040.

19. Wu G, Poethig RS.(2006). Temporal regulation of shoot development in Arabidopsis thaliana by miR156 and its target SPL3. Development.133(18):3539-47. Epub 2006/08/18. doi: 10.1242/dev.02521. PubMed PMID: 16914499; PubMed Central PMCID: PMCPMC1610107.

20. Wu G, Park MY, Conway SR, Wang J-W, Weigel D, Poethig RS.(2009). The sequential action of miR156 and miR172 regulates developmental timing in Arabidopsis. Cell.138(4):750-9.

21. Gandikota M, Birkenbihl RP, Höhmann S, Cardon GH, Saedler H, Huijser P.(2007). The miRNA156/157 recognition element in the 3′ UTR of the Arabidopsis SBP box gene SPL3 prevents early flowering by translational inhibition in seedlings. The Plant Journal.49(4):683-93.

22. Wang H, Wang H.(2015). The miR156/SPL module, a regulatory hub and versatile toolbox, gears up crops for enhanced agronomic traits. Molecular plant.8(5):677-88.

23. Xu M, Hu T, Zhao J, Park M-Y, Earley KW, Wu G, et al.(2016). Developmental functions of miR156-regulated SQUAMOSA PROMOTER BINDING PROTEIN-LIKE (SPL) genes in Arabidopsis thaliana. PLoS genetics.12(8):e1006263.

24. Ye B-B, Shang G-D, Pan Y, Xu Z-G, Zhou C-M, Mao Y-B, et al.(2020). AP2/ERF transcription factors integrate age and wound signals for root regeneration. The Plant Cell.32(1):226-41.

25. Cardon G, Höhmann S, Klein J, Nettesheim K, Saedler H, Huijser P.(1999). Molecular characterisation of the Arabidopsis SBP-box genes. Gene.237(1):91-104.

26. Sun T, Zhou Q, Zhou Z, Song Y, Li Y, Wang H-B, et al.(2022). SQUINT Positively Regulates Resistance to the Pathogen Botrytis cinerea via miR156–SPL9 Module in Arabidopsis. Plant and Cell Physiology.

27. Yin H, Hong G, Li L, Zhang X, Kong Y, Sun Z, et al.(2019). miR156/SPL9 Regulates Reactive Oxygen Species Accumulation and Immune Response in Arabidopsis thaliana. Phytopathology.PHYTO-08-18-0306-R.

28. Berens ML, Wolinska KW, Spaepen S, Ziegler J, Nobori T, Nair A, et al.(2019). Balancing trade-offs between biotic and abiotic stress responses through leaf age-dependent variation in stress hormone cross-talk. Proc Natl Acad

Sci U S A.116(6):2364-73. Epub 20190123. doi: 10.1073/pnas.1817233116. PubMed PMID: 30674663; PubMed Central PMCID: PMCPMC6369802.

29. Kanojia A, Gupta S, Benina M, Fernie AR, Mueller-Roeber B, Gechev T, et al.(2020). Developmentally controlled changes during Arabidopsis leaf development indicate causes for loss of stress tolerance with age. Journal of experimental botany.71(20):6340-54.

30. Mansfeld BN, Colle M, Kang Y, Jones AD, Grumet R.(2017). Transcriptomic and metabolomic analyses of cucumber fruit peels reveal a developmental increase in terpenoid glycosides associated with age-related resistance to Phytophthora capsici. Hortic Res.4:17022. Epub 2017/06/06. doi: 10.1038/hortres.2017.22. PubMed PMID: 28580151; PubMed Central PMCID: PMCPMC5442961.

31. Mansfeld BN, Colle M, Zhang C, Lin Y-C, Grumet R.(2020). Developmentally regulated activation of defense allows for rapid inhibition of infection in age-related resistance to Phytophthora capsici in cucumber fruit. BMC genomics.21(1):1-25.

32. Wilson DC, Carella P, Isaacs M, Cameron RK.(2013). The floral transition is not the developmental switch that confers competence for the Arabidopsis age-related resistance response to Pseudomonas syringae pv. tomato. Plant Mol Biol.83(3):235-46. Epub 2013/06/01. doi: 10.1007/s11103-013-0083-7. PubMed PMID: 23722504; PubMed Central PMCID: PMCPMC3777159.

33. Carviel JL, Al-Daoud F, Neumann M, Mohammad A, Provart NJ, Moeder W, et al.(2009). Forward and reverse genetics to identify genes involved in the age-

related resistance response in Arabidopsis thaliana. Mol Plant Pathol.10(5):621-34. Epub 2009/08/22. doi: 10.1111/j.1364-3703.2009.00557.x. PubMed PMID: 19694953.

34. He J, Xu M, Willmann MR, McCormick K, Hu T, Yang L, et al.(2018). Threshold-dependent repression of SPL gene expression by miR156/miR157 controls vegetative phase change in Arabidopsis thaliana. PLoS Genet.14(4):e1007337. Epub 2018/04/20. doi: 10.1371/journal.pgen.1007337. PubMed PMID: 29672610; PubMed Central PMCID: PMCPMC5929574.

35. Franco-Zorrilla JM, Valli A, Todesco M, Mateos I, Puga MI, Rubio-Somoza I, et al.(2007). Target mimicry provides a new mechanism for regulation of microRNA activity. Nature genetics.39(8):1033.

36. Guo A-Y, Zhu Q-H, Gu X, Ge S, Yang J, Luo J.(2008). Genome-wide identification and evolutionary analysis of the plant specific SBP-box transcription factor family. Gene.418(1-2):1-8.

37. Padmanabhan MS, Ma S, Burch-Smith TM, Czymmek K, Huijser P, Dinesh-Kumar SP.(2013). Novel positive regulatory role for the SPL6 transcription factor in the N TIR-NB-LRR receptor-mediated plant innate immunity. PLoS pathogens.9(3):e1003235.

38. Yamaguchi A, Wu M-F, Yang L, Wu G, Poethig RS, Wagner D.(2009). The microRNA-regulated SBP-Box transcription factor SPL3 is a direct upstream activator of LEAFY, FRUITFULL, and APETALA1. Developmental cell.17(2):268-78.

39. Ding P, Sakai T, Krishna Shrestha R, Manosalva Perez N, Guo W, Ngou BPM, et al.(2021). Chromatin accessibility landscapes activated by cell-surface and intracellular immune receptors. Journal of Experimental Botany.72(22):7927-41.

40. Telfer A, Bollman KM, Poethig RS.(1997). Phase change and the regulation of trichome distribution in Arabidopsis thaliana. Development.124(3):645-54. Epub 1997/02/01. PubMed PMID: 9043079.

41. Thaler JS, Humphrey PT, Whiteman NK.(2012). Evolution of jasmonate and salicylate signal crosstalk. Trends in plant science.17(5):260-70.

42. Ando K, Carr KM, Colle M, Mansfeld BN, Grumet R.(2015). Exocarp Properties and Transcriptomic Analysis of Cucumber (Cucumis sativus) Fruit Expressing Age-Related Resistance to Phytophthora capsici. PLoS One.10(11):e0142133. Epub 2015/11/04. doi: 10.1371/journal.pone.0142133. PubMed PMID: 26528543; PubMed Central PMCID: PMCPMC4631441.

43. Yang L, Teixeira PJPL, Biswas S, Finkel OM, He Y, Salas-Gonzalez I, et al.(2017). Pseudomonas syringae Type III Effector HopBB1 Promotes Host Transcriptional Repressor Degradation to Regulate Phytohormone Responses and Virulence. Cell Host Microbe.21(2):156-68. Epub 2017/01/31. doi: 10.1016/j.chom.2017.01.003. PubMed PMID: 28132837; PubMed Central PMCID: PMCPMC5314207.

44. Ding Y, Sun T, Ao K, Peng Y, Zhang Y, Li X, et al.(2018). Opposite roles of salicylic acid receptors NPR1 and NPR3/NPR4 in transcriptional regulation of plant immunity. Cell.173(6):1454-67. e15.

45. Cui H, Gobbato E, Kracher B, Qiu J, Bautor J, Parker JE.(2017). A core function of EDS1 with PAD4 is to protect the salicylic acid defense sector in Arabidopsis immunity. New Phytologist.213(4):1802-17.

46. O'Malley RC, Huang S-sC, Song L, Lewsey MG, Bartlett A, Nery JR, et al.(2016). Cistrome and epicistrome features shape the regulatory DNA landscape. Cell.165(5):1280-92.

47. Liu M, Shi Z, Zhang X, Wang M, Zhang L, Zheng K, et al.(2019). Inducible overexpression of Ideal Plant Architecture1 improves both yield and disease resistance in rice. Nature plants.1.

48. Wang J, Zhou L, Shi H, Chern M, Yu H, Yi H, et al.(2018). A single transcription factor promotes both yield and immunity in rice. Science.361(6406):1026-8.

49. Deng Y, Wang J, Tung J, Liu D, Zhou Y, He S, et al.(2018). A role for small RNA in regulating innate immunity during plant growth. PLoS pathogens.14(1):e1006756.

50. Yalpani N, Shulaev V, Raskin I.(1993). Endogenous salicylic acid levels correlate with accumulation of pathogenesis-related proteins and virus resistance in tobacco. Phytopathology.83(7):702-8.

51. Wilson DC, Kempthorne CJ, Carella P, Liscombe DK, Cameron RK.(2017). Age-Related Resistance in Arabidopsis thaliana Involves the MADS-Domain Transcription Factor SHORT VEGETATIVE PHASE and Direct Action of Salicylic Acid on Pseudomonas syringae. Mol Plant Microbe Interact.30(11):919-29. Epub 2017/08/17. doi: 10.1094/MPMI-07-17-0172-R. PubMed PMID: 28812948.

52. Kus JV, Zaton K, Sarkar R, Cameron RK.(2002). Age-related resistance in Arabidopsis is a developmentally regulated defense response to Pseudomonas syringae. The Plant Cell.14(2):479-90.

53. Fukao T, Barrera-Figueroa BE, Juntawong P, Pena-Castro JM.(2019). Submergence and Waterlogging Stress in Plants: A Review Highlighting Research Opportunities and Understudied Aspects. Front Plant Sci.10:340. Epub 20190322. doi: 10.3389/fpls.2019.00340. PubMed PMID: 30967888; PubMed Central PMCID: PMCPMC6439527.

54. Valeri MC, Novi G, Weits DA, Mensuali A, Perata P, Loreti E.(2021). Botrytis cinerea induces local hypoxia in Arabidopsis leaves. New Phytol.229(1):173-85. Epub 20200406. doi: 10.1111/nph.16513. PubMed PMID: 32124454; PubMed Central PMCID: PMCPMC7754360.

60. Holt BF, 3rd, Belkhadir Y, Dangl JL.(2005). Antagonistic control of disease resistance protein stability in the plant immune system. Science.309(5736):929-32. Epub 20050623. doi: 10.1126/science.1109977. PubMed PMID: 15976272.

61. Kim D, Paggi JM, Park C, Bennett C, Salzberg SL.(2019). Graph-based genome alignment and genotyping with HISAT2 and HISAT-genotype. Nat Biotechnol.37(8):907-15. Epub 20190802. doi: 10.1038/s41587-019-0201-4. PubMed PMID: 31375807; PubMed Central PMCID: PMCPMC7605509.

62. Lamesch P, Berardini TZ, Li D, Swarbreck D, Wilks C, Sasidharan R, et al.(2012). The Arabidopsis Information Resource (TAIR): improved gene annotation and new tools. Nucleic Acids Res.40(Database issue):D1202-10. Epub

20111202. doi: 10.1093/nar/gkr1090. PubMed PMID: 22140109; PubMed Central PMCID: PMCPMC3245047.

63. Swarbreck D, Wilks C, Lamesch P, Berardini TZ, Garcia-Hernandez M, Foerster H, et al.(2008). The Arabidopsis Information Resource (TAIR): gene structure and function annotation. Nucleic Acids Res.36(Database issue):D1009-14. Epub 20071105. doi: 10.1093/nar/gkm965. PubMed PMID: 17986450; PubMed Central PMCID: PMCPMC2238962.

64. Pertea M, Kim D, Pertea GM, Leek JT, Salzberg SL.(2016). Transcript-level expression analysis of RNA-seq experiments with HISAT, StringTie and Ballgown. Nat Protoc.11(9):1650-67. Epub 20160811. doi: 10.1038/nprot.2016.095. PubMed PMID: 27560171; PubMed Central PMCID: PMCPMC5032908.

65. Love MI, Huber W, Anders S.(2014). Moderated estimation of fold change and dispersion for RNA-seq data with DESeq2. Genome Biol.15(12):550. doi: 10.1186/s13059-014-0550-8. PubMed PMID: 25516281; PubMed Central PMCID: PMCPMC4302049.

66. Dolinski K, Dwight S, Eppig J, Harris M, Hill D, Issel-Tarver L, et al.(2000). Gene ontology: tool for the unification of biology. The Gene Ontology Consortium. Nat Genet.25(1):2529Attri.

67. Tian T, Liu Y, Yan H, You Q, Yi X, Du Z, et al.(2017). agriGO v2.0: a GO analysis toolkit for the agricultural community, 2017 update. Nucleic Acids Res.45(W1):W122-W9. doi: 10.1093/nar/gkx382. PubMed PMID: 28472432; PubMed Central PMCID: PMCPMC5793732.

68. Gu Z, Eils R, Schlesner M.(2016). Complex heatmaps reveal patterns and correlations in multidimensional genomic data. Bioinformatics.32(18):2847-9.

69. Brand L, Horler M, Nuesch E, Vassalli S, Barrell P, Yang W, et al.(2006). A versatile and reliable two-component system for tissue-specific gene induction in Arabidopsis. Plant Physiol.141(4):1194-204. doi: 10.1104/pp.106.081299. PubMed PMID: 16896232; PubMed Central PMCID: PMCPMC1533952.

70. Xue LJ, Guo W, Yuan Y, Anino EO, Nyamdari B, Wilson MC, et al.(2013). Constitutively elevated salicylic acid levels alter photosynthesis and oxidative state but not growth in transgenic populus. Plant Cell.25(7):2714-30. Epub 20130731. doi: 10.1105/tpc.113.112839. PubMed PMID: 23903318; PubMed Central PMCID: PMCPMC3753393.

71. Ricci WA, Levin L, Zhang X. Genome-Wide Profiling of Histone Modifications with ChIP-Seq. Cereal Genomics: Springer; 2020. p. 101-17.

72. Yamaguchi N, Winter CM, Wu M-F, Kwon CS, William DA, Wagner D.(2014). PROTOCOLS: Chromatin immunoprecipitation from Arabidopsis tissues. The Arabidopsis book/American Society of Plant Biologists.12.

73. Lin X, Tirichine L, Bowler C.(2012). Protocol: Chromatin immunoprecipitation (ChIP) methodology to investigate histone modifications in two model diatom species. Plant methods.8(1):1-9.

Table 2.1 Plants and primers used in Chapter 2.

| **Mutant** | **PCR size** | **primer sequences** | **Digestion** |
|---|---|---|---|
| *npr1-1* | 763 bp | GTTAGTCTTGAAAAGTCATTGCCGGAAG | NlaIII + Cutsmart buffer<br>WT=97+208+102+368;<br>npr1-1=97+306+368 |
| | | TTTCGGCGATCTCCATTGCAGC | |
| | | | |
| *eds1.2* | WT=564 bp, Mut=0 | GTGGAAATGGCTGTGAGGAGTAGA | NA. *eds1.2* has 600 bp deletion. |
| | | CAGCATTTGAAGAATGGCGTCCG | |
| | | | |
| *sid2-1* | 199 bp | AAGCTTGCAAGAGTGCAACA | MseI + Cutsmart buffer<br>WT: 129+68;<br>Mut: 100+29+68 |
| | | AAACAGCTGGAGTTGGATGC | |
| | | | |
| *pad4-1* | 392 bp | GCGATGCATCAGAAGAG | BsmF I<br>WT: 271 +124<br>Mut: indigestible |
| | | TTAGCCCAAAAGCAAGTATC | |

| Primers for qPCR and cloning | | |
|---|---|---|
| Name | Sequence (5'-3') | Description |
| *AT3G60470*_qFw | GCGCTTGAGCAATGCCATTA | 146 bp qPCR product |
| *AT3G60470*_qRv | GCCACAGAACTCTTCTCCCC | 146 bp qPCR product |

| | | |
|---|---|---|
| *BG3*_qFw | CACGGCAGTTGGACAAATCG | 93 bp qPCR product, GNS3 |
| *BG3*_qRv | TTCCGTTGTTGGTAAAGCGC | 93 bp qPCR product, GNS3 |
| *ATLTP4.4*_qFw | TCAGCTCTCGCGATGGTTTT | 169 bp qPCR product |
| *ATLTP4.4*_qRv | GGTTAGCAACTCTGGCCACT | 169 bp qPCR product |
| *PR5*_qFw | TTCATCACAAGCGGCATTGC | 122 bp qPCR product |
| *PR5*_qRv | TCAAATCCTCCATCGCCGAG | 122 bp qPCR product |
| *qTUB2*_qFw | AGCAATACCAAGATGCAACTGCG | reference gene |
| *qTUB2*_qRv | TAACTAAATTATTCTCAGTACTCTTCC | reference gene |
| *SPL10*_qFw | TGTGAGTGGCCTGGAACGTCG | 132 bp qPCR product |
| *SPL10*_qRv | CCTTGTGGCTTGCGACGCCT | 132 bp qPCR product |
| *SPL3*_qFw | ATGAGTATGAGAAGAAGCAAAGCG | 156 bp qPCR product |
| *SPL3*_qRv | TCCACTACTACTTGTAGCTTTACCT | 156 bp qPCR product |
| *rSPL3-F* | CACCATGTTGAAGAAGAAGAGGCTTTGG | XVE::35S::rSPL3-YFP |
| *rSPL3-Rns* | GTCAGTTGTGCTTTTCCGCCTTCTC | XVE::35S::rSPL3-YFP |
| *rSPL10-F* | CACCATGGACTGCAACATGGTATCTTC | XVE::35S::rSPL10-YFP |
| *rSPL10-Rns* | GATGAAATGACTAGGGAAAGTG | XVE::35S::rSPL10-YFP |
| *qSAND*_qFw | AACTCTATGCAGCATTTGATCCACT | reference gene |
| *qSAND*_qRv | TGATTGCATATCTTTATCGCCATC | reference gene |
| *PR2*_qFw | CCTTCTTCAACCACACAGCTG | 151 bp qPCR product |
| *PR2*_qRv | GCGGCAAGAGCGCCTGGGTC | 151 bp qPCR product |
| PAD4_Fw_M1_p1 | GGATCACATGCTTTGATTCGCA | 106 bp ChIP-qPCR product |
| PAD4_Rv_M1_p1 | TGCTGTGAAAGGTAGGTCCAT | 106 bp ChIP-qPCR product |
| PAD4_Fw_M1_p2 | ACCTACCTTTCACAGCATTTCT | 113 bp ChIP-qPCR product |
| PAD4_Rv__M1p2 | CTTTGCTAAGTCGTCTTCTTC | 113 bp ChIP-qPCR product |

| | | |
|---|---|---|
| PAD4_Fw_M1_p3 | AGAAGACGACTTAGCAAAGACCA | 134 bp ChIP-qPCR product |
| PAD4_Rv_M1_p3 | CGAGTAGAGAGTTGCAGAACGA | 134 bp ChIP-qPCR product |
| PAD4_Fw_n1 | TCATTGTCGCGACCTTTGGA | 86 bp ChIP-qPCR product |
| PAD4_Rv_n1 | TAAATCACTTGGGCGGACGG | 86 bp ChIP-qPCR product |
| PAD4_Fw_M2 | TCCTCAACACCACAGCAACT | 49 bp ChIP-qPCR product |
| PAD4_Rv_M2 | CCGTACCTCTGATGTTCCTCG | 49 bp ChIP-qPCR product |
| PAD4_Fw_n2 | TGAGAAGCAGATACGCGAGC | 83 bp ChIP-qPCR product |
| PAD4_Rv_n2 | CGCCTCATCCAACCACTCTT | 83 bp ChIP-qPCR product |
| proSPL10-F | CACCTTCGCATCTTCTAGTACTAAATC | SPL10 promoter forward primer |

| **Seed stocks** | |
|---|---|
| *pSPL2::rSPL2::GUS* | Xu et al., PLoS Genetics, 2016 |
| *pSPL10::rSPL10::GUS* | Xu et al., PLoS Genetics, 2016 |
| *pSPL11::rSPL11::GUS* | Xu et al., PLoS Genetics, 2016 |
| *pSPL13::rSPL13::GUS* | Xu et al., PLoS Genetics, 2016 |
| *pSPL3::rSPL3::GUS* | Xu et al., PLoS Genetics, 2016 |
| *pSPL4::rSPL4::GUS* | Xu et al., PLoS Genetics, 2016 |
| *pSPL5::rSPL5::GUS* | Xu et al., PLoS Genetics, 2016 |
| *pSPL6::rSPL6::GUS* | Xu et al., PLoS Genetics, 2016 |
| *pSPL9::rSPL9::GUS* | Xu et al., PLoS Genetics, 2016 |
| *pSPL15::rSPL15::GUS* | Xu et al., PLoS Genetics, 2016 |
| *spl2* | CS69781 |
| *spl10-2* | CS69785 |
| *spl10/11* | CS69791 |
| *spl2/10/11* | Xu et al., PLoS Genetics, 2016 |
| *spl3/4/5* | CS69790 |
| *spl9/15* | CS67865 |
| *35S::MIR156A* | CS67849 |
| *35S::MIM156* | Franco-Zorrilla et al., Nat. Genetics, 2007 |
| *XVE::35S::MIM156* | He et al., PLoS Genetics, 2018 |
| *XVE::35S::rSPL3* | this study |
| *XVE::35S::rSPL10-Citrine-HA* | this study |
| pro*SPL10::rSPL10-YFP* | this study (a 1.9kb promoter of SPL10 was cloned into pGWB40 using Gateway cloning system) |

| | |
|---|---|
| pro*PR2::GUS (BGL2::GUS)* | Zhang et al., Plant Cell, 2003 |

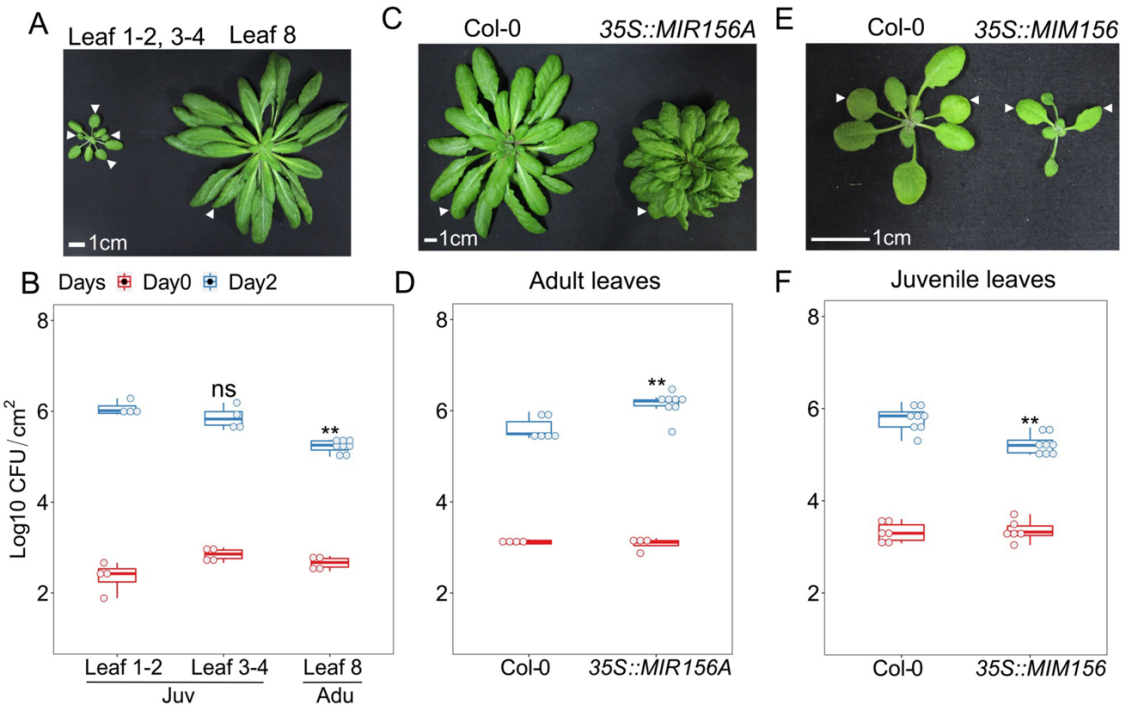


**Figure 2.1 MiR156 suppressed age-related resistance to *Pto* DC3000 in *Arabidopsis*. A**, developmental phenotype of a 4-week (left) and 7-week (right) Col-0 plant grown under short-day conditions. Arrows point to leaves 1,2,3,4 and leaf 8 in the left and right plants, respectively. **B**, *Pto* DC3000 bacterial growth in juvenile and adult leaves of Col-0. **C**, developmental phenotype of a 7-week Col-0 and *35S::MIR156A* plant. Arrows indicate an adult leaf of Col-0 or a leaf from a similar position in *35S::MIR156A*. **D**, bacterial growth in adult leaves of Col-0 and *35S::MIR156A*. **E**, developmental phenotype of a 4-week Col-0 and *35S::MIM156* plant. Arrows indicate leaves 1 and 2 on each plant. **F**, *Pto* DC3000 bacterial growth in juvenile Col-0 and *MIM156* leaves 1-2 on Day 0 and Day 2. Scale bar = 1 cm. Day 0, the day of *Pto* infection. Day 2, two days post-infection. CFU/cm$^2$, bacterial colony forming unit per square centimeter of a leaf. Juv, juvenile leaves, Adu, adult leaves. The student t-test was used for statistical

analysis. Each genotype was compared with Col-0, ns, not significant, *, $p < 0.05$, **, $p < 0.01$. Four leaf discs derived from four individual leaves were homogenized as one sample. Each sample was presented as a data point in the plot. The same annotation is used for bacterial growth dot-box plots shown in Figures 2 and 7. Repeats of bacterial growth are presented in Table S2.

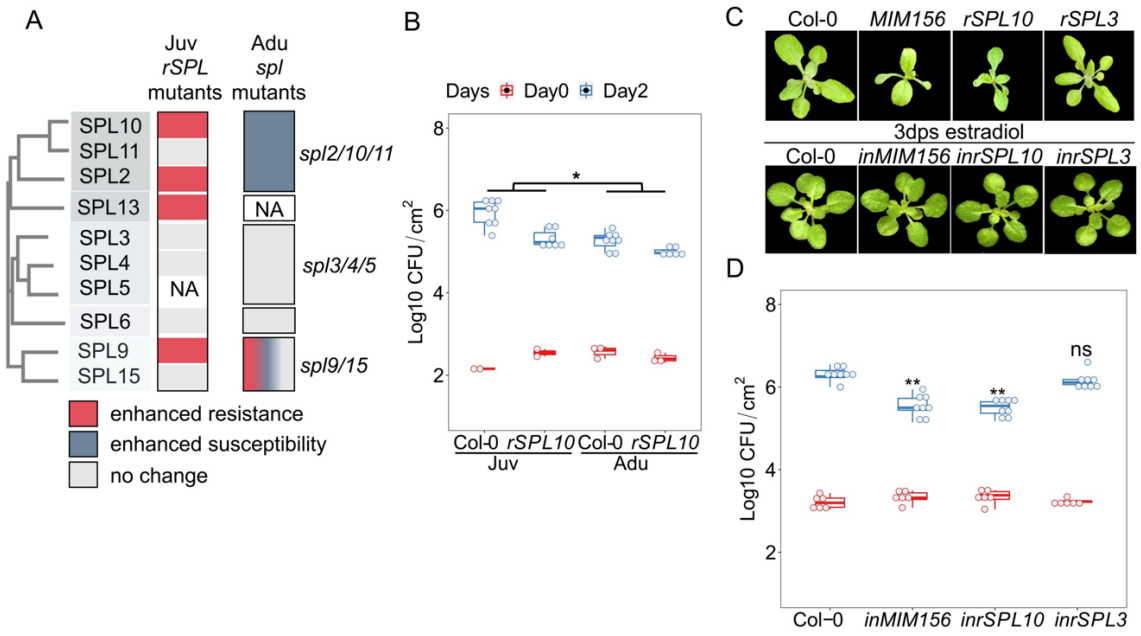


**Figure 2.2 MiR156-targeted SPL10 promoted resistance to *Pto* DC3000. A**, disease phenotype of *Pto* DC3000 in *SPL* gain and loss-of function mutants. NA, not available. **B**, bacterial growth in leaves 1-2 and leaves 11 from Col-0 and *rSPL10*. **C**, developmental phenotype of Col-0, and early phase change phenotypes of transgenic plants expressing stable *MIM156*, *rSPL10* and *rSPL3* on ½ MS plate (top panel); developmental phenotype of Col-0, *estradiol-inducible(in)MIM156*, *inrSPL10* and *inrSPL3* at 3 days-post estradiol spray (3dps, bottom panel). **D**, bacterial growth in leaves 1-2 from 4 -week-old Col-0, *inMIM156*, *inrSPL10* and *inrSPL3* on Day 0 and Day 3. Emmeans package in R was used for statistical analysis in 2 A and 2 B. The student t test was used for statistical analysis in 2 A and 2 C, and each genotype was compared with Col-0 wild type, ns, not significant, *, $p < 0.05$, **, $p < 0.01$. Repeats for the experiments here are shown in Table S2.

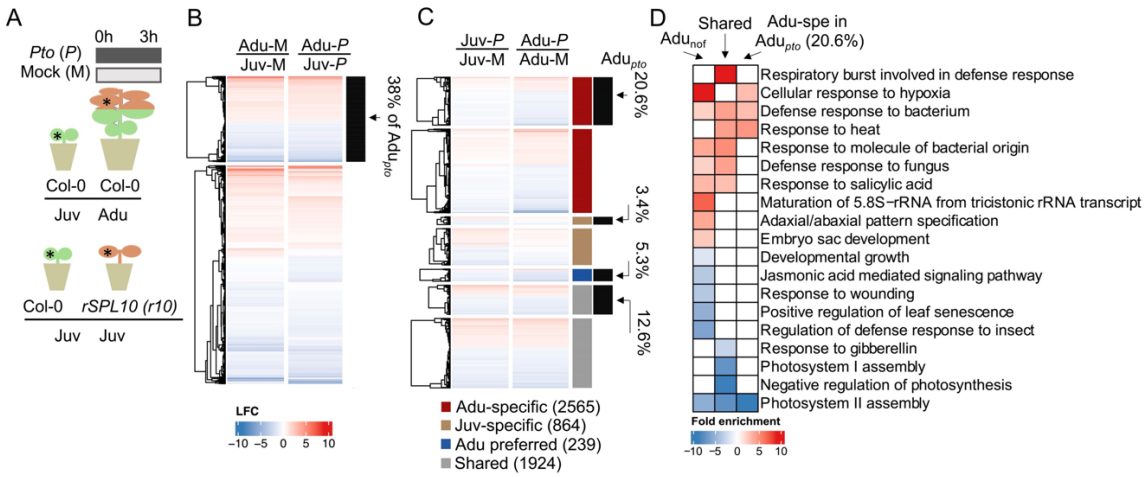


**Figure 2.3 Basal transcript level of defense genes were heightened over vegetative phase change. A**, experimental settings of RNA-seq. Non-infected state and challenged (3 hours after *Pto* inoculation) transcriptomes from leaf 1-2 (Col-0 and *rSPL10*) and leaf 11 (Col-0) were compared. * indicates examples of leaf samples that were collected for RNA-seq. Green: juvenile leaves; brown: adult leaves. **B**, an expression profiling of DEGs identified in mock-treated adults against mock-treated juvenile leaves. DEGs, differently expressed genes with LFC ≥ ±0.58 and padj ≤ 0.05. LFC, log2 fold change of gene expression. Padj, adjusted p value. Color-codes in the heatmap, blue is for down-regulated DEGs and red is for up-regulated DEGs. Euclidean distance was used for calculating distance. Complete linkage was applied to structure the hierarchical clustering. Expressing profiles of DEGs derived from Adu-M/Juv-M are mapped in the first column of the map. The expressing profiles of those DEGs in Adu-*P*/Juv-*P* are shown in the second column of the map. Genes that were DEGs in both Adu-M/Juv-M and Adu-*P*/Juv-*P* are marked by the black bar on the right. 38% indicates the percentage of those overlapping DEGs in $Adu_{pto}$. **C**, a profile of *Pto*-triggered DEGs came from Juv-*P*/Juv-M and Adu-*P*/Adu-M. Adult-specifically

*Pto*-triggered DEGs (dark red), Juvenile-specifically triggered (light brown), adult preferentially triggered (deep blue), and commonly triggered in both adults and juveniles, i.e., shared (light grey) are marked by the first column of bars on the right. The percentages (20.6%, 3.4%, 5.3%, 12.6%) and corresponding black bars indicate the proportion of each DEG category that overlaps with $Adu_{pto}$. **D**, representative GO terms enriched in DEGs of $Adu_{nof}$, DEGs triggered by *Pto* DC3000 in both adult and juvenile leaves (the Shared) and DEGs specifically triggered by *Pto* in adult phase within the total $Adu_{pto}$ (20.6%). Red and blue color blocks refer to GOs enriched in up- and down-regulated DEGs, respectively. Only GO terms with FDR < 0.05 were deemed as enriched here. Fold enrichment was based on hypergeometric tests within the range of the DEG set used for each GO analysis relative to *Arabidopsis* genome. The analysis was done using the TAIR Gene ontology website (geneontology.org). The same GO analysis and color-coding are used for Figure 4 C.

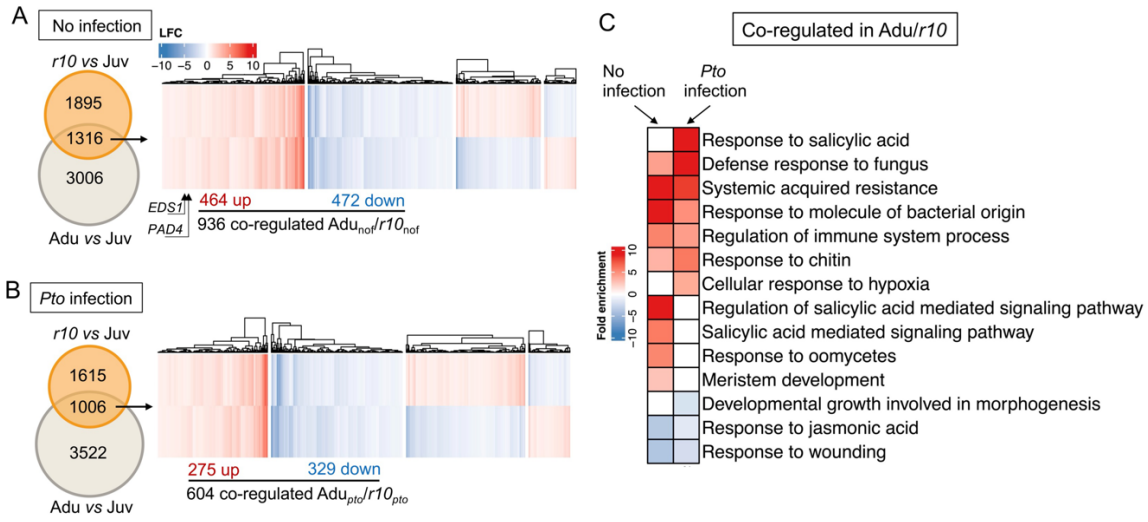


**Figure 2.4 *rSPL10* transcriptomes resembled that of adult leaves. A**, an expression profiling of co-regulated DEGs by adult and *rSPL10* leaves at non-infected state compared with juvenile leaves. *EDS1* and *PAD4* were identified as Adu/*r10* co-upregulated DEGs under non-infected state, which are indicated in the heatmap with arrows. **B**, expressing profiles of co-regulated DEGs by adult and *rSPL10* from Adu-*P* or *r10*-*P* against Juv-*P*. For the clustered heatmaps in 4 A and B, blue represents down-regulated DEGs and red is for up-regulated DEGs. Euclidean distance was used for calculating distance in the partition around medoids (PAM) clustering (k=4). **C**, GO enrichment of co-regulated adult and *r10 vs* juvenile DEGs in non-infected and *Pto*-infection states.

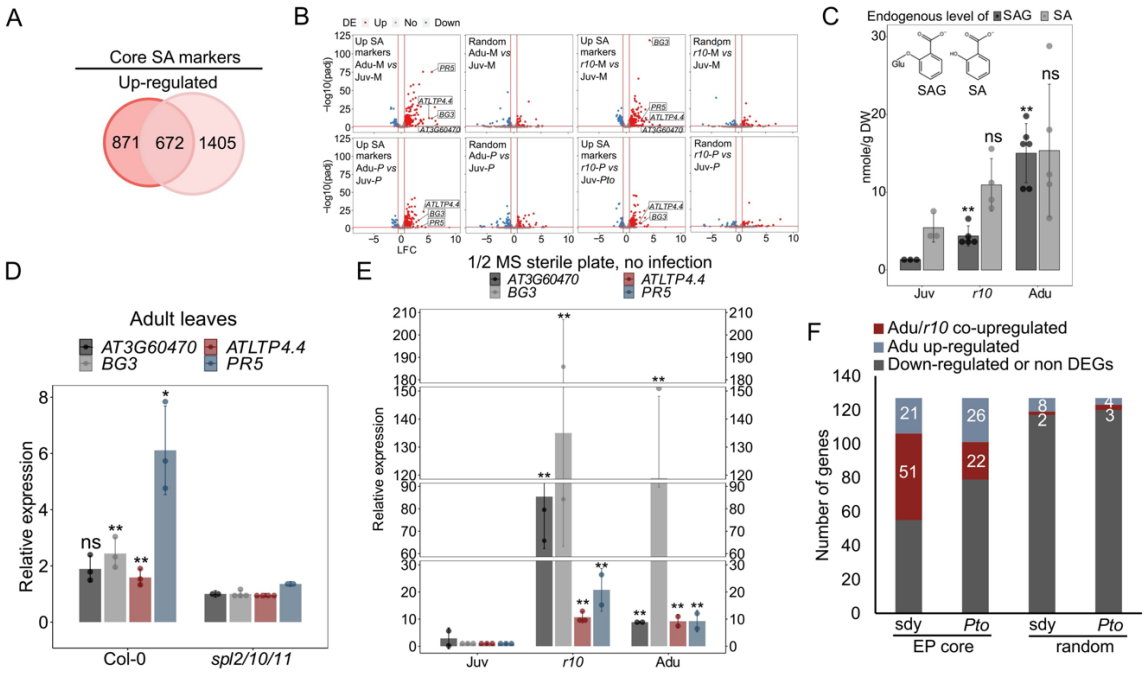


**Figure 2.5 Salicylic acid (SA) biosynthesis and signaling were enhanced by SPL10 in adult phase. A**, 672 up-regulated core SA markers were defined via overlapping DEGs pools from Ding Y *et al.*, 2018 (dark circle) and Yang L *et al.*, 2017 (light circle). **B**, expression patterns of 527 detected (out of 672) up-regulated core SA markers in adult and *r10* leaves, under non-infected and *Pto* infection states. Four random pools of detected genes (450 genes per set) derived from each pair-wise comparison exhibits here were chosen as negative controls. Up, upregulated. No, no change. Down, downregulated. Y axis shows the negative logarithm transformed adjusted p value, -log10(padj). X axis displays the value of Log2 fold change (LFC) of gene expressions. M, mock. *P, Pto* DC3000. P < 0.0001 (Hypergeometric test, done by GeneOverlap R package) was reproducibly output from each overlap between core upregulated SA markers and $Adu_{nof}$, $Adu_{pto}$, $r10_{nof}$ and $r10_{pto}$. The P values for 3 out of 4 random controls were not significant. **C**, endogenous SAG and free SA

accumulation in juvenile, *r10* and adult leaves at non-infected state. DW, dry weight. Repeats for the experiment are shown in Table S2. **D**, age-associated expression of four SA markers in adult leaves from Col-0 and in comparable leaves of *spl2/10/11*. Similar results were seen two times. **E**, the qPCR of the four SA marker genes in juvenile, *r10* and adult leaves on sterile 1/2 MS plates. Similar results were seen three times. **F**, overrepresentation of EDS1-PAD4 core regulon (EP core) in Adu/$r10_{\text{nof}}$ and Adu/$r10_{pto}$. The EP core markers were defined in Cui *et al.,* 2017 [45]. 127/155 of the EP core markers were detected in this work. Randomly selected 127 genes from our RNA-seq dataset were used as controls.

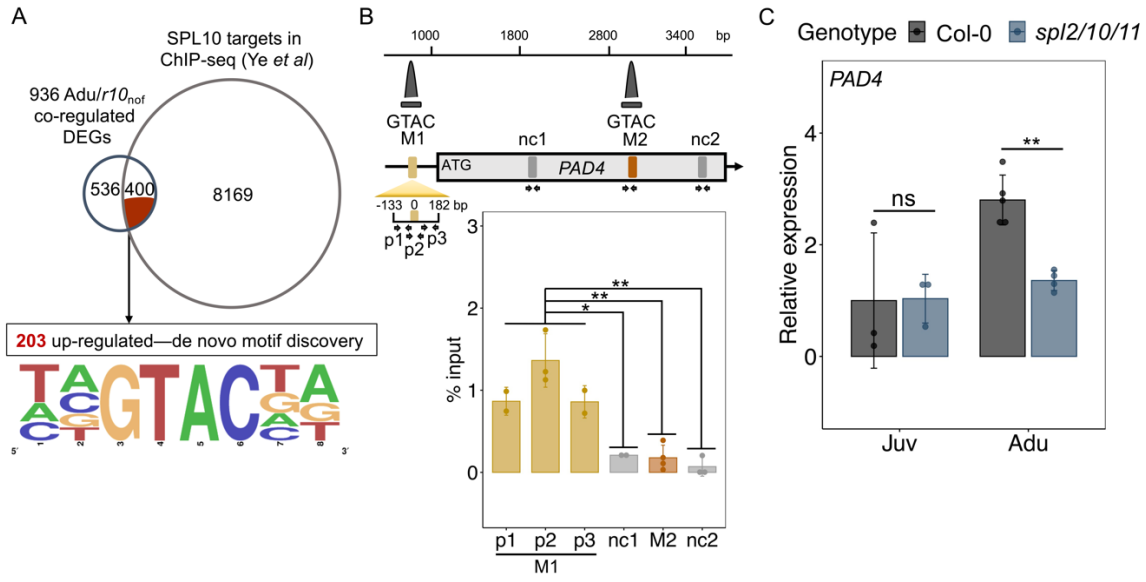


**Figure 2.6 *PAD4* was a direct target of SPL10. A**, overlap between Adu/*r10*$_{nof}$ co-regulated genes and potential SPL10 targets defined according to ChIP-seq data from *Ye et al*. (upper panel). A motif discovery and enrichment analysis of the 203 Adu/*r10*$_{nof}$ co-upregulated DEGs (lower panel). **B**, SPL10 bound to a GTAC-containing motif upstream of *PAD4*. qPCR following chromatin immunoprecipitation of *rSPL10*-YFP for motifs (M1 and M2) and negative control sites (nc1 and nc2), the latter of which are at least 600 bp away from M1 and M2 at the *PAD4* genomic region. Three primer sets (p1-p3) were used to amplify the M1 site. Relative locations of ChIP peaks (dark grey) derived from *Ye et al*, primers (arrow pairs) and the tested sites (color blocks) were indicated in the schematic diagram. The student t test was performed to compare and indicate the significance of difference between the sites. **C**, qPCR of *PAD4* transcripts level in juvenile (Juv) and adult (Adu) leaves of Col-0 and *spl2/10/11*. The student t test, ns, not significant, *, $p < 0.05$, **, $p < 0.01$.

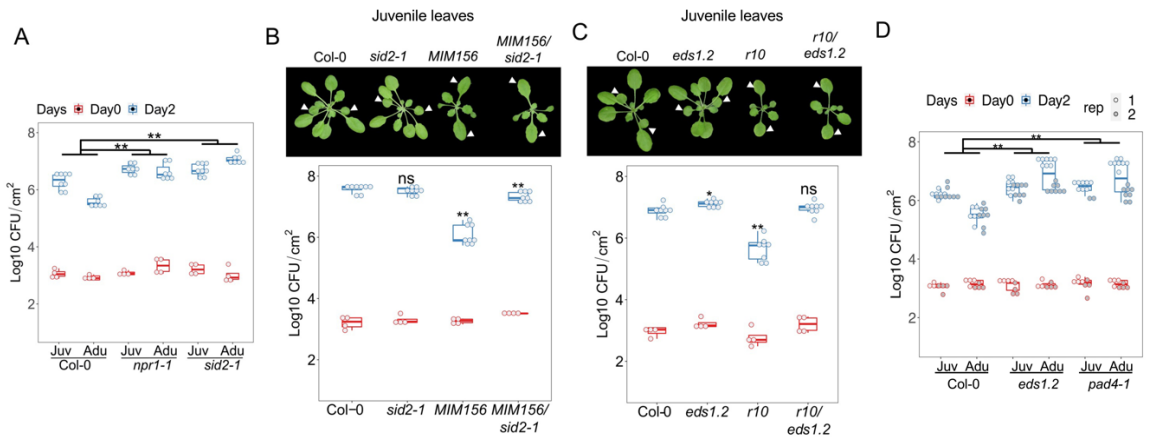


**Figure 2.7 SA biosynthesis and signaling components were required for the SPL10 regulated ARR$_{VPC}$. A**, a comparison of *Pto* DC3000 growth between the juvenile and adult leaves (ARR phenotype) of Col-0, *sid2-1* and *npr1-1*. **B**, developmental phenotype (top) and the bacterial growth (bottom) in 4-week-old leaves 1 and 2 from Col-0, *sid2-1*, *MIM156* and *MIM156/sid2-1*. **C**, developmental phenotype of 4-week-old Col-0, *eds1.2, r10* and *r10 /eds1.2*. Note the similar leaf shape between *r10* and *r10*/*eds1.2;* (bottom panel) bacterial multiplication in leaves 1 and 2 derived from Col-0, *eds1.2*, *r10* and *rSPL10/eds1.2*. Arrows indicate leaves 1-2. **D**, the ARR phenotyping of *eds1.2* and *pad4-1* infected with *Pto* DC3000. Emmeans package in R was used for statistical analysis in 7 A and D. The student t test was used for statistical analysis in 7 B-C, and each genotype was compared with Col-0 wild type, ns, not significant, *, $p < 0.05$, **, $p < 0.01$.

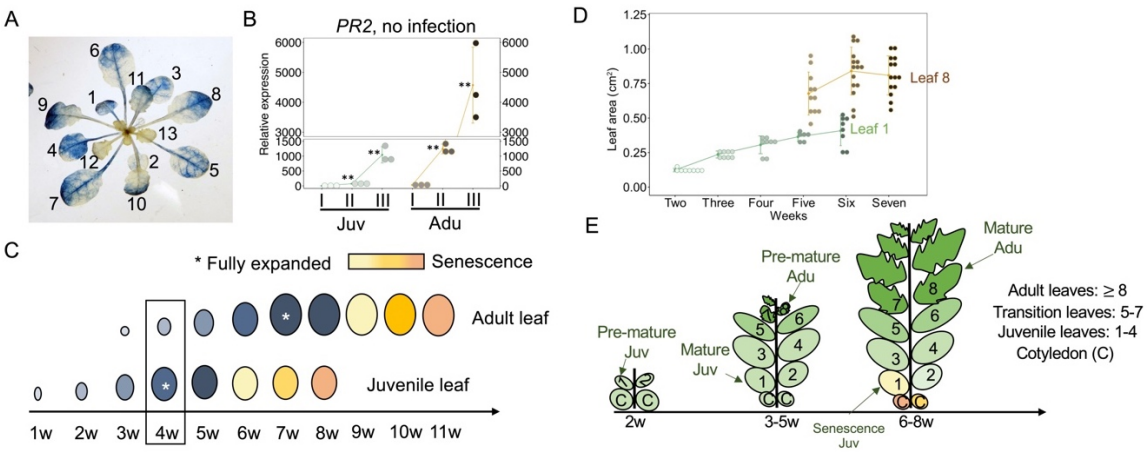


**Figure 2.8 Ontogenic change of SA response and sampling approach for examining ARR$_{vpc}$. A,** ontogenic-associated promoter activities of pro*PR2*::GUS in an uninfected plant. Note the high activity in fully expanded juvenile leaves (1-4) and low in young adult leaves (12-13). The indicated leaf numbers were based on the order of the leaves on shoot. **B**, the incremental expression of *PR2* gene spanning the expansion of juvenile and adult leaves. I, premature leaves. II, intermediate premature leaves. III, mature leaves. **C**, An outline of the ontogenic maturation of a juvenile leaf and an adult leaf. The boxed region indicates distinct ontogenic age of juvenile and adult leaves from the same plant; asteroids indicate juvenile and adult leaves of the same ontogenic age. **D,** The quantified leaf expansion rate in juvenile and adult leaves. Leaf areas were quantified and normalized through Fiji software. **E**, a cartoon depiction of shoot development and leaf maturation that are concurrent during the vegetative phase change.

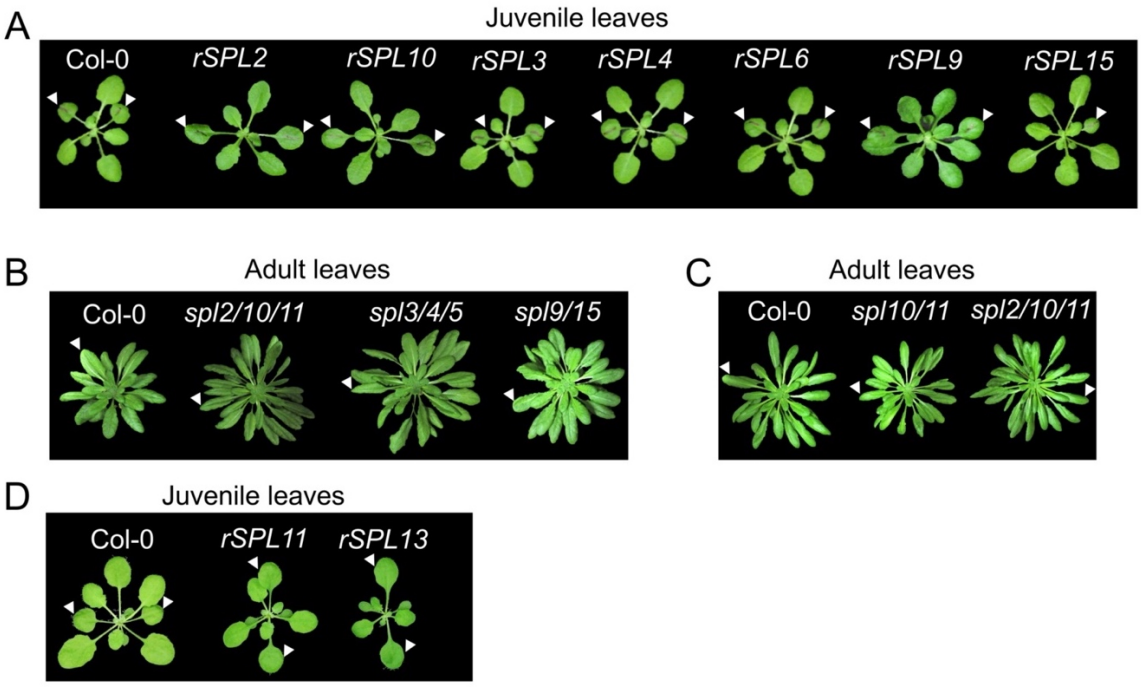


**Figure 2.9 Developmental phenotypes of *rSPLs* and *spl* mutants. A and D**, arrows indicate leaf 1-2 of juvenile Col-0 and *rSPLs*. **B-C**, arrows indicate representative adult leaves of Col-0 and *spl* mutants.

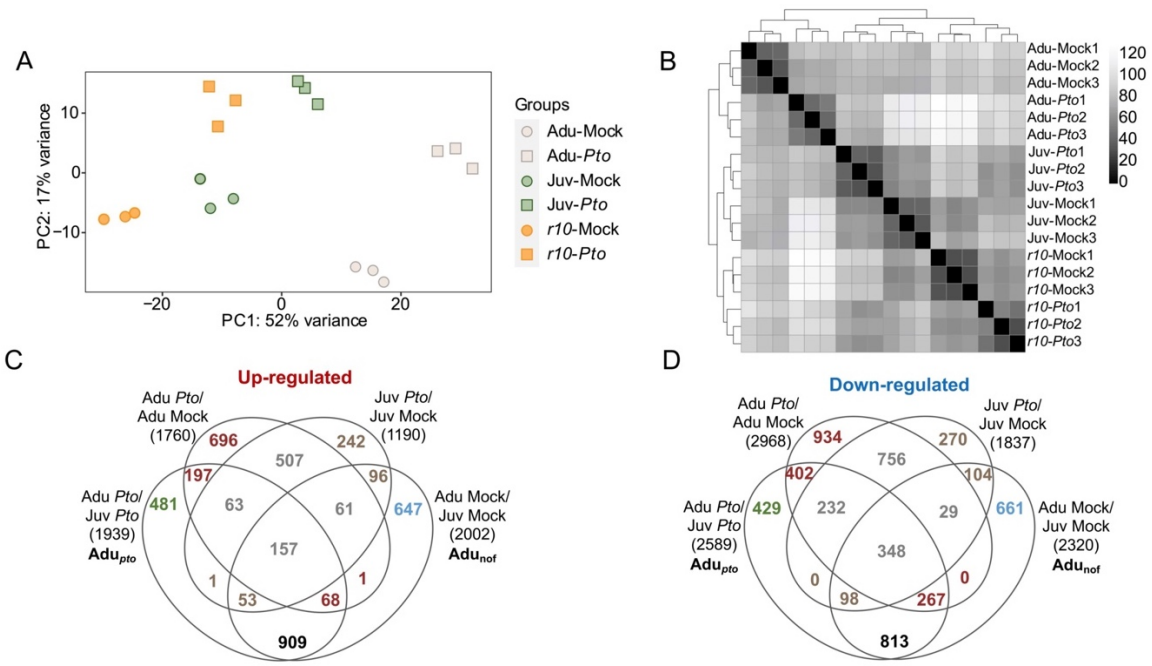


**Figure 2.10 Quality control of RNA-seq datasets and Venn diagrams of adult *vs* juvenile DEGs. A**, principal component analysis showed that the effect of age and genotype may contribute to explain 52% variance of the samples, and *Pto* infection effect may contribute to explain 17% variance of the samples. **B**, the sample-to-sample distance matrix showed that biological replicates (Mock1-3 and *Pto*1-3) were well correlated (in close distance) per genotype per treatment. The column names of the matrix are in the same order as the row names--from the “Adu-Mock1” (the first on the left) to the *“r10-Pto3*” (the first on the right). **C**, venn diagrams of Adu-DEGs generated from the indicated pair-wise comparisons. Color-coding of numbers, adult-specifically *Pto*-triggered DEGs (red), Juvenile-specifically triggered (brown), commonly triggered in both adults and juveniles, i.e., shared (grey), and overlap DEGs between $Adu_{nof}$ and $Adu_{pto}$ (black). Green numbers indicate the 20.1% synergistic DEGs that mentioned in

the main text. Blue numbers refer to DEGs that were $Adu_{nof}$ but not $Adu_{pto}$. Adult preferentially *Pto*-triggered DEGs are listed in Table S3.

A

| Alt ID | P-value | E-value | Q-value (FDR) | TP (Primary seq Match to the motif) | FP (% control seq match to the motif) | Enrichment Ratio (Primary relative to control) | Threshold (set TP/FP) |
|---|---|---|---|---|---|---|---|
| SPL1 | 2.60e-4 | 2.27e-1 | 6.95e-3 | 25/183 (13.7%) | 6/183 (3.3%) | 3.71 | 12.56 |
| SPL5 | 2.40e-3 | 2.1e0 | 2.69e-2 | 24/183 (13.1%) | 8/183 (4.4%) | 2.78 | 12.38 |
| SPL15 | 3.69e-3 | 3.22e0 | 3.60e-2 | 29/183 (15.8%) | 12/183 (6.6%) | 2.31 | 9.14 |

B


**Figure 2.11 A table of enriched SPL-binding motifs within the upregulated 203 and plant phenotype of *proSPL10::rSPL10-YFP*. A,** Frequency-based DNA logos are shown for each enriched motif. The analysis was performed in the simple enrichment analysis-MEME Suite. Details were described in the method section. **B,** plant phenotype of proSPL10::rSPL10-YFP. Note the elongated leaves 1 and 2 in the transgenic plant.

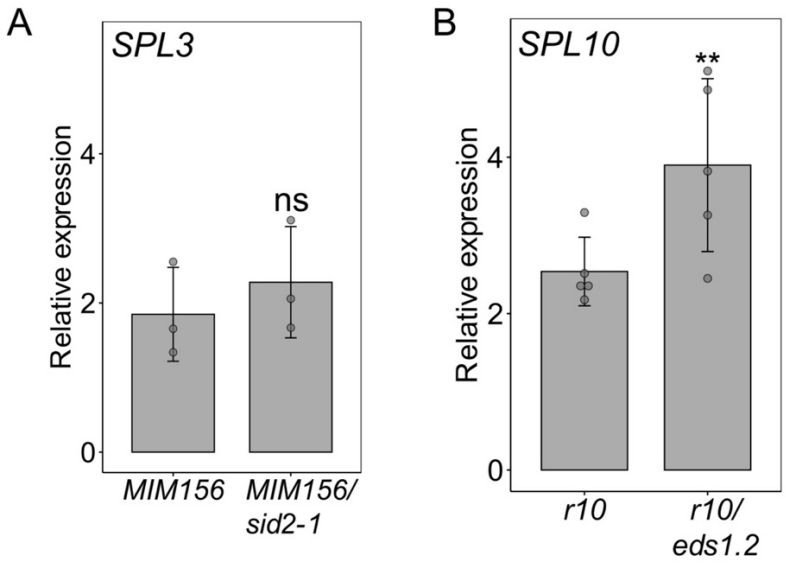


**Figure 2.12 Expression of *SPL3* and *SPL10* in *MIM156/sid2-1* and *r10/eds1.2*.**

A, *SPL3* was used as an indicator of *MIM156* function. No difference was observed in *MIM156* and *MIM156/sid2-1.* B, *SPL10* was expressed at comparable level in *rSPL10* and *rSPL10/eds1.2.* Student t test, ns, not significant, *, $p < 0.05$, **, $p < 0.01$.

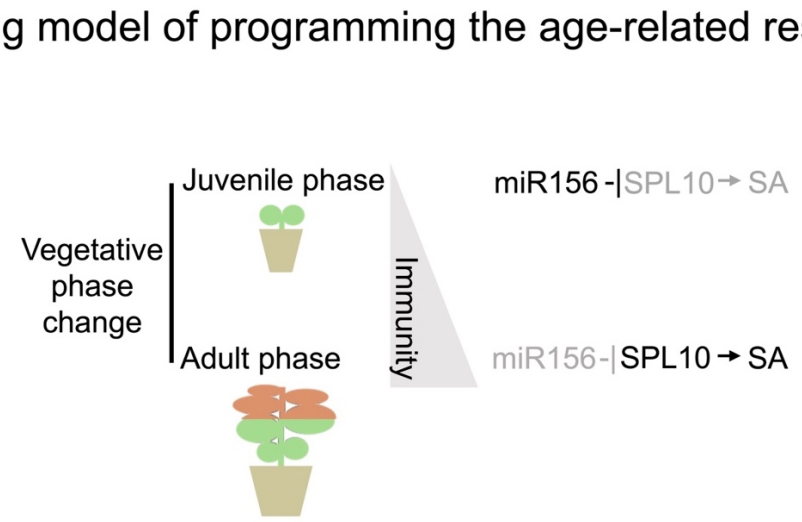


**Figure 2.13 A model of miR156-SPL10 regulated age-related resistance during the vegetative phase change.** In brief, miR156 suppressed the resistance in juvenile phase through inhibiting SPL10. The increased expression of *SPL10* followed by the decline of miR156 level gives rise to a high immune output in adult phase. That is achieved via promoting the expression of *PAD4* as well as enhancing expressions of other components in SA biosynthesis and signaling pathways.

# CHAPTER 3

## SHOOT MATURATION STRENGTHENS FLS2-MEDIATED RESISTANCE TO PSEUDOMONAS SYRINGAE.

Reproduced, by permission, from Hu L., Kvitko B., Yang Li. 2023. *Shoot maturation strengthens FLS2-mediated resistance to Pseudomonas syringae. Submitted to MPMI.*

**ABSTRACT**

A temporal-spatial regulation of immunity components is essential for properly activating plant defense response. Flagellin-sensing 2 (FLS2) is a surface-localized receptor that recognizes bacterial flagellin. The immune function of FLS2 is compromised in early stages of shoot development. However, the underlying mechanism for the age-dependent FLS2 signaling is not clear. Here, we show that the reduced basal immunity of juvenile leaves against *Pseudomonas syringae* pv. tomato DC3000 is independent of FLS2. The flg22-induced marker gene expression and ROS activation were comparable in juvenile and adult stage, but callose deposition was more evident in the adult stage than that of juvenile stage. We further demonstrated that microRNA156, a master regulator of plant aging, suppressed callose deposition in juvenile leaves in response to flg22 but not the expression of *FLS2* and *FRK1 (Flg22-induced receptor-like kinase 1)*. Altogether, we revealed an intrinsic mechanism that regulates the amplitude of FLS2-mediated resistance during aging.

## INTRODUCTION

At the cell surface, some receptor kinases and receptor-like proteins act as pattern recognition receptors (PRRs) to recognize evolutionarily conserved microbe/pathogen-associated molecular patterns (M/PAMPs) and activate the Pattern-triggered immunity (PTI) (Ngou et al., 2022, Couto & Zipfel, 2016). The PTI response can be hindered by effectors, which are pathogen-derived molecules secreted into plant cells or apoplastic spaces, resulting in effector-triggered susceptibility (Jones & Dangl, 2006). Flagellin-sensing 2 (FLS2) is a receptor-like kinase localized at plasma membrane. FLS2 recognize flg22, a 22 amino acid peptide derived from bacterial flagellin, and activates PTI (Zipfel et al., 2004; Couto & Zipfel, 2016). Hallmarks of the FLS2-mediated PTI occur within minutes include changes of ion-flux at the plasma membrane, increase of cytosolic $Ca^{2+}$ level and production of reactive oxygen species (ROS) (Seybold et al., 2014; Couto & Zipfel, 2016). Within hours, transcriptional reprogramming is induced (Li et al., 2016). In the following hours and days, deposition of callose papillae occurs to reinforce cell walls (Li et al., 2016; Couto & Zipfel, 2016). Then, synthesis of hormones amplifies immune signaling through triggering second transcriptional waves (Li et al., 2016; Couto & Zipfel, 2016). The sum of those events limit pathogen invasion and multiplication.

Misfiring of immune responses often leads to compromised growth (J. K. M. Brown, 2002, 2003; Nelson et al., 2018). Temporal-spatial regulation of activation

and expression dosage of immune components are necessary to fine-tuning growth and defense (Fröschel et al., 2021; H. Wu et al., 2020; Zheng et al., 2015). FLS2-mediated signaling is developmentally regulated. In the *Arabidopsis* root, the promoter of *FLS2* was active in the differentiation zone, specifically in the vascular cylinder (Beck et al., 2014). Flg22-activated expressions of *FRK1 (FLG22-INDUCED RECEPTOR-LIKE KINASE)* and *PER5 (PEROXIDASE 57)* were confined at the cortical cell layer during lateral root formation, where root primordia pushed and damaged neighboring cortical cells (Zhou et al., 2020). FLS2 promoter activity was high in tissues that were potential bacterial entry sites, such as stomata, hydathodes, and lateral roots (Beck et al., 2014). During leaf ontogenesis, the *FLS2* transcripts were less abundant in expanding (young) leaves than that in expanded (mature) leaf, and its expression became undetectable later in senescent leaves (Klepikova et al., 2016). Zou *et al* demonstrated that the expression of *FLS2* was suppressed in early development of *Arabidopsis* cotyledon (Zou et al., 2018), leading to the higher susceptibility to bacterial pathogen *Pseudomonas syringae* (*P. syringae*) in 2-day-old seedlings than that in 6-day-old seedlings (Zou et al., 2018). In the transition from inflorescence meristem to floral meristem in *Arabidopsis*, *FLS2* was inhibited by a transcription factor, LEAFY (LFY). LFY suppressed the *FLS2* expression through binding to the promoter of *FLS2* (Winter et al., 2011). Hence, cauline leaves in *lfy* mutant were more resistant than that of wild type to *P. syringae* (Winter et al., 2011). Interestingly, the susceptible mutant phenotype of *fls2* to *P. syringae* was only evident in leaves generated late on the Arabidopsis shoot (Zipfel et al.,

2004). To date, we are not clear about how the strength of the FLS2-mediated PTI response is adjusted across different stages of shoot maturation.

In this work, we revealed that the FLS2-mediated resistance to *Pseudomonas syringae pv.* tomato DC3000 (*Pto* DC3000) (Cuppels, 1986) was increased during shoot maturation in *Arabidopsis*. We expanded the observation about *fls2* mutant phenotype in leaf from adult stage to juvenile stage. We showed that flg22-induced ROS accumulation and marker gene expression were comparable in juvenile and adult leaves. However, the level of callose deposition was higher in adult leaves than that in juvenile leaves. MiR156-regulated aging pathway showed limited impact on flg22-induced ROS production and gene activation but reduced callose deposition in fully expanded juvenile leaves. We propose that the intrinsic control of callose deposition in juvenile leaves mediates the maturation of FLS2 immune response.

## MATERIALS AND METHODS

### Plant material and growth conditions

Planting and growing conditions (9 hours light/15 hours darkness) are the same as described in (Hu et al., 2022). All juvenile leaves of Col-0 and leaf 1 and 2 of mutants that were used in this work coming from 4-5 weeks old plants in soil. All adult leaves of Col-0 and leaves at the similar positions of mutants were from 6-7

weeks old plants in soil. *Fls2-101*, *fls2* (SALK_141277), and *npr1-1* mutant were obtained from the Arabidopsis Biological Resource Center (Ohio State University, Columbus, OH). *Fls2/efc/cerk1* mutant was kindly provided by Kvitko Lab (University of Georgia). The cross of *fls2-101* and *35S::MIM156* were generated from this research, and genotyped with primers in supplementary Table. S2. Progenies in F3 and F4 of *fls2/MIM156* were used for phenotypic tests.

**Bacterial growth assay**

*Pto* DC3000 and *Pto* mutants were grown at 28 °C on King's B medium (40 g $l^{-1}$ proteose peptone 3, 20 g $l^{-1}$ glycerol, 15 g $l^{-1}$ agar) with Rifamycin (final concentration 100 $\mu$g/mL). An overnight fresh plate culture of each bacterial strain was prepared. For needleless syringe infiltration, bacteria were scraped off the plate and resuspended in 10 mM $MgCl_2$ (OD=0.1 and then with 500 times of dilution). For spraying the DC3000 strain, bacterial cell suspension (OD=0.1) was prepared in 10 mM $MgCl_2$ with 0.01% Silwet L-77. After inoculation, leaves from four individual juvenile or four adult plants were collected separately and homogenized (homogenizer, OMNI International) in one biological replicate. The homogenized samples were then loaded on fresh King's B plate with serial dilutions. Two days after loading, single colonies were counted manually. Usually three-four biological replicates per genotype/age per treatment were collected at Day0, and six-eight biological replicates were used for Day2 and Day4.

**Flg22-induced protection assay**

1$\mu$M of flg22 or mock (1 $\mu$M DMSO in ddH2O) were infiltrated in leaves with needleless syringe 24 hour prior to the bacteria infection. Infiltration of *Pst* DC3000 and sampling are the same as described in the bacterial growth assay.

**Gene expression analysis**

To detect flg22-induced activation of *FLS2* and *FRK1*, 1 $\mu$M, 100 nM, 10 nM, 1nM, 100 pM, 10 pM and 1 pM of flg22 (GenScript) were infiltrated in leaves with a needleless syringe. Since flg22 was dissolved in DMSO, 1 $\mu$M DMSO in ddH2O was used as mock. Samples were harvested at 1 hpi. Twenty juvenile leaves or 20 adult leaf discs from at least three individual plants were collected and homogenized (homogenizer, OMNI International) as one biological replicate. One to two biological repeats were used in a single experiment. Total RNAs were extracted using E.Z.N.A. Total RNA kit (Omega BIO-TEK) and reversely transcribed with GoScript reverse transcriptase (Promega). The qPCR was performed using SYBR Green master mix (Applied Biosystems) in the QuantStudio 1 Real-Time PCR system (Applied Biosystems). qPCR conditions were the same as described in Hu et al., 2022. Reference genes were *TUB2* (*AT5G62690*) and *SAND* (*AT2G28390*). Primers of qPCR were shown in supplementary Table. S2.

**Callose deposition assay**

The protocol was adapted from (Yu et al., 2019). 1 $\mu$M flg22 or mock (1 $\mu$M DMSO in ddH2O) was hand-infiltrated in juvenile and adult leaves of Col-0, *fls2-101* as well as the leaf 1 and 2 of *inMIM156*. Nine to twenty leaves from 8 plants (sample size varied between experimental repeats but was kept similar in an experiment between groups) were harvested 24h post the treatments. Leaf discs were collected from the same position among adult leaves using a corer that has comparable sampling area with the size of juvenile leaves. The samples were fixed with FAA solution (10% formaldehyde, 5% acetic acid and 50% ethanol) via vacuum infiltration followed by an overnight incubation under 37 °C. Using 95% ethanol to incubate the samples 24h to clear chlorophyll pigment. Rinse the samples with 75% ethanol each day over 2-3 days, until leaves became transparent. Rinse samples once with dd$H_2O$. Stain the samples for 30 min with 0.01% aniline blue solution (150 mM $KH_2PO_4$, pH 9.5). At the same day after the staining, imaging all the samples using fluorescence microscope (Zeiss). The number of callose was quantified using Fiji software.

**ROS assay**

Following the protocol derived from (Sang & Macho, 2017), Biopsy punch with plunger (4 mm diameter; Miltex, USA) was used to collect leaf disc from juvenile and adult leaves of Col-0, *fls2-101*, *inMIM156* (leaf 1-2) and *in156* (leaves at the

same position with that of adult Col-0). At least 24 leaf discs per phenotype per treatment was used for each experiment. Each leaf disc was placed in an opaque 96-well plate (OptiPlate$^{TM}$-96, Perkin Elmer) and submerged in 100 $\mu$L of dd$H_2O$ overnight. After 16-18 hrs, the water in the plate was replaced by a master mix with the same volume in each well. The total of 10 mL master mix solution was made of 10 $\mu$L of Luminol (Sigma) from 100 mM stock solution in DMSO, 10 $\mu$L of Horseradish Peroxidase (Sigma) from 20 mg/mL stock solution in dd$H_2O$, 5 $\mu$L of flg22 peptide (100 $\mu$M working stock) and supplemented with dd$H_2O$. To make the 100 $\mu$M of flg22 working stock, 10 $\mu$L of elicitor at 10 mM (dissolved in DMSO) was added in 990 $\mu$L of dd$H_2O$. As a negative control, the same master mix solution was made with flg22 replaced by DMSO. The $H_2O_2$-reacted luminescence was detected under luminometer (Molecular Devices, SpectraMax iD3) from 2 min up to an hour. The data was collected and analyzed in Excel software.

**Construction of inducible MIR156A**

The estradiol-inducible *MIR156A* line (*inmiR156*) was constructed using a Gateway compatible version of the XVE system (Brand et al., 2006).
The *MIR156A* stem loop sequence was cloned into pMDC160. Homozygous transgenic line was crossed to plants containing pMDC150-35S (Brand et al., 2006) and selected for double homozygous. The working concentration of 20 $\mu$M 17-ß-estradiol (dissolved in DMSO and diluted with ddH2O plus 0.01% Silwet 77)

was sprayed onto leaves at 12 hours before collecting leaf samples for ROS assay. For qPCR assay, estradiol was treated 24 hours before sample collections.

### Data visualization and statistics

The data visual was done using Microsoft Excel and RStudio 2022.07.1+554 (RStudio Team, 2022) with package ggplot2 3.3.6/ggpubr0.4.0 (Wickham, 2016), package magrittr 2.0.3 (Stefan Milton Bach & Hadley Wickham, 2022), and package RColorBrewer 1.1-3 (Brewer et al., 2003). The student t test was performed in the T test calculator, GraphPad, https://www.graphpad.com/quickcalcs/ttest1.cfm. Emmeans package 1.8.1-1 was conducted in RStudio (Searle et al., 1980).

## RESULTS

### FLS2-mediated defense against Pto DC3000 was dispensable in juvenile leaves.

To confirm and expand the observation of age-dependent requirement of FLS2 in resistance against *Pto* DC3000 (Zipfel et al., 2004), we measured bacterial growth in juvenile (leaves 1 & 2) and adult (leaves 13-17) leaves. Because transcriptional regulation of FLS2 occurs during leaf expansion, we used fully

expanded juvenile and adult leaves to focus on the impact of shoot maturation and minimize the consequence of leaf ontogeny (Figure 3.8). The fully expanded leaves 1 & 2 and leaves 13-17 were harvested from plants grown under short-day conditions (Figure 3.1 A and Figure 3.8). *Pto* DC3000 bacterial multiplications in two independent *fls2* alleles were not different from Col-0 juvenile leaves, while *fls2* adult leaves were more susceptible than Col-0 adults (Figure 3.1 A-B), which was consistent with a previous report (Zipfel et al., 2004). Many studies on FLS2 immune function have used bacterial surface inoculation (Zipfel et al., 2004; Zeng & He, 2010; Orosa et al., 2018). We found that juvenile *fls2* leaves were not more susceptible than Col-0 juvenile's when *Pto* DC3000 was applied either through syringe infiltrated or spray. These results confirmed that the susceptibility of *fls2* relative to Col-0 wild type was age-dependent.

We first speculated that the lack of phenotype in *fls2* juvenile leaves was due to a redundancy of FLS2-mediated defense with other PTI pathways. We tested bacterial growth in *fec,* the triple mutant of loss-of-function *FLS2/EFR/CERK1* immune receptors (Gimenez-Ibanez, Ntoukakis, et al., 2009). Like *fls2*, leaves 1-2 from *fec* mutant showed the same level of susceptibility to *Pto* DC3000 as that of Col-0 (Figure 3.1 C), arguing against the possibility of the functional redundancy among the three signaling pathways. The result implied that a downstream of *FLS2/EFR/CERK1* was compromised in juvenile leaves. The *npr1-1* mutant, defective in salicylic acid perception (Cao et al., 1997), showed increased bacterial propagation in juvenile leaves (Figure 3.1 C), suggesting the

bacterial load was not constrained by the physiology of juvenile leaves. This data suggests that FLS2-mediated defense signaling to *Pto* DC3000 is hindered in juvenile leaves.

**Effectors and coronatine were not required to limit FLS2-mediated defense in juvenile leaves.**

*Pto* DC3000 delivers effector proteins and toxin coronatine to suppresses FLS2-mediated defense (Gimenez-Ibanez, Hann, et al., 2009; Shan et al., 2008; Xiang et al., 2008; Zeng & He, 2010). We sought to assess if the inefficiency of the FLS2 signaling in juvenile leaves were due to those virulent factors. We separately inoculated juvenile leaves with three *Pto* DC3000 mutant strains: *hrcC-*, defective in effector delivery through Type III Secretion System (T3SS) (Yuan & He, 1996); *cor-*, the Δ*cfl*Δ*cfa9 (cfa, coronafacic acid; cfl, cfa ligase)* (Bender et al., 1993) or the Δ*cfa6* mutant (Zeng et al., 2011) that is deficient in the phytotoxin coronatine biosynthesis, and the *hrcC-/cor-* double mutant (Worley et al., 2013). In *fls2-101* juvenile leaves the *hrcC-*, *cor-* and *hrcC-/cor-* strains reached similar respective loads to what was observed in the Col-0 juvenile leaves (Figure 3.2 A-C). Neither the high inoculum (OD600=0.1) nor the additional period of growth made a difference for *hrcC-/cor-* growth in Col-0 and *fls2* juvenile leaves (Figure 3.2 C). When compared with adult leaves, juvenile leaves were more susceptible to those mutated strains, displaying an age-dependent defense response. Thus, the evidence supports that host factors or

additional pathogen virulence factors constrained the FLS2-defense in juvenile leaves.

**A subset of FLS2-mediated defense response was compromised in juvenile leaves.**

We next investigated host factors that might limit FLS2 function in juvenile leaves. To check whether *FLS2* is differentially expressed or induced between juvenile and adult leaves, we infiltrated a series dilution of flg22 in those leaves. Both basal level and flg22-induced expression of *FLS2* were comparable in juvenile and adult leaves. Expression of a PTI marker *FRK1 (Flg22-induced Receptor-like Kinase 1)* was also indistinguishable between those two stages (Figure 3.3 A-B). Likewise, the flg22-induced production of reactive oxygen species (ROS) was not impaired in the juvenile leaves, nor was the total ROS accumulation (Figure 3.3 C).

Flg22-induced callose deposition in both juvenile and adult leaves, which was dependent on FLS2 (Figure 3.4 A-B). However, flg22-triggered callose deposition was weaker in juvenile leaves than that in adult leaves (Figure 3.4 A-B). Next, we assessed the flg22 priming effect between the two phases of leaves. The pretreatment of flg22 protected leaves against *Pto* DC3000 in juvenile leaf of Col-0 (Figure 3.4 C). Being consistent with enhanced callose deposition in the adult leaves (Figure 3.4 A-B), bacteria multiplication was still lower in adult leaves than

those in juvenile leaves after flg22 treatment. Those results indicated that low callose deposition correlates with limited FLS2-mediated defense in juvenile leaves.

**The flg22-triggered callose deposition was weakened by high miR156 level in juvenile phase.**

MicroRNA156 (miR156) is a master regulator of the shoot maturation (Poethig, 2013). miR156 accumulates highly in plants to maintain juvenile phase (J.-W. Wang et al., 2008; G. Wu et al., 2009; G. Wu & Poethig, 2006). The temporal decline of miR156 expression allows the transition to adult phase (J.-W. Wang et al., 2008; G. Wu et al., 2009; G. Wu & Poethig, 2006). Knocking down the function of miR156 by target mimicry, *MIM156*, leads to precocious adult traits on leaves 1 and 2 (Franco-Zorrilla et al., 2007; Wu et al., 2009; Wu & Poethig, 2006). We sought to test whether miR156 controls the age dependent FLS2 immune signaling. First, we examined whether the miR156 influences the flg22-induced defense outputs using estradiol-inducible transgenic lines with either knocking down of miR156 function, *est::MIM156* (*inMIM156*) (Brand et al., 2006; He et al., 2018), or overexpressing *MIR156A, est::MIR156A* (*inMIR156*) (Brand et al., 2006). The temporary expression of *MIM156* or *MIR156A* through estradiol induction minimized the impact of morphological differences caused by the altered miR156 activity or transcriptional expression. Neither *inMIM156* juvenile leaves nor adult leaves of *inMIR156* changed ROS activities, *FLS2* or *FRK1*

expression, at resting state or upon FLS2-defense activation (Figure 3.5 A-C). These observations agreed with those results that ROS activities, *FLS2* or *FRK1* expression were not differentially regulated in the juvenile and adult leaves (Figure 3.3).

Notably, induced *MIM156* led to an increased number of deposited callose at cell wall in juvenile leaves after flg22 treatment (Figure 3.6 A-B), suggesting that the high accumulation of miR156 compromised this defense output of FLS2 signaling. However, the callose deposition phenotype in *inMIM156* juvenile leaves was still significantly lower than that in wild type adult leaves (Figure 3.6 A-B), indicating additional age-dependent mechanisms contribute to high callose deposition potential in the adult stage or suppress which in the juvenile stage. We subsequently crossed 35S::*MIM156* (Franco-Zorrilla et al., 2007; Wu et al., 2009; Wu & Poethig, 2006) into *fls2-101* mutants to endow adult feature to the leaves 1&2 of *fls2* (Figure 3.6 C). Consistent with our previous observation (Hu et al., 2022) that knocking down miR156 function enhanced resistance against *Pto* DC3000, leaves 1&2 in *MIM156* plants showed low bacterial multiplication. Loss of *fls2* in the *MIM156* background did not increase disease susceptibility in leaves 1&2 (Figure 3.6 D). The similar disease phenotype of *MIM156* and *fls2/MIM156* indicates that miR156 acts downstream or in parallel with FLS2. We conclude that miR156 suppressed flg22-induced callose deposition, which together with miR156-independent factors restrict the output of FLS2 signaling in early shoot development.

## Discussion

In this research, we reported FLS2 contributed to age-related resistance to *Pto* DC3000 in adult leaves in *Arabidopsis*. We measured FLS2 immune signaling cascade including the flg22-induced ROS burst, the level of *FLS2* and *FRK1* transcripts and callose deposition. We discovered that the callose deposition phenotype was dampened in juvenile leaves. In support of that, the pre-treatment of flg22 decreased the bacterial load in adult leaves when compared with what was in flg22-treated juveniles. Furthermore, high accumulation of miR156 in the juvenile stage hindered flg22-triggered callose deposition, with potentially additional factors together led to the inefficiency of FLS2 resistance (Figure 3.7). Our work provided a temporal regulation on a subset of FLS2-mediated PTI responses, which associates with age-dependent defense response.

The change of immune strength during vegetative phase change has been documented in various plants. The overexpressing enhancer mutant of the miR156, *Corngrass 1,* led to extended juvenile phase and increased susceptibility to common rust (*Puccinia sorghi Schw*) and European corn borer (*Ostrinia nubilalis Hubner*) (Abedon & Tracy, 1996). Silencing miR156 in *MIM156* mutant accelerated adult development in rice leaf and increased resistance to brown planthopper (Ge et al., 2018). In other cases, a weak allele of *Hm1*, $Hm1^{A}$, conferred adult resistance to northern leaf spot in maize (Marla et al., 2018); Cf-9B-mediated resistance to leaf mold in tomato was incremental over the

vegetative-reproductive transition (Panter et al., 2002). Neither *Hm1*$^{A}$ nor *Cf-9B* changed transcriptional expression within those developmental transitions (Marla et al., 2018; Panter et al., 2002). The alternative splicing of *Cf-9B* was alluded to play a role in the onset of mature resistance (Panter et al., 2002). Whether miR156 participates in those age-related resistances remains to be seen.

Callose deposition to the plant cell wall contributes to defense against pathogen invasion, especially for preventing the penetration of fungal hyphae (An, Ehlers, et al., 2006; An, Huckelhoven, et al., 2006; Nielsen et al., 2012). Many Gram-negative bacterial pathogens require T3SS-secreted effectors to suppress callose deposition. T3SS-deficient strains of *Pto* DC3000 and *Xanthomonas euvesicatoria* 85-10 induced abundant callose deposition, thickening cell walls and triggering papilla formation (Bestwick et al., 1995; I. Brown, 1995; I. Brown et al., 1998). The pathogen-induced papillae are a cell wall apposition for plants to deliver defense components, such as phytotoxin, callose and ROS (Meyer et al., 2009; Y. Wang et al., 2021). AvrPto effector derived from *Pto* DC3000 repressed callose papillae deposition and enabled considerable multiplication of the T3SS-deficient strain of *Pto* (*hrp* mutant, Hauck et al., 2003). A decrease of papillae was observed in miR156-overexpressing rice plants (Xie et al., 2012), However, overexpression of miR156 in switchgrass increased lignin content and decreased susceptibility to fungal rust (*Puccinia emaculata*), while the plant became highly susceptible to Bipolaris species (Baxter et al., 2018). As a part of constitutive defense, the biosynthesis of wax and cuticle was upregulated in adult than that of

juvenile Col-0 leaves (Hu et al., 2022). In maize and *Arabidopsis*, miR156 regulates cell wall composition during the vegetative phase change (li et al., 2019; Strable et al., 2008; Vega et al., 2002). Investigating the modulation of miR156 in cell wall-defense in the absence and presence of pathogens would be of next interests.

The magnitude of flg22-triggered ROS signaling and the *FRK1* expression are maintained during the vegetative transition, indicating the early inducibility of the defense is intact. Since miR156 functions in the absence of pathogen attack, it is plausible that the high level of miR156 inhibited basal activities of defense, which then attenuated a subsector of FLS2-mediate PTI. To which extent that a high level of defense gene expression at steady state contribute to defense activation is unclear in plants. Future research is required to determine the regulatory components and their modes of action pre- and post-infection in the age-related resistance. Quantitatively analyze different sectors of PTI responses in the distinct stage of development would be informative to pinpoint the composition of aging-immunity crosstalk at molecular levels and strategize disease managements accordingly. The age-related resistance can be maintained for more than 30 years when crops grow substantially in the region exposed with multiple races of pathogens (Roland F. Line & Xianming Chen, 1995). The adult resistance in wheat is conferred by different nonclassical R genes, which cannot be overcame by a single genetic variation (Ellis et al., 2014; Moore et al., 2015; Schwessinger, 2017). Limiting the population size of multiple pathogens without

demanding a fast genomic expansion of resistance gene can make the age-related resistance an efficient tactic for plants to stay resilient under turbulent environmental conditions.

Table 3.1 Plants, bacterial strains and primers used in Chapter 3.

| **Seed stocks** | **Source** |
|---|---|
| *35S::MIR156A* | CS67849 |
| *35S::MIM156* | Franco-Zorrilla et al., Nat. Genetics, 2007 |
| *XVE::35S::MIM156* | He et al., PLoS Genetics, 2018 |
| *XVE::35S::MIR156A* | this study |
| *fec* | Gimenez-Ibanez, Ntoukakis, et al., 2009 |
| *npr1-1* | Cao et al., 1997 |

| **Bacteria stocks** | **Source** |
|---|---|
| *Pto.* DC3000 | Cuppels, 1986; Zeng et al., 2011 |
| *Pto. hrcC-* | Yuan & He, 1996 |
| *Pto. cor-* | Bender et al., 1993 |
| *Pto. hrcC-/cor-* | Worley et al., 2013 |

| **Primers for genotyping** | | |
|---|---|---|
| **Mutant** | **PCR size** | **primer sequences** |
| *fls2-101* | WT=908 bp,<br>Mut=no band | CTTCTTTGGCATTGCACTAGC |
| | | ACCCCAAATGGGTTAACTGAG |

| Primers for qPCR | | |
|---|---|---|
| Name | Sequence (5'-3') | Description |
| *qTUB2*_qFw | AGCAATACCAAGATGCAACTGCG | reference gene |
| *qTUB2*_qRv | TAACTAAATTATTCTCAGTACTCTTCC | reference gene |
| *SPL3*_qFw | ATGAGTATGAGAAGAAGCAAAGCG | 156 bp qPCR product |
| *SPL3*_qRv | TCCACTACTACTTGTAGCTTTACCT | 156 bp qPCR product |
| *qSAND*_qFw | AACTCTATGCAGCATTTGATCCACT | reference gene |
| *qSAND*_qRv | TGATTGCATATCTTTATCGCCATC | reference gene |
| *qPCR_FRK1_qFw* | ATCTTCGCTTGGAGCTTCTC | 108 bp qPCR product |
| *qPCR_FRK1_qRv* | TGCAGCGCAAGGACTAGAG | 108 bp qPCR product |
| *qPCR_FLS2_qFw* | GGTTTGCGTGGGAAAGCGGC | 95 bp qPCR product |
| *qPCR_FLS2_qRv* | CGGTGCTGCAGAGCCGTGAA | 95 bp qPCR product |

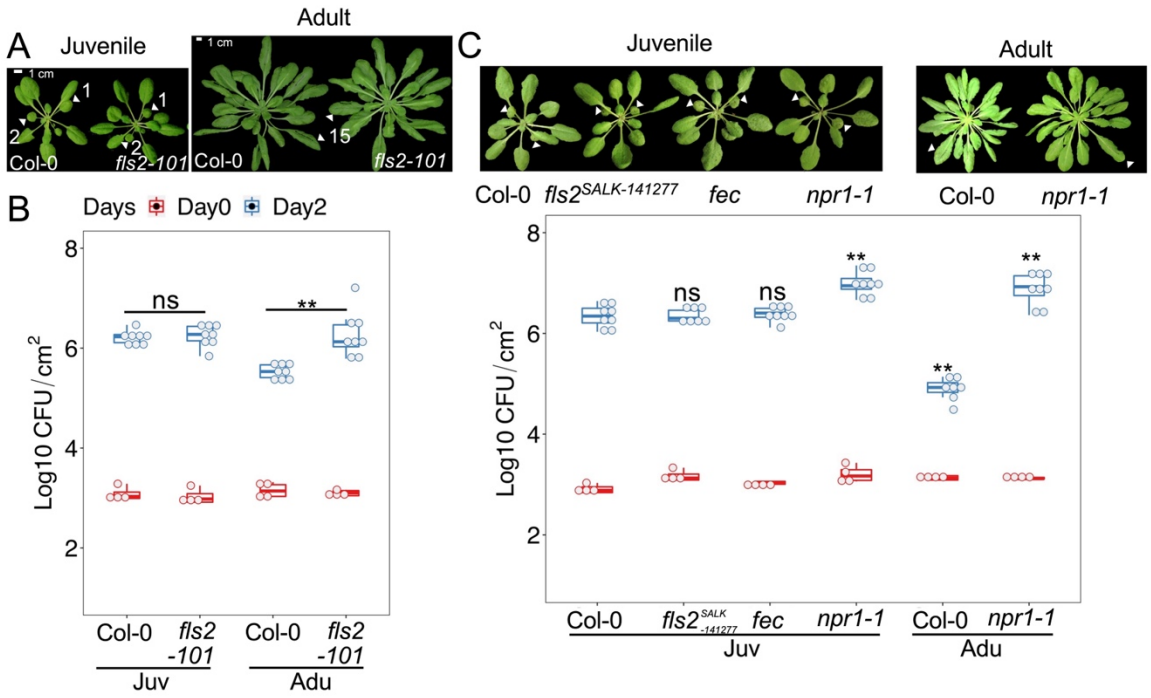


**Figure 3.1 The age-related resistance to *Pto* DC3000 was abolished in *fls2* mutant. A**, plant morphology of juvenile and adult Col-0 and *fls2-101*. **B**, *fls2* mutant was more susceptible than Col-0 in the adult stage, but not in the juvenile stage. Juv, juvenile leaves. Adu, adult leaves. Arrows indicate the leaves used for juvenile (leaves 1 and 2) and adult samples (leaf 15). **C**, *fls2 (SALK_141277)*, *fls2/efr/cerk1* but not *npr1-1* showed bacterial growth similar to Col-0 in juvenile phase. Juv, juvenile leaves. Adu, adult leaves. Arrows indicate leaves 1 and 2 in juvenile samples; and leaves 15 in adult samples. Images of plants were taken one day before bacterial inoculation. In boxplots, each dot represents a sample that was homogenized with four leaf discs derived from four individual leaves. Red boxes indicate the initial inoculation of *Pto* DC3000 in leaves. Blue boxes indicate bacterial growth in leaves two days post-inoculation (dpi). The bacteria growth was estimated by counting bacterial colony forming unit/cm$^2$ (CFU/cm$^2$). *

$P < 0.05$, ** $P < 0.01$, student t-test. The data are representative of three experimental repeats that were performed with similar results.

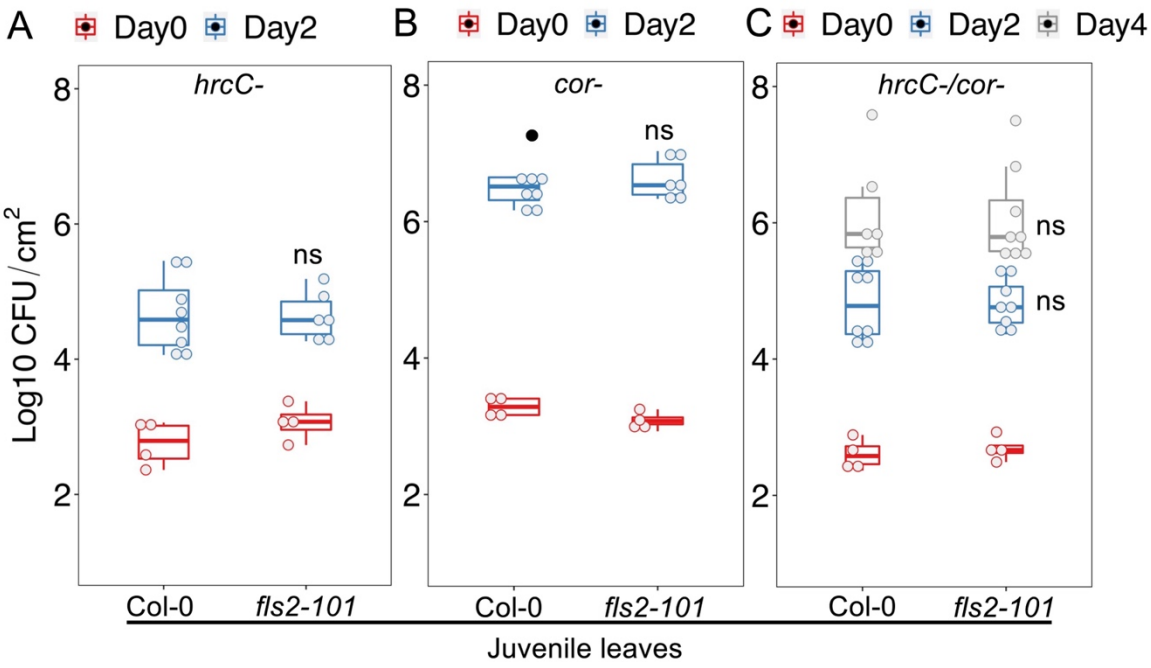


**Figure 3.2 The growth of *Pto* mutants was comparable in juvenile leaves of *fls2* and Col-0.**

**A**, comparable bacterial growth of *hrcC-* in juvenile Col-0 and *fls2*. Each dot represents a sample containing 4 leaf discs. **B**, a comparable growth of *cor-* in juvenile leaves of Col-0 and *fls2*. **C**, the similar growth of *hrcC-/cor-* in juvenile Col-0 and *fls2*. Red boxes indicate the initial inoculation of *Pto* DC3000 and *hrcC-* in leaves. Blue boxes indicate bacterial growth in leaves two days post-inoculation (dpi). Grey boxes indicate bacterial growth four days post-inoculation (dpi). The bacteria growth was estimated by counting bacterial colony forming unit/cm$^2$ (CFU/cm$^2$). The outliers indicated by black dots were determined by mean$\pm$two standard deviations (sds) in R. * $P < 0.05$, ** $P < 0.01$, student t-test. The data are representative from at least three experimental repeats that were performed with similar results.

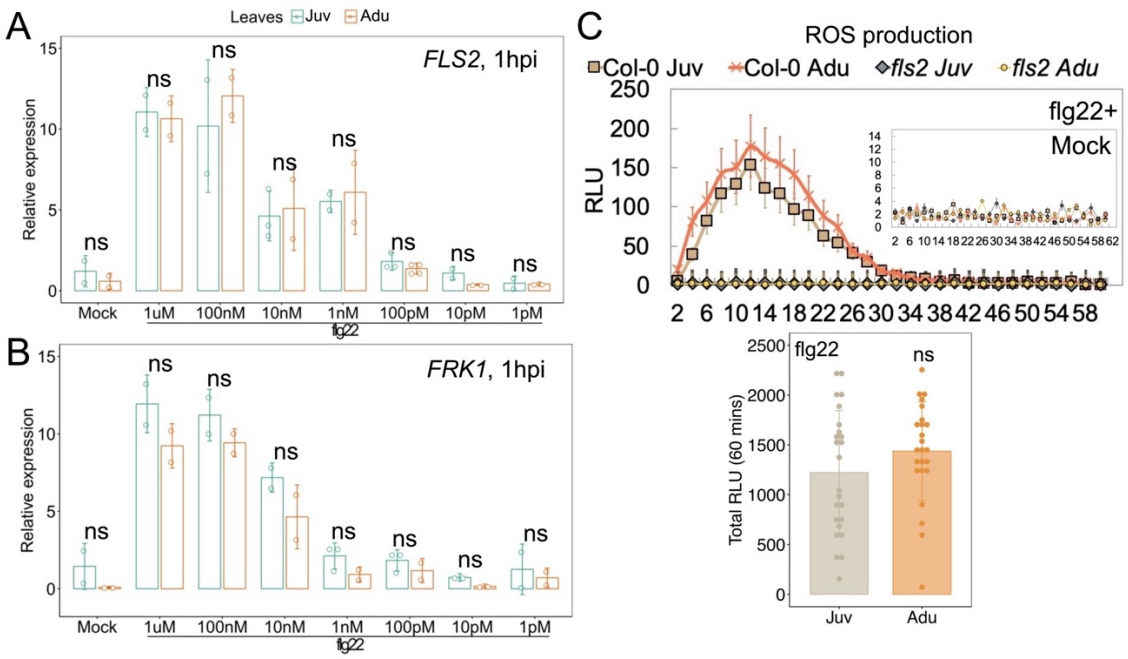


**Figure 3.3 The early FLS2 immune responses were independent of shoot maturation.**

**A-** **B**, the transcript quantity of *FLS2* and *FRK1* was not temporally regulated. Juv, juvenile leaves. Adu, adult leaves. 1 $\mu$M flg22-treated juvenile and adult leaf samples were harvested at 1-hour post-infiltration (hpi). Mock, 1 $\mu$M DMSO in dd$H_2O$. Each dot represents a technical repeat. Error bars stand for standard deviation (±SD). * P < 0.05, ** P < 0.01, student t-test. The data are representative from three experimental repeats that were performed with similar results. **C**, ROS induction and accumulation within an hour reached to the similar amplitude in juvenile and adult Col-0 leaves. See details of mock prep in methods. Flg22: 50 nM. Each symbol in the curve plot stands for an average value of at least 24 individual leaf

discs. Each dot in the bar plot represents the sum of values of a single leaf disc evaluated within 60 minutes. RLU, relative light unit.

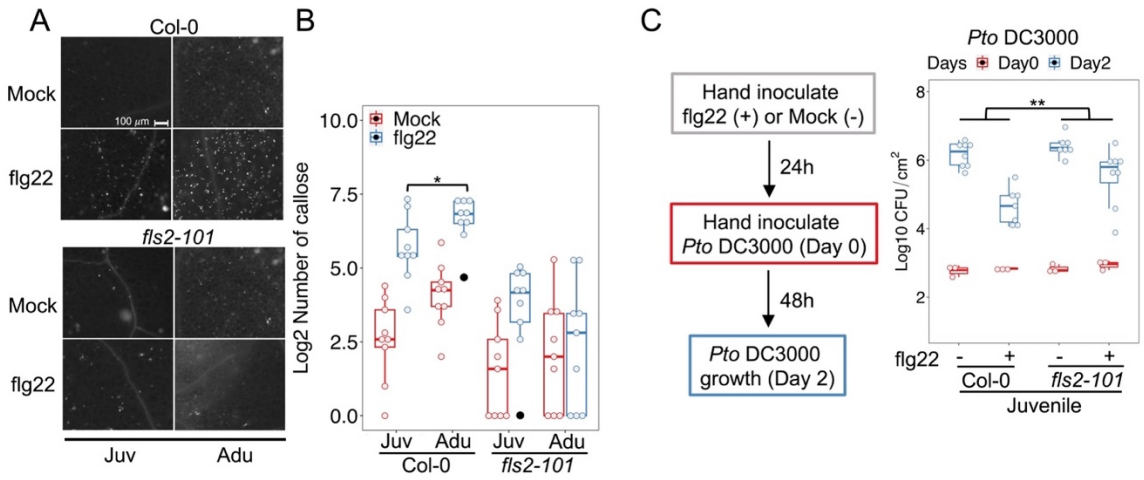


**Figure 3.4 Perception of flg22 activated a weak callose deposition in juvenile leaves. A**, visualization of callose deposited in juvenile and adult leaves of Col-0 24 hours post flg22 treatment. Flg22: 1 $\mu$M. **B**, quantification of the callose deposition depicted in Fig 4A. Juv, juvenile leaves. Adu, adult leaves. The outliers indicated by black dots were determined by checking the statistical model in R. The treatment effect within each genotype or age was determined by student t test, $P < 0.05$, ** $P < 0.01$. **C**, Flg22-priming protected juvenile Col-0 compared with that in *fls2*. Flg22 was infiltrated in leaves 24h prior to inoculation of *Pto* DC3000. Left panel, a diagram of procedures of flg22-protection assay. Right panel, each dot represents a sample with four leaf discs. Red boxes indicate the initial inoculation of *Pto* DC3000 in leaves. Blue boxes indicate bacterial growth in leaves two days post-inoculation (dpi). The bacteria growth was estimated by counting bacterial colony forming unit/cm$^2$ (CFU/cm$^2$). The outliers indicated by black dots were determined by mean $\pm$ two standard deviations (sds) in R. Emmeans in R (Searle et al., 1980) was used in Fig 4C to determine the genotype effect on bacterial growth between treatments. The data

are representative from three experimental repeats that were performed with similar results.

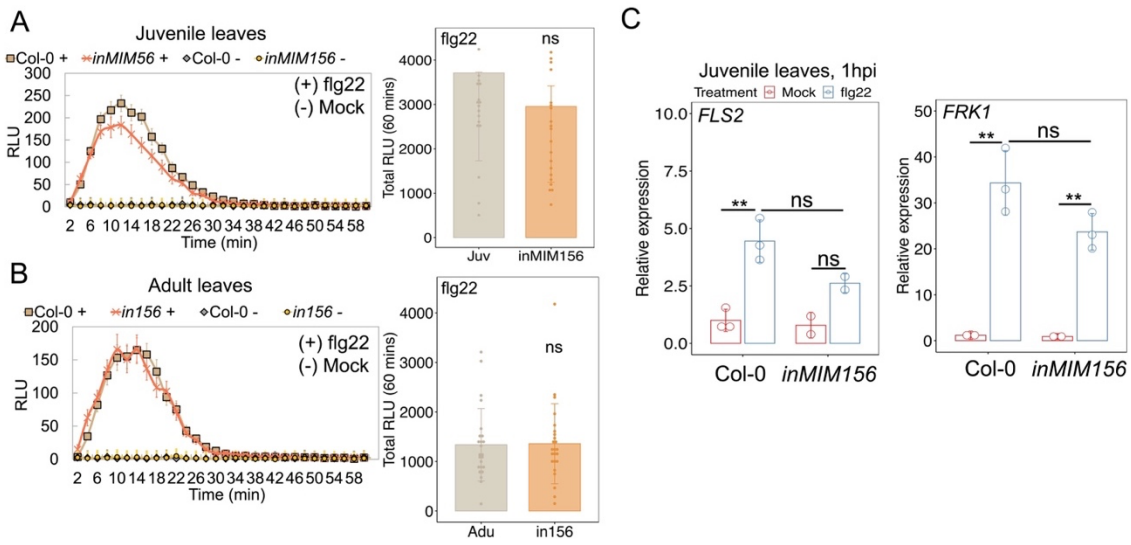


**Figure 3.5 Early defense signaling in juvenile leaves was independent of miR156. A,** Similar levels of ROS induction and total accumulation of juvenile Col-0 and *inMIM156* leaf 1-2 within an hour. **B**, Similar levels of ROS activation and accumulation of adult Col-0 and *in156* leaf 13-17. Treatments and the meaning of symbols were the same as described in Fig 3C. **C**, *FLS2* and *FRK1* expressions were not higher in leaf 1-2 of *inMIM156* than juvenile leaves of Col-0. Mock treatment refers to leaves infiltrated with 1 $\mu$M DMSO. Flg22, 1 $\mu$M. Samples were harvested at 1 hpi of treatments. Each dot represents a technical repeat. Error bars represent standard deviation (±SD). P < 0.05, ** P < 0.01, student t-test. The Data are representative from three experimental repeats that were performed with similar results.

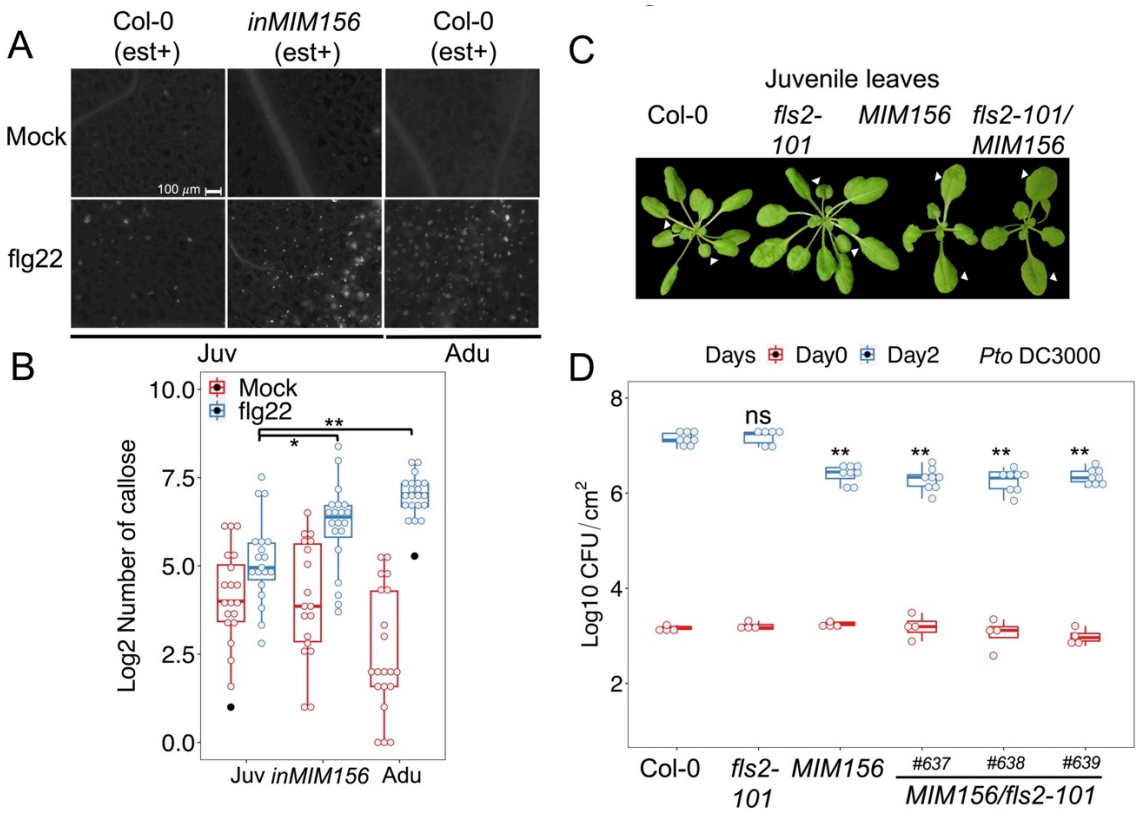


**Figure 3.6 The low level of miR156 allows enhanced callose deposition and disease resistance. A**, flg22 induced less callose deposition in juvenile Col-0 leaves than those from *inMIM156* and adult Col-0. **B**, Quantification of the callose deposition in Fig 6A. Juv, juvenile leaves. Adu, adult leaves. The black square indicated numbers of callose calculated from wounded tissue. The outliers indicated by black dots were determined by mean ± two standard deviations (sds) in R. The student t test was used between treatments within a single genotype/age, $P < 0.05$, ** $P < 0.01$. Emmeans in R (Searle et al., 1980) was used to determine genotype/age effects on the accumulation of flg22-induced callose. **C**, plant morphology of *fls2/MIM156* relative to *fls2* and *MIM156*. The photo was taken one day before the bacterial infiltration. **D**, Bacterial growth in

leaves 1 and 2 from *MIM156* and *MIM156*/*fls2*. Each dot represents a sample. Red boxes indicate the initial inoculation of *Pto* DC3000 in leaves. Blue boxes indicate bacterial growth in leaves two days post-inoculation (dpi). The bacteria growth was estimated by counting bacterial colony forming unit/$cm^2$ (CFU/$cm^2$). P < 0.05, ** P < 0.01, student t-test. The Data are representative from three experimental repeats with similar results.

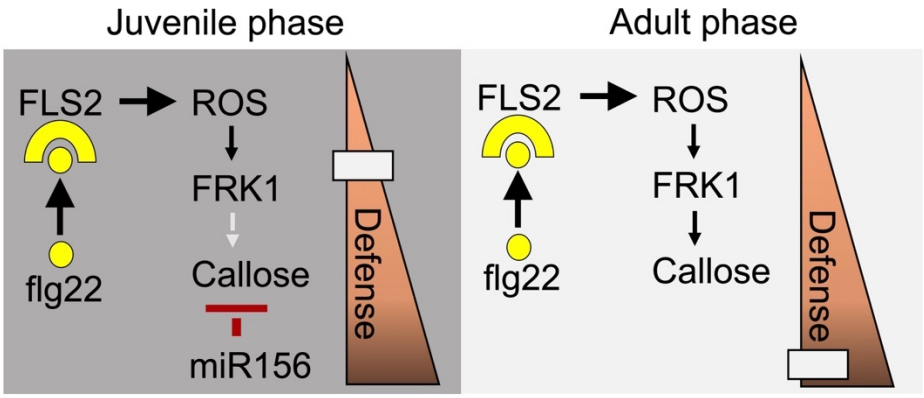


**Figure 3.7 A diagram for the proposed model.** Flg22 induces FLS2-mediated PTI in juvenile and adult phase. Callose deposition, but not ROS signaling, accumulation or early marker activation, was compromised in the juvenile phase. Temporal reduction of miR156 contributed to the increase of callose deposition in adult stage. Additional host factors may limit FLS2-mediated PTI or promote which in the juvenile stage.

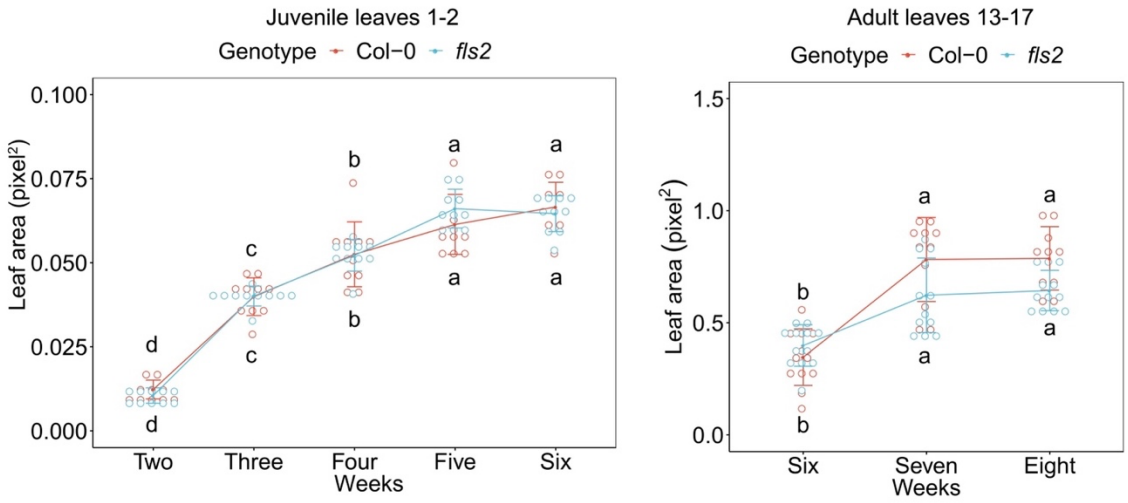


**Figure 3.8 *Fls2* mutant had comparable leaf expansion rates as that of Col-0.** In the curve-dot plots, each dot stands for a single leaf. Tukey test was applied for statistics.

## LITERATURE CITED


Abedon, B. G., & Tracy, W. F. (1996). Corngrass1 of maize (Zea mays l.) delays development of adult plant resistance to common rust (Puccinia sorghi Schw.) and European corn borer (Ostrinia nubilalis Hubner). *Journal of Heredity*, *87*(3), 219–223.

An, Q., Ehlers, K., Kogel, K., van Bel, A. J. E., & Hückelhoven, R. (2006). Multivesicular compartments proliferate in susceptible and resistant *MLA12* - barley leaves in response to infection by the biotrophic powdery mildew fungus. *New Phytologist*, *172*(3), 563–576.

An, Q., Huckelhoven, R., Kogel, K.-H., & van Bel, A. J. E. (2006). Multivesicular bodies participate in a cell wall-associated defense response in barley leaves attacked by the pathogenic powdery mildew fungus. *Cellular Microbiology*, *8*(6), 1009–1019.

Baxter, H. L., Mazarei, M., Dumitrache, A., Natzke, J. M., Rodriguez, M., Gou, J., Fu, C., Sykes, R. W., Turner, G. B., Davis, M. F., Brown, S. D., Davison, B. H., Wang, Z., & Stewart, C. N. (2018). Transgenic miR156 switchgrass in the field: growth, recalcitrance and rust susceptibility. *Plant Biotechnology Journal*, *16*(1), 39–49.

Bender, C. L., Liyanage, H., Palmer, D., Ullrich, M., Young, S., & Mitchell, R. (1993). Characterization of the genes controlling the biosynthesis of the polyketide

phytotoxin coronatine including conjugation between coronafacic and coronamic acid. *Gene*, *133*(1), 31–38.

Bestwick, C. S., Bennett, M. H., & Mansfield, J. W. (1995). Hrp Mutant of Pseudomonas syringae pv phaseolicola Induces Cell Wall Alterations but Not Membrane Damage Leading to the Hypersensitive Reaction in Lettuce. *Plant Physiology*, *108*(2), 503–516.

Brand, L., Hörler, M., Nüesch, E., Vassalli, S., Barrell, P., Yang, W., Jefferson, R. A., Grossniklaus, U., & Curtis, M. D. (2006). A Versatile and Reliable Two-Component System for Tissue-Specific Gene Induction in Arabidopsis . *Plant Physiology*, *141*(4), 1194–1204.

Brewer, C. A., Hatchard, G. W., & Harrower, M. A. (2003). ColorBrewer in Print: A Catalog of Color Schemes for Maps. *Cartography and Geographic Information Science*, *30*(1), 5–32.

Brown, I. (1995). *hrp* Genes in *Xanthomonas campestris* pv. *vesicatoria* Determine Ability to Suppress Papilla Deposition in Pepper Mesophyll Cells. *Molecular Plant-Microbe Interactions*, *8*(6), 825.

Brown, I., Trethowan, J., Kerry, M., Mansfield, J., & Bolwell, G. P. (1998). Localization of components of the oxidative cross-linking of glycoproteins and of callose synthesis in papillae formed during the interaction between non-pathogenic strains of *Xanthomonas campestris and* French bean mesophyll cells. *The Plant Journal*, *15*(3), 333–343.

Brown, J. K. M. (2002). Yield penalties of disease resistance in crops. *Current Opinion in Plant Biology*, *5*(4), 339–344.

Brown, J. K. M. (2003). A cost of disease resistance: paradigm or peculiarity? *Trends in Genetics*, *19*(12), 667–671.

Cao, H., Glazebrook, J., Clarke, J. D., Volko, S., & Dong, X. (1997). The Arabidopsis NPR1 gene that controls systemic acquired resistance encodes a novel protein containing ankyrin repeats. *Cell*. 10;88(1):57-63.

Cuppels, D. A. (1986). Generation and Characterization of Tn5 Insertion Mutations in Pseudomonas syringae pv. tomato. *Applied and Environmental Microbiology*, *51*(2), 323–327.

Ellis, J. G., Lagudah, E. S., Spielmeyer, W., & Dodds, P. N. (2014). The past, present and future of breeding rust resistant wheat. *Frontiers in Plant Science*, *5*: 641.

Franco-Zorrilla, J. M., Valli, A., Todesco, M., Mateos, I., Puga, M. I., Rubio-Somoza, I., Leyva, A., Weigel, D., García, J. A., & Paz-Ares, J. (2007). Target mimicry provides a new mechanism for regulation of microRNA activity. *Nature Genetics*, *39*(8), 1033–1037.

Fröschel, C., Komorek, J., Attard, A., Marsell, A., Lopez-Arboleda, W. A., le Berre, J., Wolf, E., Geldner, N., Waller, F., Korte, A., & Dröge-Laser, W. (2021). Plant roots employ cell-layer-specific programs to respond to pathogenic and beneficial microbes. *Cell Host & Microbe*, *29*(2), 299-310.e7.

Ge, Y., Han, J., Zhou, G., Xu, Y., Ding, Y., Shi, M., Guo, C., & Wu, G. (2018). Silencing of miR156 confers enhanced resistance to brown planthopper in rice. *Planta*. 248(4):813-826.

Gimenez-Ibanez, S., Hann, D. R., Ntoukakis, V., Petutschnig, E., Lipka, V., & Rathjen, J. P. (2009). AvrPtoB Targets the LysM Receptor Kinase CERK1 to Promote Bacterial Virulence on Plants. *Current Biology*, *19*(5), 423–429.

Gimenez-Ibanez, S., Ntoukakis, V., & Rathjen, J. P. (2009). The LysM receptor kinase CERK1 mediates bacterial perception in Arabidopsis. *Plant Signaling & Behavior*, *4*(6), 539–541.

Hauck, P., Thilmony, R., & He, S. Y. (2003). A *Pseudomonas syringae* type III effector suppresses cell wall-based extracellular defense in susceptible *Arabidopsis* plants. *Proceedings of the National Academy of Sciences*, *100*(14), 8577–8582.

He, J., Xu, M., Willmann, M. R., McCormick, K., Hu, T., Yang, L., Starker, C. G., Voytas, D. F., Meyers, B. C., & Poethig, R. S. (2018). Threshold-dependent repression of SPL gene expression by miR156/miR157 controls vegetative phase change in Arabidopsis thaliana. *PLoS Genetics*. 14(4): e1007337.

Hu, L., Peng, Q., Peper, A., Kong, F., Yao, Y., & Yang, L. (2022). Distinct function of SPL genes in age-related resistance in Arabidopsis. *BioRxiv*.

Jones, J. D. G., & Dangl, J. L. (2006). The plant immune system. *Nature*, *444*(7117), 323–329.

Klepikova, A. v., Kasianov, A. S., Gerasimov, E. S., Logacheva, M. D., & Penin, A. A. (2016). A high resolution map of the *Arabidopsis thaliana* developmental transcriptome based on RNA-seq profiling. *The Plant Journal*, *88*(6), 1058–1070.

Li, B., Meng, X., Shan, L., & He, P. (2016). Transcriptional Regulation of Pattern-Triggered Immunity in Plants. In *Cell Host and Microbe*. 19(5):641-50.

li, R.-J., Li, L. M., Liu, X. L., Kim, J. C., Jenks, M. A., & Lu, S. (2019). Diurnal Regulation of Plant Epidermal Wax Synthesis through Antagonistic Roles of the Transcription Factors SPL9 and DEWAX. *The Plant Cell*, 31(11):2711-2733.

Marla, S. R., Chu, K., Chintamanani, S., Multani, D. S., Klempien, A., DeLeon, A., Bong-suk, K., Dunkle, L. D., Dilkes, B. P., & Johal, G. S. (2018). Adult plant resistance in maize to northern leaf spot is a feature of partial loss-of-function alleles of Hm1. *PLoS Pathogens*. 14(10):e1007356.

Meyer, D., Pajonk, S., Micali, C., O'Connell, R., & Schulze-Lefert, P. (2009). Extracellular transport and integration of plant secretory proteins into pathogen-induced cell wall compartments. *The Plant Journal*, *57*(6), 986–999.

Moore, J. W., Herrera-Foessel, S., Lan, C., Schnippenkoetter, W., Ayliffe, M., Huerta-Espino, J., Lillemo, M., Viccars, L., Milne, R., Periyannan, S., Kong, X., Spielmeyer, W., Talbot, M., Bariana, H., Patrick, J. W., Dodds, P., Singh, R., & Lagudah, E. (2015). A recently evolved hexose transporter variant confers resistance to multiple pathogens in wheat. *Nature Genetics*, *47*(12), 1494–1498.

Nelson, R., Wiesner-Hanks, T., Wisser, R., & Balint-Kurti, P. (2018). Navigating complexity to breed disease-resistant crops. *Nature Reviews Genetics*, *19*(1), 21–33.

Ngou, B. P. M., Ding, P., & Jones, J. D. G. (2022). Thirty years of resistance: Zig-zag through the plant immune system. *The Plant Cell*, *34*(5), 1447–1478.

Nielsen, M. E., Feechan, A., Böhlenius, H., Ueda, T., & Thordal-Christensen, H. (2012). *Arabidopsis* ARF-GTP exchange factor, GNOM, mediates transport

required for innate immunity and focal accumulation of syntaxin PEN1. *Proceedings of the National Academy of Sciences*, *109*(28), 11443–11448.

Orosa, B., Yates, G., Verma, V., Srivastava, A. K., Srivastava, M., Campanaro, A., de Vega, D., Fernandes, A., Zhang, C., Lee, J., Bennett, M. J., & Sadanandom, A. (2018). SUMO conjugation to the pattern recognition receptor FLS2 triggers intracellular signalling in plant innate immunity. *Nature Communications*, *9*(1), 5185.

Panter, S. N., Hammond-Kosack, K. E., Harrison, K., Jones, J. D. G., & Jones, D. a. (2002). Developmental control of promoter activity is not responsible for mature onset of Cf-9B-mediated resistance to leaf mold in tomato. *Molecular Plant-Microbe Interactions : MPMI*, *15*(11), 1099–1107.

Poethig, R. S. (2013). Vegetative phase change and shoot maturation in plants. *Current Topics in Developmental Biology*, *105*, 125–152.

Roland F. Line, & Xianming Chen. (1995). Successes in breeding for and managing durable resistance to wheat rusts. *Plant Disease*, *79*(12), 1254–1255.

RStudio Team. (2022). *RStudio: Integrated Development Environment for R* (2022.07.1+554). http://www.rstudio.com/.

Sang, Y., & Macho, A. P. (2017). *Analysis of PAMP-Triggered ROS Burst in Plant Immunity* (pp. 143–153).

Schwessinger, B. (2017). Fundamental wheat stripe rust research in the 21 st century. *New Phytologist*, *213*(4), 1625–1631.

Searle, S. R., Speed, F. M., & Milliken, G. A. (1980). Population Marginal Means in the Linear Model: An Alternative to Least Squares Means. *The American Statistician*, *34*(4), 216–221.

Seybold, H., Trempel, F., Ranf, S., Scheel, D., Romeis, T., & Lee, J. (2014). Ca2+ signalling in plant immune response: From pattern recognition receptors to Ca2+ decoding mechanisms. *New Phytologist*. 204(4):782-90.

Shan, L., He, P., Li, J., Heese, A., Peck, S. C., Nürnberger, T., Martin, G. B., & Sheen, J. (2008). Bacterial Effectors Target the Common Signaling Partner BAK1 to Disrupt Multiple MAMP Receptor-Signaling Complexes and Impede Plant Immunity. *Cell Host & Microbe*, *4*(1), 17–27.

Stefan Milton Bach, & Hadley Wickham. (2022). *magrittr: A Forward-Pipe Operator for R*. https://magrittr.tidyverse.org, https://github.com/tidyverse/magrittr.

Strable, J., Borsuk, L., Nettleton, D., Schnable, P. S., & Irish, E. E. (2008). Microarray analysis of vegetative phase change in maize. *The Plant Journal*, *56*(6), 1045–1057.

Vega, S. H., Sauer, M., Orkwiszewski, J. A. J., & Poethig, R. S. (2002). The early phase change Gene in Maize. *The Plant Cell*, *14*(1), 133–147.

Wang, J.-W., Schwab, R., Czech, B., Mica, E., & Weigel, D. (2008). Dual Effects of miR156-Targeted *SPL* Genes and *CYP78A5/KLUH* on Plastochron Length and Organ Size in *Arabidopsis thaliana*. *The Plant Cell*, *20*(5), 1231–1243.

Wang, Y., Li, X., Fan, B., Zhu, C., & Chen, Z. (2021). Regulation and Function of Defense-Related Callose Deposition in Plants. *International Journal of Molecular Sciences*, *22*(5), 2393.

Wickham, H. (2016). *ggplot2*. Springer International Publishing. ISBN: 978-3-319-24275-0.

Winter, C. M., Austin, R. S., Blanvillain-Baufumé, S., Reback, M. A., Monniaux, M., Wu, M.-F., Sang, Y., Yamaguchi, A., Yamaguchi, N., Parker, J. E., Parcy, F., Jensen, S. T., Li, H., & Wagner, D. (2011). LEAFY Target Genes Reveal Floral Regulatory Logic, cis Motifs, and a Link to Biotic Stimulus Response. *Developmental Cell*, *20*(4), 430–443.

Worley, J. N., Russell, A. B., Wexler, A. G., Bronstein, P. A., Kvitko, B. H., Krasnoff, S. B., Munkvold, K. R., Swingle, B., Gibson, D. M., & Collmer, A. (2013). Pseudomonas syringae pv. tomato DC3000 CmaL (PSPTO4723), a DUF1330 Family Member, Is Needed To Produce L-allo-Isoleucine, a Precursor for the Phytotoxin Coronatine. *Journal of Bacteriology*, *195*(2), 287–296.

Wu, G., Park, M. Y., Conway, S. R., Wang, J. W., Weigel, D., & Poethig, R. S. (2009). The Sequential Action of miR156 and miR172 Regulates Developmental Timing in Arabidopsis. *Cell*, *138*(4), 750–759.

Wu, G., & Poethig, R. S. (2006). Temporal regulation of shoot development in Arabidopsis thaliana by miRr156 and its target SPL3. *Development*. 133(18):3539-47.

Wu, H., Qu, X., Dong, Z., Luo, L., Shao, C., Forner, J., Lohmann, J. U., Su, M., Xu, M., Liu, X., Zhu, L., Zeng, J., Liu, S., Tian, Z., & Zhao, Z. (2020). WUSCHEL triggers innate antiviral immunity in plant stem cells. *Science*, *370*(6513), 227–231.

Xiang, T., Zong, N., Zou, Y., Wu, Y., Zhang, J., Xing, W., Li, Y., Tang, X., Zhu, L., Chai, J., & Zhou, J.-M. (2008). Pseudomonas syringae Effector AvrPto Blocks Innate Immunity by Targeting Receptor Kinases. *Current Biology*, *18*(1), 74–80.

Xie, K., Shen, J., Hou, X., Yao, J., Li, X., Xiao, J., & Xiong, L. (2012). Gradual Increase of miR156 Regulates Temporal Expression Changes of Numerous Genes during Leaf Development in Rice. *Plant Physiology*, *158*(3), 1382–1394.

Yu, X., Li, B., Jang, G.-J., Jiang, S., Jiang, D., Jang, J.-C., Wu, S.-H., Shan, L., & He, P. (2019). Orchestration of Processing Body Dynamics and mRNA Decay in Arabidopsis Immunity. *Cell Reports*, *28*(8), 2194-2205.e6.

Yuan, J., & He, S. Y. (1996). The Pseudomonas syringae Hrp regulation and secretion system controls the production and secretion of multiple extracellular proteins. *Journal of Bacteriology*, *178*(21), 6399–6402.

Zeng, W., & He, S. Y. (2010). A Prominent Role of the Flagellin Receptor FLAGELLIN-SENSING2 in Mediating Stomatal Response to *Pseudomonas syringae* pv *tomato* DC3000 in Arabidopsis. *Plant Physiology*, *153*(3), 1188–1198.

Zeng, W., Brutus, A., Kremer, J. M., Withers, J. C., Gao, X., Jones, A. D., & He, S. Y. (2011). A Genetic Screen Reveals Arabidopsis Stomatal and/or Apoplastic Defenses against Pseudomonas syringae pv. tomato DC3000. *PLoS Pathogens*, *7*(10), e1002291.

Zheng, X., Zhou, M., Yoo, H., Pruneda-Paz, J. L., Spivey, N. W., Kay, S. A., & Dong, X. (2015). Spatial and temporal regulation of biosynthesis of the plant immune

signal salicylic acid. *Proceedings of the National Academy of Sciences*, *112*(30), 9166–9173.

Zhou, F., Emonet, A., Dénervaud Tendon, V., Marhavy, P., Wu, D., Lahaye, T., & Geldner, N. (2020). Co-incidence of Damage and Microbial Patterns Controls Localized Immune Responses in Roots. *Cell*, *180*(3), 440-453.e18.

Zou, Y., Wang, S., Zhou, Y., Bai, J., Huang, G., Liu, X., Zhang, Y., Tang, D., & Lu, D. (2018). Transcriptional Regulation of the Immune Receptor FLS2 Controls the Ontogeny of Plant Innate Immunity. *The Plant Cell*. 30(11):2779-2794.

## SUMMARY

Age-associated change of immunity is a widespread phenomenon in animals and plants. How organisms integrate immune maturation into their developmental clock is a fundamental question. Heterochronic microRNAs are key regulators of developmental timing. We found that a conserved heterochronic microRNA (miRNA) in *Arabidopsis*, microRNA156, regulates the timing of age-related resistance associated with a transition from the juvenile to the adult vegetative phase. In one case, the coordination between developmental maturation and gain of disease resistance is achieved through miR156-controlled SPL transcription factors with distinct functions. A subset of SPL transcription factors promoted resistance by directly activating key genes in defense signaling. In another case, miR156 acts in downstream or in parallel with FLS2 signaling, inhibiting an age-dependent callose deposition. These works bridge the knowledge gap between vegetative development and age-related resistance. Pinpointing mechanisms of the developmental regulation on immunity may pave a way for unlocking the age limit on plant immunity and lay a foundation to applications in the precision agriculture.

Plant innate immunity shares similarities to human innate immunity, ranging from structures and functionality of innate immune receptors and their downstream signaling cascades [55, 56]. Our discovery of miR156-SPL signaling in $ARR_{VPC}$ provides further evidence that heterochronic miRNAs coordinate aging and

immunity *in planta*. In *Caenorhabditis elegans*, *let-7* family microRNAs are well-characterized regulators of developmental timing by specifying stage-specific cell fates in the hypodermal seam cell lineages [57, 58]. Interestingly, let-*7-fam* miRNAs also repress the worm's resistance to *Pseudomonas aeruginosa*, an opportunistic human pathogen [59]. The dual function of *let-7-fam* in developmental timing and immunity is fulfilled through integrating downstream heterochronic genes and the p38 MAPK pathway [59]. Thus, deploying heterochronic microRNAs pathway can be a cross-kingdom strategy to integrate immunity and developmental timing. It will be exciting to further dissect the genetic components and regulatory architecture of coordinated maturation of immunity and development.

## LITERATURE CITED

55. Jones JD, Vance RE, Dangl JL.(2016). Intracellular innate immune surveillance devices in plants and animals. Science.354(6316):aaf6395.

56. Rossez Y, Wolfson EB, Holmes A, Gally DL, Holden NJ.(2015). Bacterial flagella: twist and stick, or dodge across the kingdoms. PLoS pathogens.11(1):e1004483.

57. Reinhart BJ, Slack FJ, Basson M, Pasquinelli AE, Bettinger JC, Rougvie AE, et al.(2000). The 21-nucleotide let-7 RNA regulates developmental timing in Caenorhabditis elegans. nature.403(6772):901-6.

58. Abbott AL, Alvarez-Saavedra E, Miska EA, Lau NC, Bartel DP, Horvitz HR, et al.(2005). The let-7 MicroRNA family members mir-48, mir-84, and mir-241 function together to regulate developmental timing in Caenorhabditis elegans. Developmental cell.9(3):403-14.

59. Ren Z, Ambros VR.(2015). Caenorhabditis elegans microRNAs of the let-7 family act in innate immune response circuits and confer robust developmental timing against pathogen stress. Proceedings of the National Academy of Sciences.112(18):E2366-E75.

APPENDIX. 203 genes used for the de novo motif discovery in Figure 2.6.

| | | | | | | |
|---|---|---|---|---|---|---|
| AT5G15160 | AT2G36870 | AT3G30180 | AT4G14400 | AT1G72930 | AT5G64770 | AT5G20700 |
| AT4G31840 | AT3G23010 | AT5G08760 | AT1G17745 | AT5G57700 | AT4G11300 | AT4G34380 |
| AT2G40610 | AT4G34250 | AT3G11650 | AT5G02890 | AT1G59590 | AT1G76980 | AT2G21850 |
| AT3G26200 | AT3G48240 | AT3G44326 | AT1G67865 | AT1G10990 | AT5G03760 | AT4G29110 |
| AT2G27300 | AT1G35230 | AT1G64390 | AT1G33560 | AT5G15230 | AT1G58420 | AT1G68710 |
| AT3G23290 | AT5G18470 | AT1G20850 | AT3G22410 | AT3G51920 | AT1G56020 | AT5G66320 |
| AT1G75090 | AT1G27130 | AT1G17140 | AT2G47800 | AT1G19320 | AT1G65490 | AT1G19330 |
| AT4G23020 | AT2G40100 | AT2G20950 | AT5G19240 | AT3G03450 | AT4G11660 | AT1G04770 |
| AT1G78320 | AT1G29720 | AT3G23000 | AT3G62110 | AT4G11900 | AT5G46880 | AT3G18370 |
| AT5G66690 | AT3G56710 | AT4G21903 | AT5G53830 | AT1G64080 | AT3G56090 | AT1G07930 |
| AT3G57240 | AT5G39010 | AT5G10380 | AT2G40740 | AT1G17920 | AT4G14740 | AT5G50150 |
| AT5G60760 | AT1G64710 | AT1G14880 | AT3G59010 | AT3G61280 | AT5G53370 | AT5G08380 |
| AT5G51560 | AT2G21650 | AT1G24470 | AT4G26270 | AT2G44290 | AT2G25000 | AT3G27270 |
| AT2G20750 | AT2G40475 | AT2G47750 | AT2G15090 | AT3G52430 | AT2G26190 | AT3G59100 |
| AT1G76800 | AT5G47610 | AT5G06330 | AT1G47670 | AT1G69730 | AT2G33310 | AT3G11580 |
| AT1G12380 | AT4G27460 | AT3G60420 | AT1G10060 | AT1G21590 | AT5G15310 | AT2G28950 |
| AT3G44350 | AT1G21270 | AT2G33580 | AT1G31580 | AT4G23030 | AT2G24160 | AT1G72480 |
| AT5G22380 | AT5G62940 | AT5G10760 | AT5G08240 | AT1G21520 | AT3G49260 | AT4G00180 |
| AT1G56600 | AT5G24530 | AT1G78820 | AT4G18250 | AT1G79110 | AT3G29320 | AT1G75500 |
| AT5G26690 | AT5G57130 | AT2G36970 | AT5G45800 | AT2G46420 | AT5G17600 | AT2G38120 |
| AT3G13980 | AT5G66400 | AT3G53150 | AT2G43150 | AT4G20000 | AT3G08030 | AT2G01670 |
| AT5G55450 | AT5G17760 | AT4G27300 | AT1G69530 | AT4G36280 | AT4G24780 | AT2G46270 |
| AT1G75040 | AT5G60690 | AT5G26230 | AT1G14730 | AT2G41180 | AT4G02520 | AT5G05460 |
| AT4G02420 | AT5G63180 | AT5G58930 | AT4G39830 | AT3G13222 | AT1G66970 | |

| | | | | | | |
|---|---|---|---|---|---|---|
| AT1G71390 | AT4G13840 | AT2G37640 | AT4G22130 | AT1G55210 | AT5G38212 | |
| AT2G43570 | AT5G60800 | AT4G34950 | AT1G50420 | AT3G20600 | AT3G29030 | |
| AT5G12940 | AT1G74670 | AT4G00820 | AT5G52310 | AT3G51950 | AT2G05920 | |
| AT1G51440 | AT5G41761 | AT3G50930 | AT1G65800 | AT3G46090 | AT3G21560 | |
| AT3G54820 | AT1G56150 | AT1G05630 | AT2G30010 | AT5G65590 | AT5G61210 | |
| AT2G01505 | AT2G29980 | AT4G37650 | AT3G62820 | AT5G41460 | AT5G64860 | |